# THERMODYNAMIC ANALYSIS OF ENVIRONMENTAL EFFECT OF IC ENGINE

## Thesis

*Submitted in partial fulfilment for the award of the Degree*
*of*

**DOCTOR OF PHILOSOPHY**

*in*

*Mechanical Engineering*

by


**Neeraj Kumar**

**(Roll No.- 2K18/Ph.D./ME/06)**


*Under the Supervision*

*of*


**Prof. B.B. Arora**
(Department of Mechanical Engg. DTU)

**Prof. S. Maji**
(Department of Mechanical Engg. DTU)

**Department of Mechanical Engineering,Delhi Technological University**
**(Formerly Delhi College of Engineering)**
**Main Bawana Road, Shahabad Daulatpur, Delhi- 110042, India**

**2024**

# DECLARATION

To fulfill the requirements for the award of the degree of Doctor of Philosophy , I hereby certify that the work being presented in this thesis titled "**THERMODYNAMIC ANALYSIS OF ENVIRONMENTAL EFFECT OF IC ENGINE** " is a record of proper research work conducted from July 2018 to Dec. 2024 under the supervision of Prof. B.B. Arora and Prof. S. Maji, the professor, Mechanical Engineering Department, Delhi Technological University, New Delhi, India.

Neeraj Kumar

(2K18/PHD/ME/06)

# CERTIFICATE

It is certified that the work contained in the thesis entitled **"Thermodynamic analysis of environmental effect of IC engine"** by Neeraj Kumar (Roll No: 2K18/PhD/ME/06), in partial fulfillment ofthe requirements for the award of the Degree of **DOCTOR OF PHILOSOPHY** in **Mechanical Engineering**, is an authentic record of the researcher scholar work conducted under my supervision. This is certified that this work has not been submitted to any other Institute or Universityfor the award of any other diploma or degree.

| | |
|---|---|
| Prof. B.B. Arora | Prof. S. Maji |
| (Department of Mechanical Engg. DTU) | (Department of Mechanical Engg. DTU) |

# ACKNOWLEDGEMENTS

I am deeply thankful to my supervisors, Prof. B.B. Arora and Prof. S. Maji, from the Department of Mechanical Engineering at Delhi Technological University, New Delhi, for granting me the opportunity to undertake this enriching research journey. Their guidance, wisdom, and encouragement have been invaluable throughout this Ph.D. endeavor.

Prof. Arora and Prof. Maji have not only provided expert advice and expertise but also inspired me with their profound knowledge and passion for the subject matter. Their perceptive insights, infectious enthusiasm, and unwavering support have significantly contributed to the success of this research project.

I extend my sincere gratitude to Dr. Akhilesh Arora, Dr. Rajiv Chaudhary, and Dr. Vipin, Professorsat Delhi Technological University, for their invaluable support, encouragement, and insightful suggestions.

I would like to express my gratitude to my doctoral research scholars Mr. Rashin Khera, Mr. Ashutosh Mishra, and Dr. Deepak Kumar (Mechanical Engineering Department), Delhi Technological University, New Delhi for their assistance and direction. I also want to express my gratitude to all the professors and staff who directly and indirectly assisted me in completing this project.

I will forever hold dear the love and blessings bestowed upon me by my beloved father, Mr. Satish Rao , and my mother, Mrs. Sunita Devi. Their unwavering support and guidance have been the cornerstone of my professional journey. I am deeply grateful for their tireless efforts in nurturing and shaping me into the person I am today.

I am also indebted to my wife, Mrs. Nalini, and my sister, Miss. Dheeraj, for their unwavering support and assistance whenever it was needed. Their encouragement, understanding, and willingnessto lend a helping hand have been invaluable throughout this journey. Their belief in me and their selfless contributions have played a significant role in the completion of this work. I am truly grateful for their presence in my life and their continuous support.

Lastly, I would like to express my gratitude to the Almighty, God, for granting me the strength, perseverance, and patience to see this work through to completion. It is through His blessings that I have been able to overcome challenges and achieve success in all aspects of this endeavor.

Neeraj Kumar

# ABSTRACT

Diesel engines are widely used in various applications, including automobiles (especially in trucks and buses), ships, locomotives, construction equipment, agricultural machinery, and generators. Diesel engines emit high concentrations of nitrogen oxide (NOx) particulate matter (PM) and hydrocarbons (HC) into the environment compared to other fuel engines. These pollutants contribute to smog formation, respiratory problems, and other health issues. PM emissions, in particular, are associated with lung cancer, asthma, and cardiovascular diseases. The combustion of diesel fuel also releases $CO_2$, a major contributor to global warming and climate instability. Diesel engines can have adverse effects on ecosystems and wildlife. Acid rain is caused by the emission of nitrogen oxides and sulfur dioxide ($SO_2$), which can harm aquatic life, vegetation, and soil quality.

To minimize the harmful effects of diesel engines, it is necessary to use eco-friendly fuels in the diesel engines either partially or completely replacing conventional fuels. CNG is recognized for its better combustion properties, high calorific value, and lower greenhouse gas emissions compared to diesel fuel. Implementing CNG in diesel engines through the dual fuel technique offers an improved option for the environment.

To examine the effects of CNG in dual fuel mode, an experiment with a diesel engine at different compression ratios, engine speeds, and injection pressures was conducted. The energy share of CNG is taken as 0-80% for this experiment. The present experiment evaluated the performance and emission characteristics of diesel/CNG dual-fuel engine.

The experimental results were also analysed by using Taguchi method.The experimental results demonstrated significant impacts on performance and emissions when CNG was added to diesel engines in dual-fuel combustion. Compared to single diesel fuel combustion, dual-fuel combustion led to increased brake thermal efficiency (BTE) of up to 43.6% and brake specific

fuel consumption (BSFC) of 32.46%. Carbon monoxide (CO) and hydrocarbon (HC) emissions were increased by 11.3% and 27.8% while carbon dioxide ($CO_2$), nitrogen oxide ($NO_X$), and smoke opacity were decreased by 13.8%, 15.1%, and 40.2 % in dual-fuel combustion.

# LIST OF CONTENTS

# LIST OF FIGURES

# LIST OF TABLES

# LIST OF ABBREVIATIONS

| | |
|---|---|
| A/F | air/fuel |
| AFR | air-fuel ratio |
| BDC | bottom dead centre |
| bTDC | before top dead centre |
| BTE | brake thermal efficiency |
| BSFC | brake specific fuel consumption |
| BP | brake power |
| CA | crank angle |
| CI | compression ignition |
| CNG | compressed natural gas |
| CO | carbon monoxide |
| $CO_2$ | carbon dioxide |
| CRDI | common rail direct injection |
| COPD | chronic obstructive pulmonary disease |
| CR | compression ratio |
| $CH_4$ | methane gas |
| CN | cetane number |
| DI | direct injection |
| D | diesel |
| DF | dual fuel |
| EPA | environmental Protection Agency |
| ECU | electronic control unit |
| EGR | exhaust gas recirculation |
| HC | hydrocarbon |
| HRR | heat release rate |
| IC | internal combustion |
| IT | injection timing |
| IP | injection pressure |
| kW | kilowatts |
| LPG | liquified petroleum gas |

| | |
|---|---|
| LNG | liquified natural gas |
| MN | methane number |
| ms | millisecond |
| mm | millimeter |
| NG | natural gas |
| $NO_X$ | nitrogen oxide |
| PM | particulate matter |
| ppm | parts per million |
| PPR | pulse per revolution |
| RON | research octane number |
| rpm | revolution per minute |
| SI | spark ignition |
| SNR | signal noise ratio |
| $SO_x$ | sulfur oxide |
| TDC | top dead centre |
| VCR | variable compression ratio |
| w.r.t. | with respect |

# CHAPTER 1. INTRODUCTION

The invention of the modern internal combustion engine (IC) in the last decade of the 19th century by Étienne Lenoir, Nikolaus Otto, and Rudolf Diesel has been a major contributor to the economic development of modern society. The IC engine is used in a variety of applications, such as power production, industrial uses, and the transportation of people and cargo over land and water, in part due to its high power-to-weight ratio. For IC engines, the 4-stroke cycle is the most usual operating mechanism. The rotation of the piston during its top and bottom positions in the cylinder is referred to as a stroke. Usually, the top position is referred to as the top dead centre (TDC), and the bottom as the bottom dead centre (BDC). Here is a simplified explanation of the 4-stroke direct injection (DI) diesel engine working concept. The cycle has been split into four different strokes. The piston shifted from TDC to BDC during the intake stroke as the intake valve was open and the air was drawn into the cylinder. When the intake valve is closed, the second stroke begins as the piston shifts from BDC to TDC, and air is compressed. As a result, the combustion chamber confronts an increase in pressure and temperature. After that, using a fuel injector, an appropriate quantity of liquid fuel is delivered to the combustion chamber near the TDC position. This fuel mass vaporizes, combines with the air around it, and then spontaneously ignites in the combustion chamber. This results in a rapid increase in temperature and pressure in the combustion chamber, and transmits mechanical energy to the piston, connecting rod, and crankshaft-based crank mechanism. During this expansion stroke, the piston shifts from TDC to BDC till the exhaust valve opens. At this point, the exhaust stroke begins, and the piston shifts from BDC to TDC with the exhaust valve open to release the cylinder's residual exhaust gases. Finally, the cycle is then completed by closing the exhaust valve, opening the intake valve, and repeating the process.

## 1.1 *Diesel engine emissions*

A diesel engine's emissions strongly depend on its equivalence ratio ($\Phi$) [1]. Nitrogen oxides (NOx), particulate matter (PM), carbon monoxide (CO), unburned hydrocarbons (HC), and carbon dioxide ($CO_2$) are typical exhaust pollutants from diesel engines. NOx emission is formed by the oxidation of atmospheric nitrogen and is highly influenced by cylinder combustion temperature. Total NOx emission in a CI engine is higher than in a lean burn spark-ignition (SI) engine because combustion occurs as a diffusion flame at an equivalence ratio ($\Phi$) close to 1.0. The stoichiometric air-fuel ratio achieves extremely high temperatures in this region, resulting in a high quantity of NOx. Diesel engines that run at a highly lean mixture with excess air help to decrease NOx emissions. The combustible gas in the lean mixture sustains to mix with the excess air, resulting in lower temperatures that decrease the NOx formation kinetics. Compared to CI engines, SI engines that run close to stoichiometric generate high NOx emissions. Nitrogen is dissociated at the maximum flame temperature, which occurs at the stoichiometric air-fuel ratio, and then it mixes with oxygen to produce NOx emission. Due to the non-homogeneity of the air-fuel mixture in lean mixture diesel engines, some local regions of the cylinder may become too lean to ignite, resulting in a misfire and poor combustion. Other regions could be too rich with oxygen-deficient for all the carbons to react together. High HC emission is produced in both lean and rich mixture conditions. Since CO emissions are generated if an engine operates at a rich mixture, its forming is not dependent on the intake mixture conditions. PM emissions in diesel engines originate primarily in the fuel-rich zone, where $\Phi$ superior to 1.0 inside the cylinder during combustion because of the incomplete combustion by fuel hydrocarbons [2]. $CO_2$ is produced during combustion when the carbon atom from the fuel is combined with the oxygen from the air.

### *1.2 The Effects of Exhaust Emission*

Figure 1.1 shows the global energy-related $CO_2$ emissions of various sectors from 2019-2022. The USA contributes 14.02 % of global $CO_2$ emissions, China (29.18%), the European Union (12%), India (7.09%), Russian Federation (4.65%) and Japan (3.7%) [3]. The majority of air pollution comes from road transport, with 95% of carbon dioxide emissions [4]. The consequences of greenhouse and other emissions are serious. These emissions harm air pollution, the health of people, and the environment in many ways. These air pollutants are closely related to COPD, coughing, breathing, wheezing, asthma, respiratory illnesses, and premature death [5]. Urban areas citizens are most affected by air pollution because diesel engine emissions degrade the air quality. Millions of people are exposed daily to toxic air pollution from IC engine-operated road transport. The air quality in Delhi is severely compromised due to the presence of harmful exhaust emissions, posing a significant threat to public health and well-being [6].

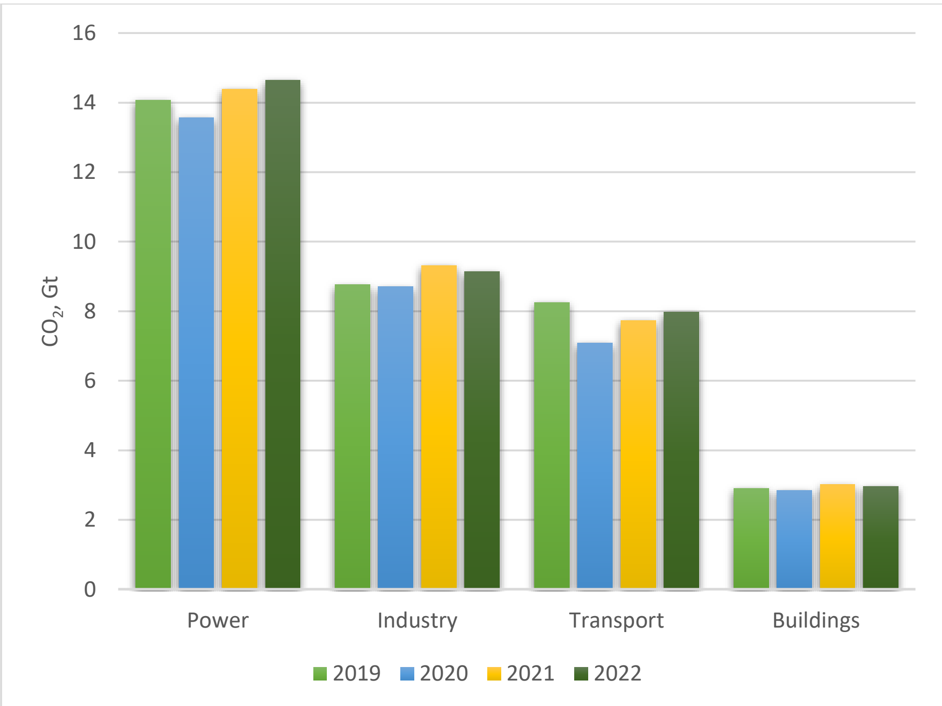


Fig. 1.1. global energy-related $CO_2$ emissions of various sectors

With the deteriorating Air Quality Index in Delhi from exhaust gas emissions, It is the most polluted city in India [7]. The health impacts of these harmful pollutants are serious in the short term and ongoing in the long term and periodic use. As a result, it is critical to manage the production of air pollution. One technique to reduce emissions is by engine design and management of engine parameters, but this frequently has unexpected consequences. The reduction of PM emissions in the diesel engine to an acceptable level cannot be achieved purely through engine design and control. Typically, an after-treatment system is needed to reduce emission levels under regulator standards. Emission restrictions are used to control and handle emissions from light-duty, heavy-duty, and stationary engines.

The Environmental Protection Agency (EPA) established some emission regulations for non-road and stationary diesel engines, which are listed in Table 1.1. Tier 4 mandates a reduction of more than 90% in NOx emissions. Tier 4 also demands significant reductions in HC and PM emissions. Since Tiers 2 and 3, CO emission restrictions have remained unchanged. According to the data below, standards have been substantially reduced over time. As a result, it is difficult for engine makers to constantly enhance engine efficiency and technology to meet standards.

Table 1.1: Emission standard for non-road and stationary diesel engines with more than 900 Kw of power

| Year Released | Tier 1 | Tier 2 | Tier 3 | Tier 4 |
|---|---|---|---|---|
| | 2004 | 2006 | 2011 | 2015 |
| NOx Limit (g/kWh) | 9.2 | 6.4 | 0.67 | 0.67 |
| HC Limit (g/kWh) | 1.3 | 6.4 | 0.4 | 0.19 |
| CO Limit (g/kWh) | 11.4 | 3.5 | 3.5 | 3.5 |
| PM Limit (g/kWh) | 0.54 | 0.2 | 0.1 | 0.03 |

Fuel costs are another source of concern for diesel engine manufacturers. Diesel fuel prices are normally high, and they rise as the global need for diesel fuel and other crude oil rises. As the cost of alternative fuels, especially natural gas, is significantly less expensive, using natural gas in diesel engine operations may result in fuel cost savings. Many researchers have offered different techniques to combine cleaner and less costly gaseous fuel with diesel fuel to reduce undesired emissions and expensive diesel fuel costs. Gaseous fuels are regarded as viable alternative fuels for transportation, and stationary engines, capable of decreasing pollutant emissions while also providing energy security [8]. Most combustion devices can be simply converted to use gaseous fuels for power generation. Natural gas and biogas, which have high octane numbers, have a knock resistance, making them acceptable for engines with relatively high compression ratios. If the proper conditions for mixing and combustion are met, gaseous fuels emit less harmful exhaust emissions [9].

### *1.3 Gaseous Fuels in Diesel Engines*

Numerous research works have been published regarding the utilization of gaseous fuels, including biogas, producer gas, natural gas, and liquefied petroleum gas (LPG), in diesel engines. The Different chemical compositions of these fuels have a considerable impact on engine performance and emissions.

Biogas is also referred to as swamp gas, sewer gas, fuel gas, marsh gas, and wet gas It is produced by using bacterial cells to ferment organic material in the absence of air. The process breaks the substance down into intermediates like fatty acids and alcohols, and then into methane, carbon dioxide, and water. The process is called anaerobic fermentation [10]. The primary components of biogas are methane and carbon dioxide ($CO_2$) [11]. Because of its high octane number and autoignition temperature, biogas is a good choice for diesel engines as an alternative fuel. When utilized as a primary fuel in diesel engines, it reduces NOx and PM emissions while increasing premixed combustion. However, because of the prolonged ignition delay and poor flame propagation of the gaseous fuel-air mixture, it has a severe impact on engine performance and HC and CO emissions, particularly at part load [12]. The existence of $CO_2$ in biogas affects the cylinder's burning velocity and peak pressure, resulting in a reduction in maximum power [13].

Producer gas in dual fuel mode shows a decrease in power output due to its lower heating value compared to natural gas [14]. Due to the lower energy density of producer gas, the engine output was lowered by 20–30% in one instance [15]. This fuel reduces CO emissions and engine efficiency because of its prolonged ignition delay [16].

LPG, typically known as Autogas, is a blend of propane and butane. When LPG is used in diesel engines, it generates significantly less PM and NOx and increases the also amount of HC emission [17]. LPG has a high octane and a low cetane number. Because of this property, it works well in SI engines but is challenging to self-ignite in traditional CI engines. If LPG is to be utilized as an alternative fuel to diesel fuel, the presence of a cetane enhancer can promote the auto-ignition characteristic and attain constant engine running [18][19]. LPG is used as a secondary fuel in diesel engines using a fumigation process in which the LPG fuel is introduced into the intake air stream via a low-pressure injector [20]. Due to its tendency to self-ignite earlier, using this strategy with diesel as a pilot fuel resulted in a lower power output and lower thermal efficiency than pure methane and natural gas. Out of all the fuels, the noise produced during combustion in the cylinder is the most prominent. Introducing LPG into diesel engines results in a decrease in NO and PM emissions, although there is a noticeable rise in CO and HC emissions [21].

One way to enhance the fuel performance is by blending LPG with hydrogen in a 70:30 ratio [22][23]. When LPG is used as a secondary fuel in diesel engines, this combination can cause fluctuations in HC emissions. It causes an increase in the maximum pressure rise rate, the HRR (heat release rate), the peak cylinder pressure, and the total time of the combustion.

In recent years, the replacement of diesel fuel with natural gas has been substantially increased. Because natural gas has a higher heating value than LPG, it produces more torque and has a higher thermal efficiency in DF engines [8]. It also contributes to reducing NOx emissions by lowering charge temperature [24][25]. Methane, the primary component of natural gas, has a high octane number, making it knock-resistant and suited for high-compression ratio engines. Natural gas is beneficial because it contains less harmful substances such as sulfur and mixed with diesel in dual fuel operation, tends to minimize PM levels than diesel engines [26] [27]. Generally, Natural gas comprises 85-99 % methane and some proportion of ethane and propane. Natural gas held at high pressure is known as compressed natural gas (CNG), and natural gas stored as a sub-cooled liquid is known as liquefied natural gas (LNG). If CNG or LNG is utilized in diesel engines, a pressure regulator is required to reduce the pressure to an acceptable level.

Natural gas is considered the most promising primary alternative fuel in dual-fuel operations [28]. It is abundant, reasonable in cost, and decreases NOx and PM emissions.

### *1.4 Natural Gas*

Methane is known as Natural gas. The percentage of methane is different in different pipelines. Methane is produced naturally through processes such as anaerobic decomposition of organic matter in wetlands, termites, and methane hydrates in ocean sediments. It was formed millions of years ago by dead animals and plants, which grew up in thick layers and became trapped beneath the earth's surface. Over time, excessive heat and pressure transformed these fossils into black oils, coals, and natural gases. Natural gas is taken from the underground formation via a well along with other liquid petroleum products and nonhydrocarbons, which are subsequently purified and distributed through pipelines. Domestic power generation in Canada, China, the Netherlands, Poland, Germany, and the United States has increased fast due to its technological advancements [29]. The advancement of horizontal drilling and hydraulic fracturing technology has increased natural gas exploration from shale reserves. Shale gas, which is natural gas trapped within shale formations, has become the fastest-growing natural gas supply in the United States. Since 1860, at least 2 million oil and shale gas wells have been hydraulically fractured in the United States. Today, hydraulically fractured wells account for 95% of new wells, accounting for more than 43% of total US crude oil generation and 67% of natural gas production [30].

Although natural gas-fumigated diesel engines may decrease NOx and PM emissions while CO and HC emissions were increased, particularly at part load than conventional diesel engines [31]. The ignition of natural gas-fumigated diesel engines is slower at part load but faster at full load. This method of decreasing diesel exhaust pollutants is becoming more popular.

### *1.5 Dual Fuel Operation*

Operating a dual fuel internal combustion (IC) engine involves using two different fuels simultaneously for power production. The most common combination is diesel as the primary fuel and gaseous fuel such as natural gas (CNG/LNG) or biogas as the secondary fuel. In comparison to normal diesel fuel, gaseous fuels frequently have a low cetane number and a high autoignition temperature. These characteristics of gaseous fuel make it challenging to employ in a traditional diesel engine alone. As a result, the diesel engine under dual fuel mode plays an active role in the effective utilization of gaseous fuels as alternate fuel with reduced exhaust emissions [32]. The dual fuel CI engines are based on diesel technology. The primary fuel is a gaseous fuel, while the pilot fuel is a liquid fossil fuel. A simple modification allowed the diesel engine to function in dual fuel mode.

Here's how the operation generally works:

1. Fuel Injection System

- Dual fuel IC engines are equipped with a specialized fuel injection system capable of injecting both primary and secondary fuels into the combustion chamber.
- The engine control unit (ECU) monitors various parameters to control the injection timing and quantity of each fuel for efficient combustion.

2. Compression Stroke:

- CNG is injected in the air stream during suction stroke.
- A mixture of CNG and air is compressed.
- Diesel is injected at 20$^{o}$ bTDC at a higher temperature mixture of CNG and air.
- Initially, diesel auto ignition, with a result rest of the mixture burns.

3. Combustion:

- Ignition of the air-fuel mixture is initiated by the compression ignition of the primary fuel (diesel).
- The combustion process propagates throughout the combustion chamber, with the secondary fuel contributing to the overall energy release.

4. Power Stroke:

- The combustion of the air-fuel mixture generates high-pressure gases that exert force on the piston, driving it downward.

- The downward motion of the piston produces mechanical work, which is transferred to the crankshaft to produce rotational motion.

**5.** Exhaust Stroke:

- The exhaust stroke expels the combustion products, including unburned hydrocarbons and combustion by-products, from the combustion chamber.

The engine's internal workings or the diesel injection system are not modified. Natural gas will replace some of the diesel fuel to run the engine [33]. Figure 1.2 depicts the fundamental workings of diesel/CNG dual-fuel engines.

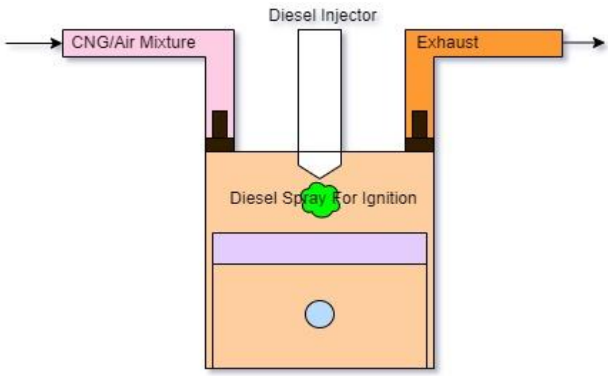


Fig. 1.2. Fundamental dual fuel operation

## *1.6 Dual Fuel Advantages and Applications*

The main advantages of the dual fuel natural gas-diesel engine are lower NOx, $CO_2$, and PM emissions, as well as lower fuel costs due to natural gas being significantly cheaper than diesel. Other potential benefits include increased thermal efficiency and lower fuel transport costs if natural gas is accessible nearby. If the majority of the engine parts stay constant, the maintenance costs will not increase after the conversion. Carbonization is reduced in the dual fuel engine because a substantial amount of diesel is supplanted by natural gas, up to 80%. As a result, the number of de-carbonization and overhauls required for the engine is reduced [34]. Transitions between diesel and dual fuel modes in the dual fuel natural gas-diesel engine can be accomplished while the engine is running without interfering with the required engine load. If natural gas is not available, the control valve is closed and the engine runs on diesel fuel as a traditional diesel engine. Various companies, like Solaris, Green Fuel Pro, Altronic, Hythane, and Landi Renzo USA, provide dual-fuel systems for engines.

### *1.7 Motivation*

Air pollution from IC engines caused an estimated 74,000 deaths in India in 2015. Out of which two-thirds (66%) could be attributed to tailpipe emissions from diesel engine vehicles on the road. Worldwide, emissions from all sources caused an estimated 33.70 lakh deaths. Out of which 3.85 lakh were attributable to IC engine transportation. Out of the transportation-attributable deaths, diesel vehicles on the road contributed an estimated 47% worldwide. Due to ongoing environmental conditions, an urgent need to find a solution to decrease the pollution level. To ensure long-term sustainability, it would be beneficial to reduce it even further, if possible.

The current study aims to reduce dependency on diesel fuel and minimize exhaust emissions by using alternative fuels.

### *1.8 Thesis outline*

The Ph.D. thesis is structured into six distinct chapters, each addressing specific aspects of the research. The organization of these chapters is as follows:

In **Chapter 1** of this thesis, an extensive introduction to internal combustion engines is provided, focusing particularly on Compression Ignition (CI) engine emissions and their effects on exhaust emissions. The utilization of gaseous fuel in CI engines is explored, along with an in-depth discussion on the concept of dual fuel operation, highlighting its advantages and diverse applications.

**Chapter 2** delves into an extensive review of existing literature concerning dual fuel operations using compressed natural gas (CNG) and diesel fuel. Numerous researchers' experimental works on engine performance, emissions, and various engine characteristics are thoroughly examined, shedding light on their impacts on engine performance and emission characteristics.

**Chapter 3** meticulously describes the detailed experimental setup, procedure, working principles, equipment utilized, and the methodology employed for data analysis in this research. This chapter provides comprehensive insights into the experimental framework adopted for conducting the study.

**Chapter 4** defines the system or phenomenon of the model. Identify the key variables, parameters, and governing equations that describe the behaviour of the system. Use fundamental principles, physical laws, empirical data, and assumptions to develop mathematical equations that represent the behavior of the system. Validate the mathematical model by comparing its predictions with experimental data or benchmark solutions.

**Chapter 5** unveils the findings derived from the experimental study. A meticulous comparison between diesel and dual-fuel engines at different compression ratios, engine speeds, and injection pressures is presented, offering detailed insights into their respective performances.

Finally, **Chapter 6** offers a conclusive discussion of the present study's findings and future perspectives for diesel/CNG dual-fuel CI engines. This section presents key conclusions drawn from the study and explores potential avenues for further research and development in this area.

# CHAPTER 2. LITERATURE REVIEW

This chapter provides an extensive review of the existing literature focusing on dual fuel operations utilizing both compressed natural gas (CNG) and diesel fuel. Numerous researchers have conducted experimental studies investigating various aspects such as engine performance, emissions, and engine characteristics. The chapter synthesizes these studies, highlighting their findings and their implications for engine performance and emission characteristics. Furthermore, it delves into the utilization of gaseous fuels in dual fuel operations, examining their effects on engine behavior and emissions. Additionally, the chapter explores the influence of key factors such as gas substitution ratio, injection timing, engine speed, injection pressure, and other engine-affecting parameters on both emissions and performance in DF engines. Through a comprehensive analysis of the literature, this chapter provides valuable insights into the complexities and nuances of DF operation and its impact on engine behavior.

## *2.1 Overview of diesel and CNG fuels*

Diesel and Compressed Natural Gas (CNG) are two types of fuels commonly used in transportation and industrial applications. Here's an overview of each:

### *2.1.1 Diesel Fuel:*

- Composition: Diesel fuel is a type of fuel derived from petroleum, specifically designed for diesel engines. It is composed of hydrocarbons, typically containing molecules with 12 to 20 carbon atoms.
- Energy Density: Diesel fuel has a higher energy density compared to gasoline, meaning it provides more energy per unit volume.

- Combustion: Diesel engines operate on the principle of compression ignition, where air is compressed to a high temperature, causing the diesel fuel injected into the combustion chamber to ignite spontaneously.
- Applications: Diesel fuel is commonly used in heavy-duty vehicles such as trucks, buses, and some cars, as well as in industrial equipment and generators.
- Emissions: While diesel engines are more fuel-efficient than gasoline engines, they often produce higher levels of nitrogen oxides (NOx) and particulate matter (PM), contributing to air pollution. However, advancements in diesel engine technology and the introduction of ultra-low sulphur diesel (ULSD) have helped reduce emissions significantly.

### *2.1.2 Compressed Natural Gas (CNG) :*

- Composition: CNG is a natural gas that has been compressed to a pressure of around 3,600 psi to 3,000 psi (250 bar to 200 bar) to become a more viable transportation fuel.
- Energy Density: CNG has a lower energy density compared to diesel fuel and gasoline but still provides a viable alternative due to its lower cost and cleaner emissions.
- Combustion: CNG is predominantly composed of methane and requires a dedicated CNG engine or conversion kit to operate. These engines use spark ignition and compression ignition engines.

- Applications: CNG is used primarily in light-duty and medium-duty vehicles, such as taxis, buses, and some cars. It is also used in industrial applications and as a fuel for heating and cooking in some households.

- Emissions: CNG combustion produces lower levels of pollutants compared to diesel and gasoline, including significantly reduced levels of particulate matter and nitrogen oxides. It also emits lower levels of greenhouse gases, making it a cleaner alternative fuel.

## *2.2 Historical perspective on dual fuel combustion*

Dual fuel combustion, also known as dual-fuel technology, has been utilized in various forms throughout history, evolving alongside advancements in combustion engines and fuel systems. This approach involves the simultaneous combustion of two different fuels within an engine, often with one acting as the primary fuel and the other as a supplementary or ignition enhancer. While modern applications often focus on internal combustion engines, the concept itself has historical roots dating back to the early days of engine development.

### *2.2.1 Early Experiments and Steam Engines :*

The concept of utilizing multiple fuels for combustion dates back to the early experiments with steam engines in the 18th and 19th centuries. Engineers and inventors experimented with various combinations of fuels, including coal, wood, and even oil, to improve engine efficiency and performance.

### *2.2.2 Gasoline and Diesel Blend*

In the early 20th century, as internal combustion engines became more prevalent, there were experiments with blending gasoline and diesel fuels to improve engine performance and efficiency. This approach was particularly relevant during times of fuel scarcity or economic constraints.

### 2.2.3 *World War II and Alternative Fuels :*

During World War II, several countries explored alternative fuel options due to shortages and logistical challenges. Dual-fuel systems were experimented with, including the use of natural gas, hydrogen, and various biofuels alongside traditional gasoline or diesel.

### 2.2.4 *Industrial and Marine Applications :*

In industrial and marine applications, dual-fuel engines have been used for decades to take advantage of multiple fuel sources, including natural gas, diesel, and heavy fuel oils. These engines are often designed to switch between fuels based on availability or cost, offering flexibility in operation.

### 2.2.5 *Modern Automotive and Transportation :*

In recent decades, dual-fuel technology has gained renewed interest, particularly in the automotive and transportation sectors. Natural gas-diesel dual-fuel engines, for example, have been developed for commercial vehicles to reduce emissions and dependence on conventional diesel fuel.

### 2.2.6 *Renewable Energy Integration :*

With a growing emphasis on renewable energy sources, dual-fuel combustion has also been explored in the context of integrating renewable fuels such as biofuels, hydrogen, and ethanol alongside conventional fossil fuels. This approach aims to reduce greenhouse gas emissions and promote sustainability in transportation and energy systems.

### 2.2.7 *Research and Development :*

Ongoing research and development efforts continue to explore the potential of dual-fuel combustion in various applications. Advanced engine designs, optimized fuel injection systems, and sophisticated control strategies are being developed to enhance the efficiency, performance, and environmental impact of dual-fuel engines.

## ***2.3 Engine Modification :***

Gaseous fuels are unable to be used alone in diesel engines due to their low cetane number. Experimentally, Naber et al. [35] observed that methane ignites with a local temperature of 1200 K and an ignition time of 2 ms. However, in a diesel engine, the temperature is approximately 1000 K at the end of the compression stroke [36]**.** Consequently, the gaseous fuels cannot ignite in the diesel engine within the needed time. Therefore, it is necessary to investigate alternative strategies for utilizing gaseous fuel in diesel engines. As per Liu et al. [37], the following method can be used to do this:

(a) Converting the CI engine to a SI engine with a higher compression ratio.

(b) Supplying the gaseous fuel with air by the CI engine's suction port while retaining the fuel injection system for pilot fuel.

(c) Directly provide gaseous fuel to the engine while retaining the fuel injection system for pilot fuel.

Another technique for dual fuel engines was ideal because the typical diesel engine required minimal alterations. Figure 2.1 illustrates the functioning of a DF engine. A dual-fuel diesel engine sucks and compresses the air/gaseous fuel mixture. The optimum quantity of pilot diesel fuel is provided by the diesel engine's fuel injection system to ignite the air-gas mixture [38]. The quantity available for pilot fuel depends on the engine characteristics and engine load conditions. A valve is used to reduce the gas supply under part load. However, the air intake to the engine decreases, which results in a decrease in engine power and efficiency. As a result, DF engines do not throttle on the air side. At varied loading conditions of the dual-fuel engine, the optimal ratio of pilot fuel and gaseous fuel supply is required [39].

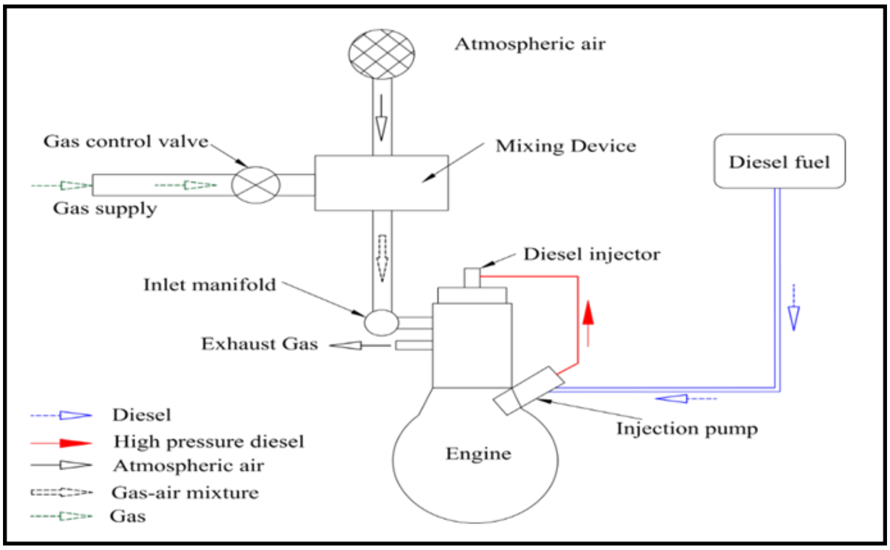


Fig.2.1. Schematic diagram of dual fuel engine

## *2.4 Previous research on diesel/CNG dual fuel combustion*

The dual fuel technique permits the use of gaseous fuel in a diesel engine. However, the performance limitations of a dual-fuel engine present many challenges that must be addressed. Changes in engine parameters such as injection pressure, injection timing, pilot fuel quantity, engine speed, compression ratio, engine load, and gaseous fuel substitution. All of these parameters affect the efficiency as well as emissions of the dual-fuel engine. Many studies have been performed by different scholars to investigate the effect of the factors mentioned above on the performance and emission characteristics of a dual-fuel engine. Several studies examined the effects of injection pressure using the various CNG substitution ratios of a diesel/CNG dual-fuel engine.

According to Kim et al. [40], the ignition performance of the primary fuel has a crucial influence on engine performance and pollution in dual fuel combustion. The experiment on a heavy single-cylinder engine revealed that fuel having a high cetane number improved combustion performance, lowered methane leaking, and reduced HC and CO emissions, but increased NOx emission.

Lee et al. [41] investigated the emission characteristics of non-methane hydrocarbons and methane on a six-cylinder heavy engine under low-load conditions. Due to the low combustion efficiency, methane accounted for the most share of the emissions (52-87%) in dual-fuel combustion. With the advanced injection timing, this problem can be resolved.

Millo et al. [42] examined the ignition mechanism of dual-fuel engines using comprehensive experimental investigation. A highly -precision ignition delay model was created using the precise chemical reaction mechanism of 0-D.

Increasing the amount of pilot fuel and advancing the injection timing may have a greater influence on engine output as well as CO and HC emissions but increased NOx emission[43].

It has been shown that advancing diesel injection timing at low load-low speed and medium load-high speed conditions reduces unburned methane and greenhouse gas emissions[44,45,46].

Wang et al. [47] studied the influence of pre-injection approach using a six-cylinder turbocharged intercooled NG/diesel dual-fuel heavy-duty engine under light-load conditions. The study shows that the pilot diesel ignition mode and quality are dependent on the pre-injection timing. When the injection timing is set to 42.5 crank angle (°CA), the effects are optimized (35% BTE, 0.4% HC emissions, and 60 ppm NOx).

Nithyanandan et al. [48] experimentally studied the effects of single and double injection on combustion and emissions using single-cylinder diesel engines via optical access. A high-speed color camera was utilized to discriminate between lean premixed methane combustion and diffusion combustion. The outcomes showed that pre-injection diesel improves flame propagation while lowering diesel fuel usage and soot emissions.

Papagiannakis et al. [49] investigated the influence of injection timing and substitution ratio on combustion and exhaust emissions in a single-cylinder engine operating at part load. It showed that when methane ($CH_4$) content increased, specific energy consumption, CO, and maximum pressure increased, whereas nitric monoxide (NO) and soot emission decreased. By advancing the injection timing specific energy consumption, soot, and CO emissions were decreased. But the peak pressure and NO increased dramatically.

Liu et al. [50] investigated the emission characteristics of a diesel/CNG dual-fuel engine varying the injection angle and amount of diesel fuel pilot dose. The findings of the studies revealed that the CO emission in the dual-fuel operation was significantly higher and the NOx emission was 30% lower on average than in a regular diesel engine. HC emissions are higher in dual-fuel combustion operations, particularly at low and medium loads.

Yang et al. [51] examined the influence of pilot injection timing on combustion performance and emission characteristics at low load conditions. The results revealed that advancing the pilot injection timing increased cylinder pressure and HRR while considerably reducing HC and CO emissions but increased NOx emissions.

Guerry et al. [52] examined the impact of pilot injection timing on the combustion performance and emissions of diesel/Methane DF engines using low-temperature combustion (LTC) under low and high loads. The examination shows that improving the injection time of diesel pilots increases the pressure in the cylinder and HRR, as well as reduces the HC and CO emissions. Further advancing the diesel injection timing, decreased combustion performance and raised the exhaust emission.

Shu et al. [53] examined the impact of injection timing on performance, and emissions on diesel/CNG dual fuel engines under low speed and load, and observed that promoting the pilot injection timing may improve cylinder pressure, thermal efficiency, and HRR whereas also increasing HC and NOx emissions.

Yuvenda et al. [54] experimented using a single cylinder engine on performance, combustion, and emissions characteristics of a diesel/CNG dual-fuel engine were examined by varying the pilot injection time from 11° to 19° BTDC within a 20-second interval. At pilot injection timing 17° BTDC under low load, the outcomes indicated the increment of 3.006% in thermal efficiency, 47.8 bar in-cylinder pressure, 52.05kl/$m^3$/°CA in HRR, and a reduction in HC, CO, and PM emissions.

Ouchikh et al. [55] experimentally investigate the effects of a diesel injection strategy on the performance and emissions of a methane/diesel dual fuel engine. The experiments were conducted on a single-cylinder diesel engine with 1500 rpm at various engine load conditions. The findings showed that the split injection approach had a substantial effect on dual-fuel engine combustion. Furthermore, when compared to the single injection approach at low load, the BTE increased by an average of 25.6%. With a pre-injection timing of 11°bTDC at 20% engine load, BSFC was reduced by 20.4%. Also, the pre-injection approach helped to reduce NOx and combustion noise while also lowering HC emissions significantly.

The combustion, performance, and emission characteristics of a CRDI diesel engine-assisted CNG dual fuel engine were studied. In this study, the engine was operated at a constant speed of 1500 rpm using variable engine loads of 16, 20, and 24 NM to evaluate the effect of fuel injection timings (7.5, 12.5, and 17.5 SOI) and fuel injection pressure (500, 750, and 1000 bar) in RCCI mode. At fuel injection pressure of 1000 bar, the BSFC of 0.42 kg/kWh was observed with a brake mean effective pressure of 3.2 bar and concluded that the most suitable input parameters are 20(Nm), 750(Bar), and 12.5% injection timing (BTDC) [56].

Dou et al. [57] evaluated the influence of the pilot diesel premixed ratio and injection timing on the engine's emissions. They observed that delayed injection timing is valuable for reducing particle emissions at higher premixed ratios.

Papagiannakis and Hountalas [58] examined the functions of dual fuel performance of a single-cylinder DI diesel engine when diesel is partially replaced by natural gas at ambient intake temperature. They investigated the effect of liquid fuel percentage replaced by natural gas on engine performance and emissions.

Karim et al. [59, 60] studied the $CH_4$ emissions on a single-cylinder diesel engine modified for operation on NG-diesel dual fuel combustion at low load. The effect of engine load, the amount of $CH_4$ fumigated into the intake mixture, and the amount of diesel fuel supplied in every cycle on $CH_4$ and CO emissions was experimentally determined.

Gatts et al. [61] experimentally studied the impact of engine load, and NG/air ratio on CO emissions of an NG/diesel dual-fuel engine. Natural gas addition at medium to high load first increased the CO emission but subsequently decreased CO emissions. Ultimately, NG-diesel dual combustion produced higher CO than single diesel fuel operation. CO emissions at low loads were considerably higher compared to medium and high loads and gradually increased with increasing NG supply.

Lyu et al. [62] investigated the influence of the CNG substitution ratio on combustible and emission properties for a CNG-Diesel DF engine. The analysis revealed that as increasing the CNG substitution ratio HC and CO emissions increased. NOx and smoke emissions show a trade-off tendency.

Gharehghani et al. [63] investigate the comparison between single diesel and dual fuel (Diesel/CNG) combustion and indicate that HC and CO emissions were increased in dual fuel combustion than in single diesel fuel combustion.

Bari et al. [64] experimentally investigate the performance and emission characteristics of a diesel engine fuelled with CNG and diesel in dual-fuel mode, with proportions of diesel ranging from 10 to 100% with different engine loads(1.1KW-2.8KW). The results indicate that BTE decreases and increases BSFC in DF mode compared to pure diesel fuel mode. At 1.1 KW load, a maximum decrease in efficiency and increased growth of 68% of specific fuel consumption were noted in dual-fuel combustion mode. The exhaust emission of $CO_2$ and soot was lower and increased CO in DF combustion.

Lounici et al. [65] experimented with investigating the effect of a dual fuel (Diesel-CNG) operating model to analyze the performance and emissions at moderate and relatively high loads. The results indicate a decrease in specific fuel consumption, NOx, and soot while increasing carbon CO and HC emissions.

Tripathi et al. [66] investigated the effect of diesel methane DF combustion on performance and emission-varying load conditions. The outcome reveals that the increased methane energy ratio decreased brake thermal efficiency, $CO_2$, and $NO_X$ while increasing CO and HC emissions at all tested loads.

Jamrozik et al. [67] studied the effect of CNG (0-95%) substitution on single-cylinder, 4-stroke diesel engines with a constant rotation speed of 1500 rpm. And results show that increasing the energy substitution ratio of CNG from 0% to 45% increases heat release rate and maximum combustion pressure, decreasing HC and NOx emission. As increased CNG substitution ratio beyond 45%-95% increases, the NOx emission, heat release rate, maximum combustion pressure, and CO emission decrease.

Lee et al. [68] experimentally determined the combustion and emission characteristics of diesel CNG dual-fuel engines with CNG substitution rates of CNG0%, CNG70%, and CNG80%, and results show that CNG80% recorded increased thermal efficiency by 2.7% and reduction in $CO_2$ emission by 22.6% than 100% diesel fuel.

Rai et al. [69] conducted an experimental study to determine the effect of injection timing on the performance and emission of a diesel/CNG dual-fuel operation. Experiments were carried out under various loading conditions to determine the effect of CNG flow rates and injection timings on BTE and emissions such as NOx, smoke opacity, and HC. The outcomes show that by advancing the IT significant reduction in NOx and smoke, but HC showed an increase. Though BTE first increased with advancing IT and then decreased.

Blasio et al. [70] experimentally performed the effects of compression ratio and injection parameters on performance and emission on a single-cylinder engine in dual-fuel combustion (diesel/methane). The results conclude that CR of 15.5 attained the best global efficiency and pollutant emissions outputs in DF combustion than D combustion.

Muammar et al. [71] performed an experiment and investigated the effect of dual fuel on emission and performance using CNG energy share of 90D10G, 80D20G, 70D30G, and 60D40G and compared it to 100% diesel fuel. The results show that CNG energy share of 90D10G, 80D20G, and 70D30G showed lower BSEC 60D40G showed higher BSEC compared to 100% diesel fuel and 90D10G and 60D40G showed higher $CO_2$ and $NO_X$ and 80D20G and 70D30G showed lower $CO_2$ and $NO_X$ than 100% diesel fuel.

Yuvenda, et al. [72] experimentally showed the performance and emission of diesel CNG dual fuel engines by optimizing the CNG injection timing. Results showed that CNG injection timing of 130oATDC and 110oCA, increased brake thermal efficiency and decreased brake specific fuel consumption, HC, CO, and PM.

Huang et al. [73] performed an experimental and simulation analysis of the impact of injection timing on diesel/CNG dual-fuel mode. Studies revealed that the amount of premixed combustion of injected diesel and the period of natural gas flame propagation showed a substantial effect on methane emissions.

Karabektas et al. [74] introduced a novel approach to enhancing diesel-CNG dual-fuel engine performance by modifying the composition of the pilot fuel dose with the addition of diethyl ether (DEE) to diesel fuel. Their study focused on three combustion scenarios: diesel alone, diesel with 40% CNG, and diesel with DEE and 40% CNG, using pilot doses of DEE at 5% and 10%. Their findings revealed that while co-combusting diesel with CNG led to decreased engine performance, particularly at low and medium loads, it also resulted in elevated CO and HC emissions across all loads and reduced NOx emissions at high loads. However, incorporating DEE as an additive to the pilot dose showed promising outcomes. It improved thermal efficiency, reduced specific energy consumption, and consequently lowered CO and NOx emissions.

Lebedevas et al. [75] focused on a CNG-diesel dual fuel engine and explored optimization techniques for CNG injection timing and duration at low load conditions. They varied the timing of CNG injection from 70° to 150° ATDC and the duration from 70° to 150°CA in 20° intervals. Their findings indicated that retarding the timing of CNG injection to 130°

ATDC resulted in the highest cylinder pressure and heat release rate (HRR). This timing configuration also led to lower emissions of hydrocarbons (HC), carbon monoxide (CO), and particulate matter (PM). Additionally, it allowed for a larger volume of CNG to be injected into the cylinder. Furthermore, the optimal CNG injection duration was identified as 110°CA. This combination of timing and duration demonstrated enhanced performance and reduced emissions in the CNG-diesel dual fuel engine operating under low load conditions.

In their experimental study, researchers investigated the use of compressed natural gas (CNG) as a substitute for diesel fuel in an indirect injection diesel engine across various operating conditions. The unique aspect of this research was the examination of different mass fractions of diesel fuel being replaced by CNG, while also considering the impact of cold exhaust gas recirculation on emissions and fuel consumption. The experiments were conducted under different equivalence ratios at engine speeds of 1200, 2000, and 3000 rpm, and at load levels of 25%, 50%, and 75% of full load for each speed setting. Replacing 40% of the diesel fuel with CNG resulted in a remarkable 74% reduction in soot emissions. This reduction was attributed to a decrease in the carbon-to-hydrogen ratio within the fuel mixture [76].

Under high load conditions, both diesel and methane-diesel dual fuel studies exhibited similar combustion pressure values, largely attributed to factors such as delayed injection timing, heightened injection pressure, and increased combustion temperature. Moreover, the coefficient of variation of indicated mean effective pressure (COVIMEP) for all tested fuels remained below 5% during medium and high load conditions. Notably, the primary concerns of diesel engines, namely NO and smoke emissions, witnessed significant reductions. With higher levels of methane addition in the dual fuel application, NO emissions showed an improvement of up to 67%, while smoke emissions saw an enhancement of up to 82%.

Despite elevated hydrocarbon (HC) and carbon monoxide (CO) emissions - common issues in dual fuel operations - the substantial decrease in NO emissions due to methane incorporation notably improved both environmental impact and economic viability. This underscores the practicality and efficacy of employing high levels of methane substitution to mitigate emissions in dual fuel operations. Furthermore, exhaust energy loss across all load conditions in the methane-diesel dual fuel mode demonstrated an average enhancement of 13.5% compared to the diesel-only mode [77].

Tripathi et al. [78] explored the impact of methane augmentation on combustion characteristics and unregulated emissions across varying engine loads in a dual fuel setup. Their findings revealed consistent trends across all load conditions: as methane augmentation increased, both the maximum cylinder pressure (Pmax) and heat release rate (HRR) decreased. They noted a prolonged ignition delay period and an expanded duration of the diffusion combustion stage. They also observed a tendency for unregulated emissions to diminish with the incorporation of methane into the fuel mixture.

Silvana et al. [79] observed that introducing methane in dual fuel operation led to a reduction in both Pmax (maximum pressure) and pressure rise rate. This decrease was attributed to the lower charge temperature associated with methane augmentation. Furthermore, they noted that the slower flame spread of methane resulted in a prolonged combustion process, shifting the peak pressure beyond the top dead center (TDC). Moreover, their study reported a decrease in particulate matter (PM) emissions when methane was added to diesel compared to conventional operation, highlighting the potential environmental benefits of this approach.

Gülcan and Ciniviz [80] investigated the effects of varying the methane energy fraction (from 0% to 50%) in a common rail direct injection (CRDI) engine with optimized diesel injection timing. Their findings revealed that as the methane energy fraction increased, combustion stability decreased compared to traditional diesel combustion. Moreover, they observed a notable increase in hydrocarbon (HC) and carbon monoxide (CO) emissions under these conditions, suggesting a trade-off between increased methane energy usage and combustion performance in terms of stability and emissions control.

Mattson et al. [81] investigated the impact of varying percentages of natural gas (%NG) on the combustion characteristics of a natural gas-diesel dual fuel engine across different engine load conditions. They observed that under low-to-medium engine load conditions, an increase in %NG resulted in a decrease in peak pressure and a delay in combustion phasing. However, they noted a shift in behavior at medium-to-high load conditions, where increasing %NG up to 60% advanced combustion phasing. Beyond this threshold, however, further increases in %NG led to a retardation in combustion phasing.

Their study also highlighted that at lower %NG levels (0–18%), combustion characteristics resembled those of traditional diesel combustion, with unchanged ignition delay and worsened unburned hydrocarbon (UHC) emissions across all load conditions. Interestingly, they found that a midrange natural gas substitution ratio (40–60%) improved engine thermal efficiency, particularly at medium-to-high load conditions.

Using the AVL BOOST model, performance, emissions, and combustion analyses were conducted by incorporating different blends of $CH_4$ (20%, 40%, 60%, and 80%) into diesel fuel. The study yielded enhancements in both effective power and effective efficiency as varying proportions of $CH_4$ were introduced into the engine. Upon scrutiny of emitted exhaust emissions, it was noted that NOx emissions experienced an increase, whereas CO emissions showed a decrease. These findings underscore the potential of blending $CH_4$ with diesel to improve engine performance while simultaneously managing exhaust emissions [82].

Meng et al. [83] observed that the potential for emission reduction in a diesel/compressed natural gas (CNG) dual-fuel engine was investigated by using blends of diesel and n-butanol as the pilot fuel. Experimental data indicated that the B20CNG70 blend (with a 70% CNG substitution rate) was particularly effective in reducing NOx emissions. Furthermore, the addition of n-butanol introduced a trade-off scenario between carbon monoxide (CO) and total hydrocarbon (THC) emissions. These findings suggest that utilizing blends of diesel and n-butanol as pilot fuels in dual-fuel engines could offer promising strategies for mitigating emissions.

Jung et al. [84], an innovative approach to mitigating emissions in a dual-fuel engine was explored. The researchers observed that as the proportion of natural gas (NG) energy increased, there was a reduction in both brake power and nitrogen oxide (NOx) emissions. This finding suggests that adjusting the energy proportion of NG could offer an effective method for decreasing emissions while potentially impacting engine performance.

Zhou et al. [85] examined the evolution of soot at various compressed natural gas (CNG) substitution ratios using the KIVA-3V R2 model integrated with a novel soot model. Their findings revealed a significant reduction in soot emissions as the CNG substitution ratio increased. Specifically, they observed that the soot mass for the CNG70 case was lower compared to the other scenarios. This reduction was attributed to a decrease in pyrene distribution, which subsequently led to a decreased generation of soot precursors. These results highlight the potential of CNG substitution in reducing soot emissions in dual-fuel engines.

Addy et al. [86] observed that nitrogen oxide (NOx), carbon dioxide ($CO_2$), and particulate matter (PM) emissions were lower in a dual-fuel diesel (DDF) engine compared to a traditional diesel engine.

The research affirmed commonly observed outcomes regarding notable reductions in smoke and carbon dioxide ($CO_2$) emissions, along with a substantial increase in total hydrocarbon emissions, primarily methane, when utilizing a gaseous fuel in Dual Fuel mode. The study highlighted a challenge related to high methane emissions at low loads, which restricts the achievable compressed natural gas (CNG) substitution ratio with diesel. Consequently, the implementation of the Dual Fuel (DF) concept remains crucial for automotive engines. Furthermore, the combustion analysis provided valuable insights into both the challenges and advantages associated with engine control technology management when adopting this innovative combustion concept. These findings underscore the importance of optimizing engine control strategies to effectively manage emissions and enhance performance in Dual Fuel engine configurations [87].

Choi and Lim [88] experimentally evaluate the effects of varying CNG mixing ratios on engine performance and emissions. The results indicated that the CNG/diesel dual-fuel engine delivered consistent and satisfactory torque and power outputs across different CNG mixing ratios. Notably, particulate matter (PM) emissions remained low across all CNG mixing ratios due to the minimal diesel pilot injection. Regarding nitrogen oxide (NOx) and hydrocarbon (HC) emissions, the study revealed that higher CNG mixing ratios resulted in lower NOx and HC emissions at low engine speeds. Conversely, at medium and high engine speeds, lower CNG mixing ratios were associated with reduced NOx and HC emissions. Therefore, optimizing engine performance and emissions control was achievable by effectively managing the CNG mixing ratio based on engine operating conditions.

Maji et al. [89] performed an experiment on a 7.35 kW four-stroke, twin-cylinder, direct injection (DI) diesel engine. This engine was operated in a dual fuel mode, where Compressed Natural Gas (CNG) replaced up to 75% of the diesel fuel. The results indicate that the substitution of CNG reduced the noise level, specific fuel consumption, and NOx, however, increased the unburned hydrocarbons.

### *2.5 Research Gaps in Existing Literature*

The comprehensive literature survey revealed a substantial amount of data on the utilization of CNG in the diesel engine. After analyzing the information presented in the literature review, several significant research gaps have been identified.

- Effects of Compression ratio and engine speeds on performance and emissions of diesel/CNG dual fuel combustion mode are little available.
- The study of soot emission is scantly available for dual fuel diesel/CNG engine combustion.
- The effects of the age of the engine on performance and exhaust emissions are missing.

### *2.6 Problem Statement and Research Objectives*

Compression ignition engine manufacturers and operators are concerned about rising fuel costs and increasingly strict emission standards. Lowering fuel costs and emissions can be achieved by changing the diesel engine to dual fuel operation and utilizing lower-cost natural gas. However, the cost savings from diesel substitution and reduced emissions must be evaluated. Thus, the primary goal of this research is to overcome the issues associated with dual fuel engines to increase efficiency and control exhaust emissions. Although dual-fuel engines emit more HC and CO than standards allow, strategies for controlling combustion and emissions should be developed. Additionally, in-cylinder combustion is quite complicated. While experimental data can approximate in-cylinder combustion, it cannot fully explain factors such as temperature field, air-fuel ratio distributions, and emission sites. As a result, detailed combustion analysis is one of the most essential fundamental variables in determining engine efficiency. Therefore, the following are the key problems of this study as well as hypotheses for the questions:

(a) Does dual fuel combustion save cost than diesel combustion?

*Hypothesis: Natural gas fuel prices have stayed significantly lower than diesel fuel prices over the last five years. When natural gas is injected into a diesel engine, it is expected to displace some of the diesel fuel in the CI engine, reducing the fuel cost in a dual-fuel engine.*

(b) Does dual-fuel combustion emit less NOx and PM than diesel engines?

*Hypothesis: As the lowest member of the paraffin family, diesel/CNG dual-fuel combustion is expected to generate less particulate matter. Furthermore, because premixed combustion occurs, the possibility of locally rich mixes forming is limited. As a result, during lean conditions, the flame temperature should be lower, lowering NOx produced in a dual-fuel combustion.*

(c) Does dual-fuel combustion produce excessive amounts of HC and CO?

*Hypothesis: The quantity of natural gas to air approaching the cylinder is not controlled. It is assumed that under these load levels, the natural gas air mixture in the cylinder is below the flammability limit, and the penetration of the diesel fuel jet does not reach across the cylinder. As a result, portions near the combustion chamber's border that contain natural gas and air mixtures that are less flammable are either unburned (HC emission) or partially burned (CO emission).*

Given the problem statement, the following are the research objectives:

- To develop an experimental setup of a dual fuel combustion.
- Investigating the impact of different compression ratios in dual fuel mode on engine performance and exhaust gas emissions, aiming to optimize these parameters through the utilization of diverse engineering analysis tools. Additionally, conducting a comparative analysis between dual fuel combustion and single diesel fuel combustion to discern their respective effects and efficiencies.
- Examining the influence of different engine speeds in dual fuel mode on both performance metrics and exhaust gas emissions, followed by a comprehensive analysis of the obtained data to assess the engine's operational characteristics and environmental impact.
- Investigate the impact of varying injection pressures across different engine speeds in both dual fuel and single diesel modes, and subsequently assess the resulting engine performance and exhaust gas emissions. Analyze the emission data obtained for both fuels and evaluate the feasibility of utilizing CNG as an alternative fuel option, considering its effects on engine performance and environmental pollution levels.

# CHAPTER 3. EXPERIMENT SETUP AND METHODOLOGY

This study aims to analyze the performance and emissions traits of an engine operating on both diesel fuel and a dual-fuel combination of compressed natural gas (CNG) and diesel. Initially, the research focuses on comparing the performance and emissions of engines running solely on diesel fuel with those using a dual-fuel configuration at various compression ratios and engine speeds. Furthermore, the study intends to explore the impact of different diesel injection pressures and varying diesel fuel volumes on the efficiency and emissions profile of dual-fuel engines. By investigating these factors, the research aims to provide insights into the optimal operational parameters for achieving improved engine efficiency and reduced emissions in dual-fuel engine configurations.

### *3.1 Experimental Set-up*

In this study a single cylinder ,water-cooled , 4-stroke variable compression ratio (VCR)was used to carry out the experiments. The engine specifications and the various devices fitted with the engine set up is given in table 3.1. To facilitate the investigation, this engine has been retrofitted with a dual fuel system. Figure 3.1 showcases a visual representation of the engine test setup, providing a clear image of the experimental configuration. Meanwhile, Figure 3.2 presents a schematic diagram illustrating the key components and layout of the test engine setup. These visuals aid in comprehending the experimental arrangement and highlight the integration of the dual fuel system into the Kirlosker diesel engine.

Table 3.1: Engine Specifications

| Parameters | Description |
|---|---|
| Engine | Make Kirloskar, Type 1 cylinder, 4 stroke, water-cooled, VCR |
| Dynamometer | Make Saj , Model AG10, Type Eddy current |
| Bore× stroke(mm) | 87.5×110 |
| Displacement (cc) | 661 |
| Rated power (kW) | 3.5 |
| Variable compression ratio range | 12:1 to 18:1 |
| Software | ICEngineSoft |
| EGR | SS, Water cooled |
| Piezo Sensor | Make PCB USA,Combustion: Range 350 Bar |
| Injector | Type Solenoid driven |
| ECU | Model Nira i7r (with solenoid injector driver) |
| Fuel Tank | Capacity 15 lit, Type: Duel compartment, with fuel metering pipe of glass |
| Temperature Sensor | Make Radix, Type RTD, PT100, and Thermocouple, Type K |
| Load Sensor | Make VPG Sensotronicst, type strain gauge, range 0-50 Kg |
| Fuel Flow Transmitter | Make Yokogawa, Model: EJA110-EMS-5A-92NN, range 0-500 mm $H_2O$ |

| | |
|---|---|
| Air Flow Transmitter | Make Wika, Model SL1, Range (-) 250 mm WC |
| Pump | Make Kirloskar, Type Monoblock |
| Overall dimension(mm) | W 2000 × D 2500 × H 1500 |

Fig.3.1. Engine setup

Equipped with essential units for calibrating both performance and emission characteristics, the test engine was further integrated with a water-cooled eddy current dynamometer to precisely measure engine load. Notably, the engine features a unique tilting cylinder block arrangement that enables the adjustment of compression ratio seamlessly, without the need to halt the engine or modify the combustion chamber's configuration. This innovative design allows for flexibility in optimizing engine performance across different operational conditions. Moreover, the engine incorporates advanced technology, such as Variable Compression Ratio (VCR), which facilitates programmable control over fuel injection time, injection angle, and ignition angle. This programmability, enabled by an open Engine

Control Unit (ECU), is based on factors like engine speed (rpm) and mass air pressure, contributing significantly to optimizing engine performance within its operational limits. Crucial parameters such as air temperature, coolant temperature, mass air pressure, and trigger sensor readings are seamlessly integrated into the Open ECU system. This integration enables precise control over fuel flow, fuel injectors, and the fuel pump, ensuring efficient engine operation. Furthermore, the experimental setup includes the necessary equipment for measuring combustion pressure and crank angle, providing comprehensive insights into engine performance and behavior during testing.

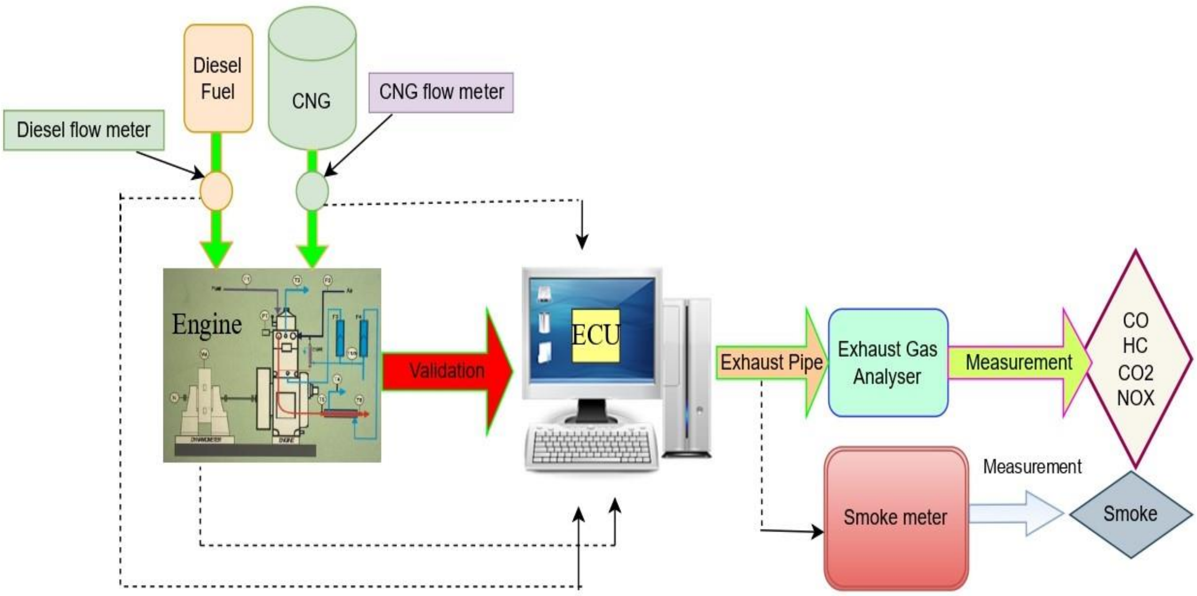


Fig.3.2. Schematic diagram of engine setup

Airflow measurements were conducted using a Wika airflow transmitter (Model SL1), while pressure readings were obtained using a piezoelectric sensor (PCB Model AX-409). Temperature measurements of both exhaust gases and intake air were captured using a K-type thermocouple manufactured by Radix. To control and manage the testing process, a Programmable Electronic Control Unit (ECU) of Model Nira i7r was employed. This ECU played a crucial role in regulating and coordinating various aspects of the experiment. Emissions from the exhaust were meticulously analyzed using an AVL Di Gas 444N gas analyzer, providing detailed insights into the composition of exhaust gases. Additionally, smoke opacity was quantified using an AVL 437 smoke meter, enabling precise measurement and characterization of smoke emissions. Overall, the combination of advanced engine features and precise control mechanisms ensures accurate assessment and optimization of engine performance and emissions characteristics throughout the experimental process.

### *3.2 Fuel used in experimentation*

In the present experiment, two distinct fuels were utilized: compressed natural gas (CNG) and diesel. While compressed natural gas is in a gaseous form, diesel is a liquid fuel. These two fuel types were selected to assess their respective impacts on engine performance and emissions in the experimental setup.

#### *3.2.1 Compressed Natural Gas (CNG)*

In the current experimental work, a single gaseous fuel, namely Compressed Natural Gas (CNG), was employed. CNG was introduced into the engine's intake manifold air stream suction port independently to facilitate dual fuel operation. This setup allowed for the systematic examination of CNG's effects on engine performance and emissions when used in conjunction with the primary fuel source. The CNG substitution ratio was calculated by equation (1).

$$\text{CNG, \%} = \frac{\dot{m}_{CNG} \times CV_{CNG}}{(\dot{m}_{CNG} \times CV_{CNG}) + (\dot{m}_{Diesel} \times CV_{Diesel})} \times 100 \tag{1}$$

$Where$ $\dot{m}_{CNG}$ and $\dot{m}_{Diesel}$ are the fuel mass flow rate of CNG and diesel fuel in Kg/s, and $CV_{CNG}$ and $CV_{Diesel}$ are the net calorific value of CNG and diesel fuel.

### *3.2.2 Diesel Fuel*

In this experiment, commercial diesel fuel sourced from a diesel tank was used. The diesel fuel was delivered to the engine via the injection pump. Volumetric measurements of fuel consumption were conducted using a graduated glass burette over one-minute intervals. These measurements were then converted to a gravimetric basis by determining the fuel density, which was subsequently recorded in the engine software. Initially, readings were taken during diesel operation using 100% diesel fuel. Subsequently, in the dual fuel tests, a combination of diesel and gaseous fuel CNG was used as the primary fuel source for dual fuel operation. The volume of pilot diesel fuel was controlled by adjusting the fuel cut-off valve.

The physicochemical properties of both diesel and CNG fuels are detailed in Table 3.2 for reference and comparison.

Table 3.2: Fuel Properties

| **Properties** | **Diesel** | **CNG** |
|---|---|---|
| CN | 52 | 0 |
| MN | 0 | 82 |
| RON | 20 | 130 |
| Density (kg/m$^3$) | 830 | 0.72 |
| Fuel calorific value (kJ/kg) | 42000 | 50000 |
| Stoichiometric A/F ratio | 14.5 | 17.05 |

## ***3.3 Injection Pressure Variation***

In this study, the injection pressure was adjusted by modifying the fuel injector opening pressure, as illustrated in Figure 3.3. The injector's opening pressure was altered by adjusting a screw located on the injector itself, and the desired pressure was monitored using a sensor positioned on the fuel line. Rotating the screw clockwise increased the injection opening pressure, while counterclockwise rotation decreased it. For this research, two distinct sets of injection pressure settings were employed: 500 and 600 bar.


Fig.3.3. Injection Pressure Variation

### *3.4 Experimentation instruments*

Through meticulous calibration, a variety of measuring instruments were integrated into the experimental setup to capture the diverse engine characteristics. The following section outlines the key instruments utilized in the experiment.

#### *3.4.1 Engine Performance Measurement*

An eddy current dynamometer was employed to apply load to the engine during testing. A computerized system was utilized to evaluate performance parameters across different compression ratio settings. These parameters include Brake Power (BP), Brake Specific Fuel Consumption (BSFC), Brake Thermal Efficiency (BTE), and fuel flow rate, which were accurately measured and analyzed.

#### *3.4.2 Air and gas flow measurement*

Air supply to the engine was measured using an orifice meter and a manometer, while an engine software system was utilized to calculate and record the air mass flow. The position of the compressed natural gas throttling valve was carefully noted during each dual-fuel test, with the upstream compressed natural gas pressure maintained at a constant level throughout the examination. For engine calibration purposes, an ELITE series Coriolis flow meter was installed. This flow meter boasts a high level of accuracy, with a mass flow accuracy of ±0.10% for liquids and ±0.25% for gases relative to the flow meter's rate. Figure 3.4 visually depicts the reading of the flow meter.

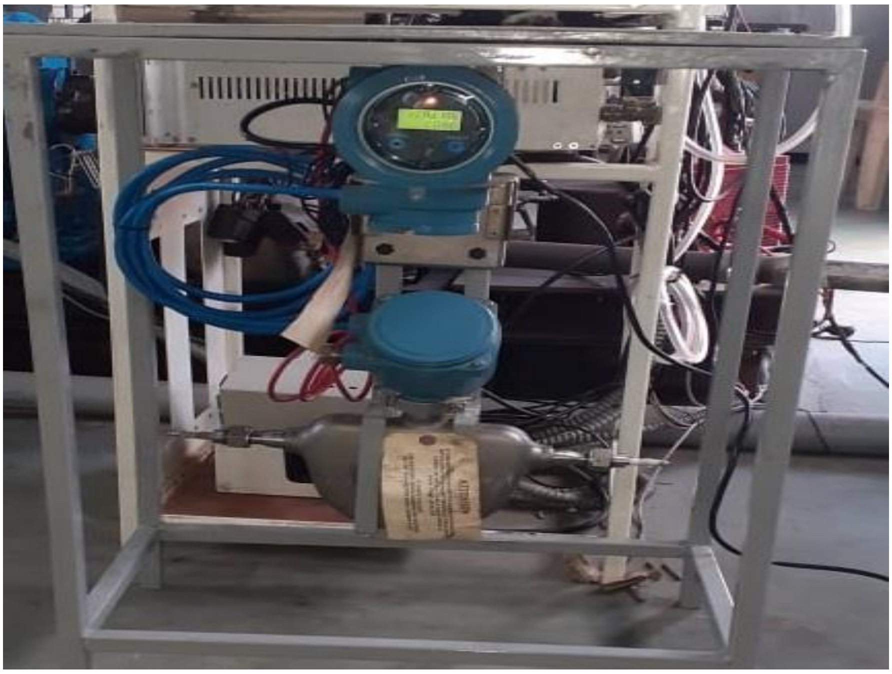

Fig.3.4. Mass flow meter reading

*3.4.3 Pressure – crank angle measurement*

A piezo sensor mounted on the engine block was utilized to measure the internal cylindrical pressure. The engine's crank motion was converted into a digital signal, which was then transmitted to a computer software system at intervals of two degrees. To calculate the crank angle, a PPR 360° encoder was employed. Figure 3.5 provides a visual representation of the PPR 360° encoder used in the experiment.

Figure 3.5. 360º degree encoder

*3.4.4 Temperature measurement*

RTD (Resistance Temperature Detector) and Type K thermocouples (specifically PT100) were strategically installed at various locations within the engine test setup to monitor temperatures. These included measuring the temperatures of the inlet and outlet cooling water from the engine, as well as those within the calorimeter. Additionally, measurements were taken for ambient temperature and the inlet temperature of the exhaust gas.

*3.4.5 Emission measurements*

The AVL Digas 444N five gas analyzers were employed to assess the composition of exhaust gases. In a controlled engine operating condition, a sample of exhaust gas was extracted from the engine's exhaust pipe and directed to the gas analyzer. This device provided clear and direct readings of CO, $CO_2$, NOx, and HC emissions. Additionally, the AVL 437 instrument was utilized to quantify the opacity of the exhaust gases. The setup of the exhaust gas analyzer and smoke meter is depicted in Figure 3.6. Further details regarding the specifications of the gas analyzer are presented in Table 3.3.

Table 3.3. Specification of exhaust gas analyzer

| Parameters | Measurement | Resolution |
|---|---|---|
| CO | 0-15% Vol. | 0.001% Vol. |
| HC | 0-20000 ppm Vol. | 1 ppm/10 ppm |
| $CO_2$ | 0-20% Vol. | 0.1% Vol. |
| NO | 0-5000 ppm Vol. | 1 ppm Vol. |
| $O_2$ | 0-25% Vol. | 0.01% Vol. |

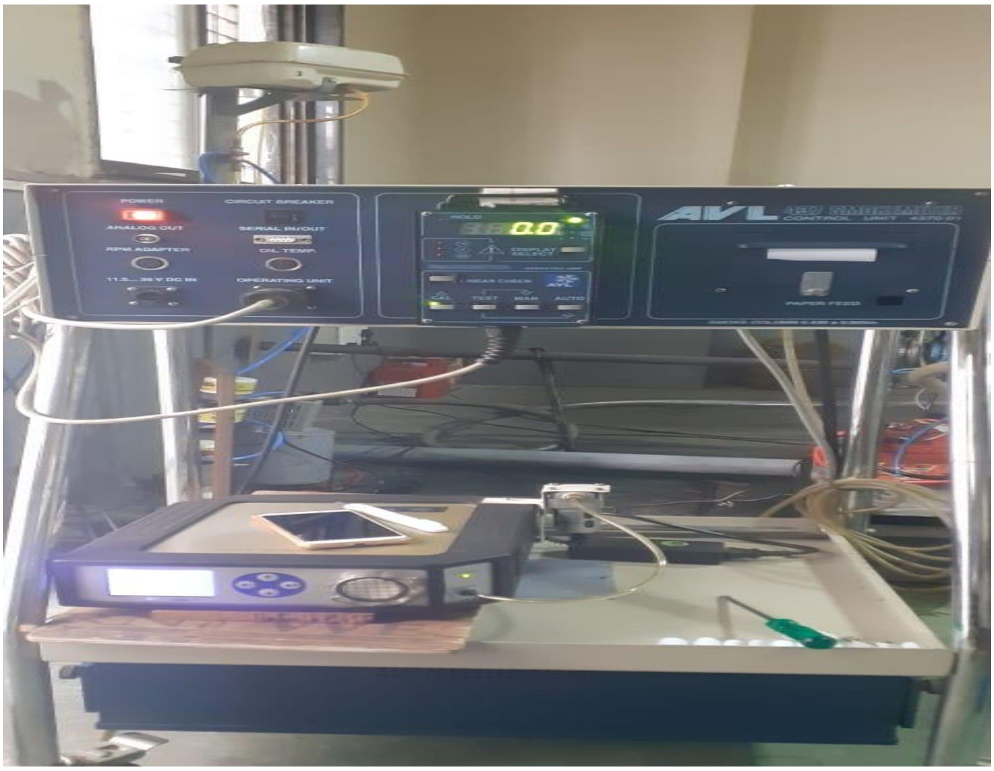


Fig.3.6. Exhaust gas analyzer and smoke meter

### *3.4.6 Engine Conversion Methodology*

Before introducing gaseous fuel, the compression ignition (CI) engine underwent modifications to enable dual fuel operation. In this setup, the flow of gaseous fuel was controlled by a valve positioned within the suction port. Experimental investigations on the dual-fuel engine, utilizing a combination of compressed natural gas (CNG) and diesel, were conducted across three distinct processes.

### *3.4.6.1 CNG/diesel dual fuel mode varying engine speeds*

The experiment was conducted with a compression ratio of 15, with engine speeds ranging from 1200 to 1500 rpm, all under a constant engine load of 10 kg. Initially, the engine operated at a compression ratio of 18 using D100 fuel (100% diesel, 0% CNG) in the first stage. Once the engine reached a state of thermal stabilization, the compression ratio was adjusted to 15 by tilting the cylinder head arrangements. Engine speeds were varied from 1200 to 1500 rpm during this stage. Engine performance data were captured using Enginesoft software, while exhaust emissions and smoke opacity were monitored using the AVL Digas 444N gas analyzer and AVL 437 smoke meter. In the second stage of the experiment, both diesel and CNG were used for dual fuel combustion.

For effective dual fuel combustion, a homogeneous air-gas mixture was crucial. This mixture was achieved by a dedicated air-gas mixing device, which supplied a consistent air-gas blend to the intake manifold. CNG was introduced into the intake manifold's air stream, while diesel injection occurred after compressing the CNG-air mixture. The experiment aimed to evaluate the impact of varying CNG energy shares, specifically at CNG40% (40% CNG, 60% diesel), CNG50% (50% CNG, 50% diesel), CNG60% (60% CNG, 40% diesel), CNG70% (70% CNG, 30% diesel) and CNG80% (80% CNG, 20% diesel). These ratios were adjusted using the CNG supply valve. Table 3.4 provides a detailed breakdown of the experiment model concerning engine speed.

Table 3.4: Experiment model w.r.t. engine speeds (Diesel-A, CNG-B)

| Engine speed (rpm) | Fuel used |
|---|---|
| 1200 | A |
| 1200 | A and B |
| 1250 | A |
| 1250 | A and B |
| 1300 | A |
| 1300 | A and B |
| 1350 | A |
| 1350 | A and B |
| 1400 | A |
| 1400 | A and B |
| 1450 | A |
| 1450 | A and B |
| 1500 | A |
| 1500 | A and B |

### *3.4.6.2 CNG/diesel dual fuel mode varying compression ratio*

In the initial phase of the experiment, the engine was set at a compression ratio (CR) of 18:1, and it commenced operation using 100% diesel (D100) fuel. Subsequently, the compression ratio was systematically adjusted from 13:1 to 15:1 in increments of 0.5:1. This adjustment was achieved by tilting the cylinder head arrangements after the engine reached a state of thermal stabilization. Throughout this phase, the engine was maintained at a constant speed of 1500 rpm and a load of 10 kg. During these tests, exhaust gas emissions and smoke were monitored using the AVL Digas 444N gas analyzer and AVL 437 smoke meter, respectively.

Moving to the second phase of the experiment, dual-fuel (DF) combustion was employed. This involved the utilization of both diesel and compressed natural gas (CNG). CNG was introduced into the intake manifold's air stream, while diesel injection occurred after the compression of the CNG-air mixture. The substitution ratios of CNG were varied, specifically CNG40%, CNG50%, CNG60%, CNG70%, and CNG80%, by adjusting the supply valve for CNG. Table 3.5 provides a comprehensive breakdown of the experiment model with respect to compression ratio.

Table 3.5: Experiment model w.r.t. compression ratio and fuel used (Diesel-A, CNG-B)

| **CR** | **Fuel used** |
|---|---|
| 13 | A |
| 13 | A and B |
| 13.5 | A |
| 13.5 | A and B |
| 14 | A |
| 14 | A and B |
| 14.5 | A |
| 14.5 | A and B |
| 15 | A |
| 15 | A and B |

*3.4.6.3 CNG/diesel dual fuel mode varying injection pressure*

The experimental test was conducted at a compression ratio (CR) of 15, with engine speeds ranging from 1200 to 1500 rpm, all under a constant engine load of 10 kg. Additionally, the injection pressure was varied between 500 and 600 bar.

Initially, the engine operated at a higher compression ratio of 18:1 using D100 fuel in the first stage. Once the engine reached a state of thermal stabilization, the compression ratio was adjusted to 15:1 by tilting the cylinder head arrangements. Throughout this phase, engine speeds varied between 1200 rpm and 1500 rpm.

Data regarding engine performance were collected using Enginesoft software, while exhaust emissions and smoke opacity were monitored using the AVL Di Gas 444N gas analyzer and AVL 437 smoke meter.

In the second stage of the experiment, dual fuel combustion was employed, utilizing diesel and compressed natural gas (CNG). Ensuring a consistent air-gas mixture for ignition was crucial in this method. This mixture was achieved through an air-gas mixing device, which supplied a homogeneous blend to the intake manifold. CNG was introduced into the intake manifold's air stream, with diesel injection occurring after the compression of the CNG-air mixture. The energy share of CNG was adjusted to CNG40%, CNG50%, CNG60%, CNG70%, and CNG80% by manipulating the CNG supply valve. Table 3.6 provides a detailed overview of the experiment model with respect to injection pressure.

Table 3.6 Experiment model w.r.t. injection pressure (Diesel-A, CNG-B)

| Engine speed (rpm) | Injection pressure (bar) | Fuel used |
|---|---|---|
| 1200 | 500 | A |
| 1200 | 500 | A and B |
| 1200 | 600 | A |
| 1200 | 600 | A and B |
| 1300 | 500 | A |
| 1300 | 500 | A and B |

| | | |
|---|---|---|
| 1300 | 600 | A |
| 1300 | 600 | A and B |
| 1400 | 500 | A |
| 1400 | 500 | A and B |
| 1400 | 600 | A |
| 1400 | 600 | A and B |
| 1500 | 500 | A |
| 1500 | 500 | A and B |
| 1500 | 600 | A |
| 1500 | 600 | A and B |

### *3.5 Experiment repeatability*

The performance and emission parameters were assessed three times under both single diesel and diesel/CNG dual fuel modes, adhering to the experimental setup. For each operating parameter, the average value was computed from these multiple assessments. These average readings were then utilized for the subsequent analysis.

### *3.6 Analysis procedure*

The calculation of various performance variables for both single diesel and diesel/CNG dual fuel modes involved employing a series of formulas and equations outlined in Annexure A. These equations were utilized to derive dependent variables, which were then compared and analyzed to discern any differences or patterns between the two operational modes.

### *3.7 Uncertainty in measurements*

In Table 3.7, the uncertainties associated with the experimental setup are outlined, covering parameters like speed, manometer readings, temperature, pressure, crank angle encoder measurements, as well as uncertainties related to brake power and specific fuel consumption. For a comprehensive understanding of these uncertainties and their calculations, detailed explanations can be found in Annexure B [90].

Table 3.7 Uncertainty errors for performance

| Performance Parameters | Diesel mode error (%) | Dual fuel mode error (%) |
|---|---|---|
| BP | 0.6 | 0.6 |
| BTE | 1.4 | 2.8 |
| Air fuel ratio | 1 | 2.1 |
| Air flow rate | 0.6 | 0.6 |
| Volumetric efficiency | 0.5 | 0.5 |
| Net heat release rate | 1.8 | 1.8 |
| Liquid fuel substitution | - | 1.2 |

# CHAPTER 4. MATHEMATICAL MODEL & VALIDATION

Modelling involves creating a simplified representation of a real-world system or process using mathematical equations, computational algorithms, or physical prototypes. Validation is the process of assessing the accuracy and reliability of a model by comparing its predictions or outputs with experimental data or observations from the real-world system.

Taguchi's method is employed to optimize the performance of engine parameters such as brake thermal efficiency (BTE), brake specific fuel consumption (BSFC), and emissions of CO, HC, $CO_2$, NOx, and smoke when utilizing various energy shares of CNG and diesel varying compression ratio and engine speed for the present study.

## 4.1 Taguchi Method

The Taguchi method, developed by Dr. Genichi Taguchi, is a statistical approach to quality improvement in manufacturing processes. It emphasizes robust design and optimization of products or processes to minimize variability and improve performance while considering factors such as cost and time. The method involves three main stages shown in Figure 4.1.

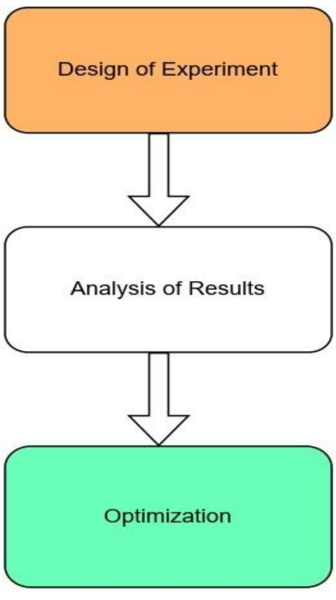


Fig. 4.1. Taguchi method Stages

### 4.1.1 Design of Experiments (DOE):

Design of experiments (DOE) is a structured approach used in engineering to tackle complex problems efficiently. It incorporates a range of principles and techniques to ensure that results are robust, reliable, and backed by solid evidence. Key principles include randomization, replication, blocking, orthogonality, and factorial experimentation.

DOE involves systematically varying independent variables, often based on hypothesized changes, to analyze their impact on the outcome. The primary objective is to achieve optimal results using the least amount of data. However, implementing DOE typically demands significant effort and time.

In engineering, processes are influenced by various factors, and the performance and emissions of a diesel engine are no exception. Design parameters such as engine size, combustion type, injection pressure, and compression ratio play crucial roles. Additionally, operational parameters like load, air pressure, speed, and air-fuel ratio significantly affect engine performance [91].

### 4.1.2 Taguchi Analysis :

When dealing with systems that involve a large number of operating parameters, traditional experimental procedures can be costly and time-consuming. The need to conduct numerous trials to explore all possible parameter combinations adds to the complexity and resource requirements. In such scenarios, employing mathematical models becomes a more efficient and time-saving approach [92].

Taguchi methodology emerges as a valuable tool in this context, facilitating the optimization of results while minimizing the number of trials needed. By leveraging mathematical models and Taguchi's principles, engineers can streamline the experimental process, leading to quicker and more effective decision-making.

In this approach, known as the Taguchi method, the focus is not just on ensuring that the output, represented by Y, remains within specified limits but also on keeping it consistently centred around a target value. This is crucial because according to Taguchi, any deviation from the target value results in a loss, even if the output remains within acceptable specifications. The larger the deviation, the greater the loss incurred.

Furthermore, in the Taguchi method, not only are the conventional factors studied through the Design of Experiments (DOE) modelled, but noise factors are also taken into account. This comprehensive modelling of both primary and noise factors helps in developing a robust model with reduced variation in the response. This approach aims to create a sustainable model that produces more consistent results, ultimately leading to improved quality and efficiency in the process.

Taguchi utilizes orthogonal arrays as part of his methodology, and the effectiveness of these arrays is closely tied to the concept of degrees of freedom. The calculation of degrees of freedom is typically represented by equation 2.

$$DOF = 1 + \sum_{i=1}^{NV}(Li - 1) \qquad (2)$$

Where NV= Number of independent variable , Li = Level , DOF = Degree of Freedom

Rather than changing one factor at a time, the Taguchi method involves simultaneously varying all factors according to a pre-designed array, while observing the corresponding response values. Table 4.0 provides an overview of the layout for 16 experiments conducted in this manner. Meanwhile, Table 4.0 (a) outlines the input parameters along with their respective levels.

The signal-to-noise (SN) ratio, as defined in the Taguchi method, incorporates both the desired output and its variation. It represents the logarithmic relationship between the energy utilized for the intended function and the energy wasted during the process. In essence, it quantifies the efficiency of a system by considering how much useful energy is produced relative to the energy lost or wasted [93].

**Table 4.0 :** $L_{16}$ Orthogonal array test layout

| **S.No.** | **CR** | **CNG (%)** | **RPM** |
|---|---|---|---|
| 1 | 13 | 0 | 1300 |
| 2 | 13 | 40 | 1400 |
| 3 | 13 | 60 | 1500 |
| 4 | 13 | 80 | 1600 |
| 5 | 14 | 0 | 1400 |
| 6 | 14 | 40 | 1500 |
| 7 | 14 | 60 | 1600 |
| 8 | 14 | 80 | 1300 |
| 9 | 15 | 0 | 1400 |
| 10 | 15 | 40 | 1500 |
| 11 | 15 | 60 | 1600 |
| 12 | 15 | 80 | 1500 |
| 13 | 16 | 0 | 1600 |
| 14 | 16 | 40 | 1300 |
| 15 | 16 | 60 | 1400 |
| 16 | 16 | 80 | 1500 |

**Table 4.0 (a):** Factors and their levels

| **Input Parameters** | **Level 1** | **Level 2** | **Level 3** | **Level 4** |
|---|---|---|---|---|
| CR | 13 | 14 | 15 | 16 |
| CNG (%) | 0 | 40 | 60 | 80 |
| RPM | 1300 | 1400 | 1500 | 1600 |

### 4.1.3 Optimization:

Based on the analysis, the optimal levels of the factors are determined to achieve the desired performance or quality characteristics. The goal is to identify the robust parameter settings that minimize the variability of the responses and are less sensitive to noise factors. In the Taguchi method, three scenarios are typically considered when optimizing a process: Larger the Better (LTB) for maximizing desirable outcomes, Smaller the Better (STB) for minimizing undesirable outcomes, and Nominal-the-Better (NTB) for selecting the best characteristic or target value.

In LTB situations, the goal is to maximize the desired output, such as improving performance or efficiency. Conversely, in STB scenarios, the aim is to minimize undesired outcomes, such as reducing defects or emissions.

For NTB cases, the objective is to choose the optimal characteristic or target value, which is often the median between specified upper and lower acceptable limits. This allows for a balanced approach where the chosen value is neither too high nor too low but rather falls within an acceptable range that meets the desired criteria explained in equations 3,4, and 5.

$$S/N\ (LTB) = -10\ [\ \log\ (\sum(1/y^2)/n)] \tag{3}$$

$$S/N\ (STB) = -10\ [\log\ (\sum\ (y^2/n))] \tag{4}$$

$$S/N\ (NTB) = -10\ [\log\ (\sum\ (s^2))] \tag{5}$$

Where Y = responses for the given factor level combination

n = number of responses in the factor level combination

s = standard deviation of the responses for all noise factors for the given factor level combination

*LTB criteria*: This means that for certain factors, such as BTE, you want to maximize their values. In other words, higher values of BTE are considered better.

*STB criteria*: Conversely, for factors like BSFC, CO, HC, $CO_2$, $NO_X$, and smoke, you want to minimize their values. Lower values of these factors are considered better in terms of environmental impact or efficiency.  The present study employs Minitab software for data modelling and validation.

## 4.2 Analysis of SN Ratios and Means for BTE

SN ratio plots for all seven response variables have been generated, showcasing the variation in signal-to-noise ratio across different parameter settings. Among these plots, the optimal value is determined as the parameter configuration corresponding to the highest mean SN ratio value.

This approach entails pinpointing the critical factors that influence the performance of the system and identifying the most effective values to attain the desired results. The investigation involved examining the Signal to Noise ratio (SNR) and the means of diesel CNG dual fuel combustion with respect to BTE through a linear model analysis. The findings of this analysis are outlined in Table 4.1 and Table 4.2, respectively. By analyzing the SN ratios with factors such as CNG (%), Compression ratio, and engine speed, the aim is to ascertain the optimal combination of these variables that maximizes the signal-to-noise ratio. This ratio serves as a representation of the desired outcome or the quality of the dual fuel combustion.

Table 4.1: Linear Model Analysis for BTE: SN ratios versus CNG (%), CR, RPM

**Estimated Model Coefficients for SN ratios**

| Term | Coef | SE Coef | T | P |
|---|---|---|---|---|
| Constant | 27.5890 | 0.1118 | 246.712 | 0.000 |
| CNG (%) 0 | -0.4543 | 0.1937 | -2.346 | 0.057 |
| CNG (%) 40 | -0.1057 | 0.1937 | -0.546 | 0.605 |
| CNG (%) 60 | -0.0517 | 0.1937 | -0.267 | 0.798 |
| CR 13 | -5.4154 | 0.1937 | -27.959 | 0.000 |
| CR 14 | 3.0088 | 0.1937 | 15.534 | 0.000 |
| CR 15 | 1.7243 | 0.1937 | 8.902 | 0.000 |
| RPM 1300 | 0.4250 | 0.1937 | 2.194 | 0.071 |
| RPM 1400 | 0.0190 | 0.1937 | 0.098 | 0.925 |
| RPM 1500 | -0.1872 | 0.1937 | -0.966 | 0.371 |

**Analysis of Variance for SN ratios**

| Source | DF | Seq SS | Adj SS | Adj MS | F | P |
|---|---|---|---|---|---|---|
| CNG (%) | 3 | 2.378 | 2.378 | 0.7928 | 3.96 | 0.071 |
| CR | 3 | 167.271 | 167.271 | 55.7572 | 278.67 | 0.000 |
| RPM | 3 | 1.128 | 1.128 | 0.3760 | 1.88 | 0.234 |
| Residual Error | 6 | 1.200 | 1.200 | 0.2001 | | |
| Total | 15 | 171.978 | | | | |

**Model Summary**

| S | R-Sq | R-Sq(adj) |
|---|---|---|
| 0.4473 | 99.30% | 98.25% |

**Response Table for Signal to Noise Ratios (Larger is Better)**

| Level | CNG (%) | CR | RPM |
|---|---|---|---|
| 1 | 27.13 | 22.17 | 28.01 |
| 2 | 27.48 | 30.60 | 27.61 |
| 3 | 27.54 | 29.31 | 27.40 |
| 4 | 28.20 | 28.27 | 27.33 |
| Delta | 1.07 | 8.42 | 0.68 |
| Rank | 2 | 1 | 3 |

Likewise, the linear model analysis of means concerning factors such as CNG (%), CR, and RPM concentrates on determining the average values of the response variable.

Table 4.2: Linear Model Analysis for BTE: Means versus CNG (%), CR, RPM

**Estimated Model Coefficients for Means**

| Term | Coef | SE Coef | T | P |
|---|---|---|---|---|
| Constant | 25.5169 | 0.3298 | 77.367 | 0.000 |
| CNG (%) 0 | -1.7044 | 0.5713 | -2.984 | 0.025 |
| CNG (%) 40 | -0.4044 | 0.5713 | -0.708 | 0.506 |
| CNG (%) 60 | -0.0494 | 0.5713 | -0.086 | 0.934 |
| CR 13 | -12.6669 | 0.5713 | -22.174 | 0.000 |
| CR 14 | 8.4006 | 0.5713 | 14.705 | 0.000 |
| CR 15 | 3.7581 | 0.5713 | 6.579 | 0.001 |
| RPM 1300 | 1.1206 | 0.5713 | 1.962 | 0.097 |
| RPM 1400 | -0.0294 | 0.5713 | -0.051 | 0.961 |
| RPM 1500 | -0.3919 | 0.5713 | -0.686 | 0.518 |

**Analysis of Variance for Means**

| Source | DF | Seq SS | Adj SS | Adj MS | F | P |
|---|---|---|---|---|---|---|
| CNG (%) | 3 | 30.91 | 30.913 | 10.304 | 5.92 | 0.032 |
| CR | 3 | 981.61 | 981.608 | 327.203 | 188.00 | 0.000 |
| RPM | 3 | 7.60 | 7.597 | 2.532 | 1.46 | 0.318 |
| Residual Error | 6 | 10.44 | 10.443 | 1.740 | | |
| Total | 15 | 1030.56 | | | | |

**Model Summary**

| S | R-Sq | R-Sq(adj) |
|---|---|---|
| 1.3193 | 98.99% | 97.47% |

**Response Table for Means**

| Level | CNG (%) | CR | RPM |
|---|---|---|---|
| 1 | 23.81 | 12.85 | 26.64 |
| 2 | 25.11 | 33.92 | 25.49 |
| 3 | 25.47 | 29.27 | 25.13 |
| 4 | 27.68 | 26.02 | 24.82 |
| Delta | 3.86 | 21.07 | 1.82 |
| Rank | 2 | 1 | 3 |

The tables reveal that the optimal values for the three inputs, specifically CR, were statistically significant. Additionally, the coefficient of determination ($R^2$), which indicates the goodness of fit of the model, was determined to be 99.30% for the SN ratio analysis and 98.99% for the means analysis.

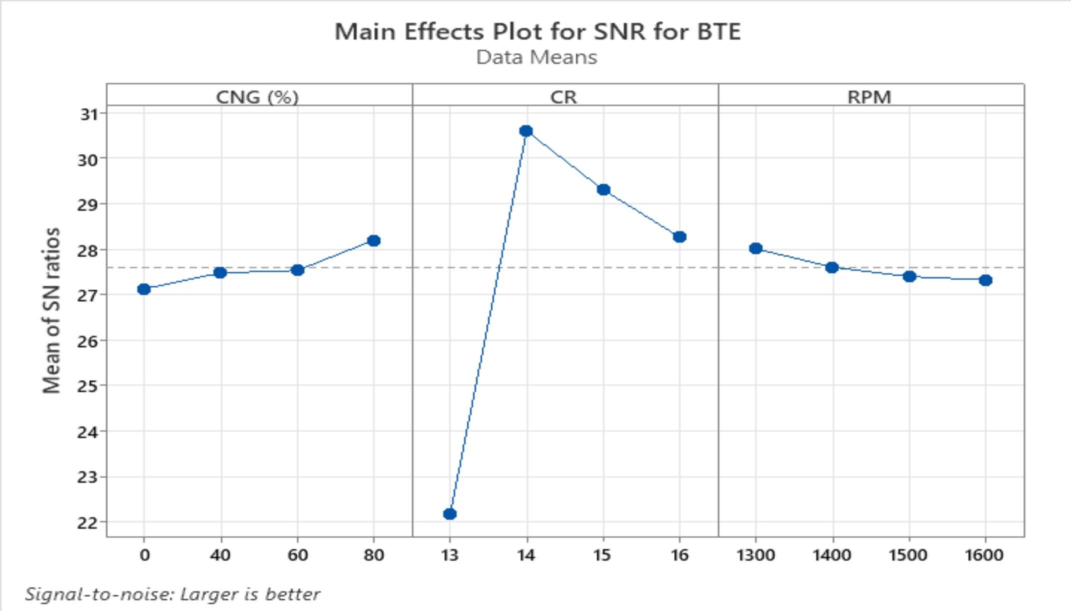


Fig. 4.2. (a) Mean of SN ratios for BTE

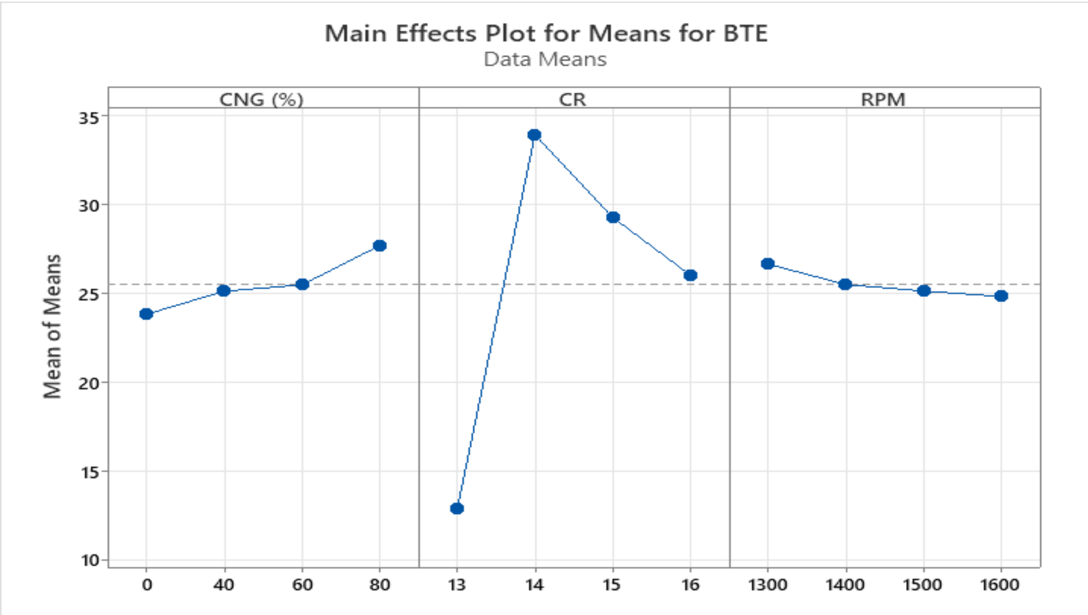


Fig. 4.2. (b) Mean of Means for BTE

This suggests that the experimental process utilizing the Design of Experiments (DOE) approach yielded results with over 98% accuracy. Furthermore, the findings were visually presented in Figure 4.2 (a and b). According to the statistical analysis of the mean SN ratio and mean of means, the optimum BTE value was achieved at CR of 15 and CNG substitution ratio of 40%.

## 4.3 Analysis of SNR and Means for BSFC

The Signal to Noise ratio (SN ratio) and the means of diesel CNG dual fuel combustion for BSFC through a linear model analysis. The findings of this analysis are outlined in Table 4.3 and Table 4.4, respectively.

Table 4.3: Linear Model Analysis for BSFC: SN ratios versus CNG (%), CR, RPM

**Estimated Model Coefficients for SN ratios**

| **Term** | **Coef** | **SE Coef** | **T** | **P** |
|---|---|---|---|---|
| Constant | 7.17307 | 0.08584 | 83.568 | 0.000 |
| CNG (%) 0 | -0.08079 | 0.14867 | -0.543 | 0.606 |
| CNG (%) 40 | -0.04731 | 0.14867 | -0.318 | 0.761 |
| CNG (%) 60 | 0.00513 | 0.14867 | 0.035 | 0.974 |
| CR 13 | 2.39382 | 0.14867 | 16.101 | 0.000 |
| CR 14 | -1.73667 | 0.14867 | -11.681 | 0.000 |
| CR 15 | -0.18633 | 0.14867 | -1.253 | 0.257 |
| RPM 1300 | 0.11604 | 0.14867 | 0.781 | 0.465 |
| RPM 1400 | 0.04456 | 0.14867 | 0.300 | 0.775 |
| RPM 1500 | -0.12001 | 0.14867 | -0.807 | 0.450 |

**Analysis of Variance for SN ratios**

| **Source** | **DF** | **Seq SS** | **Adj SS** | **Adj MS** | **F** | **P** |
|---|---|---|---|---|---|---|
| CNG (%) | 3 | 0.0956 | 0.0956 | 0.0319 | 0.27 | 0.845 |
| CR | 3 | 36.0112 | 36.0112 | 12.0037 | 101.83 | 0.000 |
| RPM | 3 | 0.1260 | 0.1260 | 0.0420 | 0.36 | 0.787 |
| Residual Error | 6 | 0.7073 | 0.7073 | 0.1179 | | |
| Total | 15 | 36.9401 | | | | |

**Model Summary**

| **S** | **R-Sq** | **R-Sq(adj)** |
|---|---|---|
| 0.3433 | 98.09% | 95.21% |

**Response Table for Signal to Noise Ratios**

Smaller is better

| Level | CNG (%) | CR | RPM |
|---|---|---|---|
| 1 | 7.092 | 9.567 | 7.289 |
| 2 | 7.126 | 5.436 | 7.218 |
| 3 | 7.178 | 6.987 | 7.053 |
| 4 | 7.296 | 6.702 | 7.132 |
| Delta | 0.204 | 4.130 | 0.236 |
| Rank | 3 | 1 | 2 |

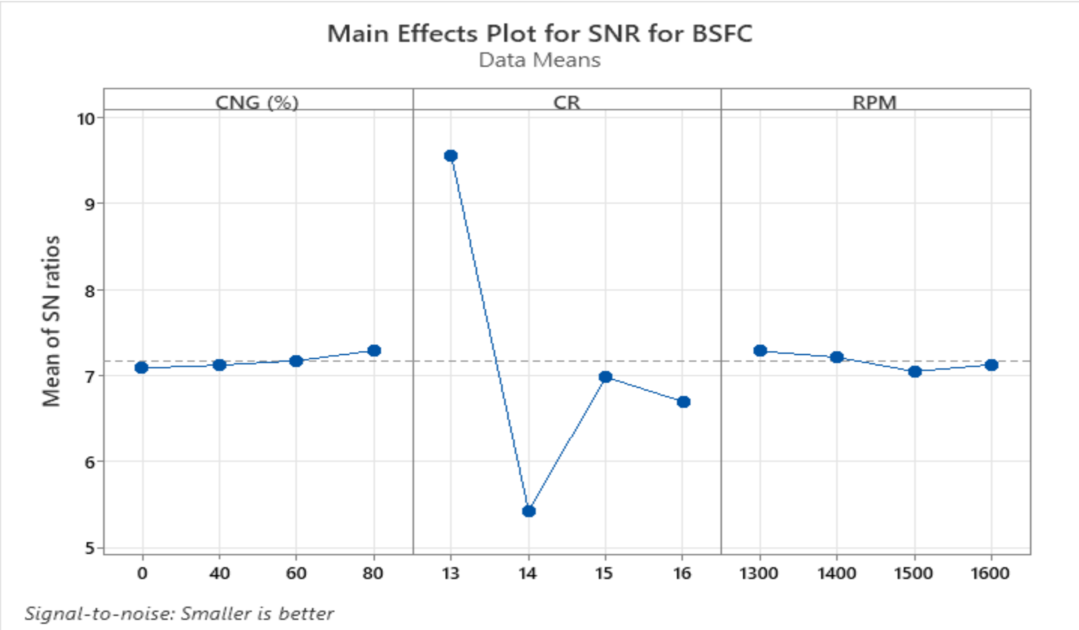


Fig.4.3. (a) Mean of SNR for BSFC

Table 4.4: Linear Model Analysis for BSFC: Means versus CNG (%), CR, RPM

**Estimated Model Coefficients for Means**

| Term | Coef | SE Coef | T | P |
|---|---|---|---|---|
| Constant | 0.444375 | 0.004492 | 98.916 | 0.000 |
| CNG (%) 0 | 0.005625 | 0.007781 | 0.723 | 0.497 |
| CNG (%) 40 | 0.003125 | 0.007781 | 0.402 | 0.702 |
| CNG (%) 60 | -0.001875 | 0.007781 | -0.241 | 0.818 |
| CR 13 | -0.111875 | 0.007781 | -14.378 | 0.000 |
| CR 14 | 0.090625 | 0.007781 | 11.647 | 0.000 |
| CR 15 | 0.003125 | 0.007781 | 0.402 | 0.702 |
| RPM 1300 | -0.004375 | 0.007781 | -0.562 | 0.594 |
| RPM 1400 | -0.001875 | 0.007781 | -0.241 | 0.818 |
| RPM 1500 | 0.005625 | 0.007781 | 0.723 | 0.497 |

**Analysis of Variance for Means**

| Source | DF | Seq SS | Adj SS | Adj MS | F | P |
|---|---|---|---|---|---|---|
| CNG (%) | 3 | 0.000369 | 0.000369 | 0.000123 | 0.38 | 0.771 |
| CR | 3 | 0.084269 | 0.084269 | 0.028090 | 86.99 | 0.000 |
| RPM | 3 | 0.000219 | 0.000219 | 0.000073 | 0.23 | 0.875 |
| Residual Error | 6 | 0.001938 | 0.001938 | 0.000323 | | |
| Total | 15 | 0.086794 | | | | |

**Model Summary**

| S | R-Sq | R-Sq(adj) |
|---|---|---|
| 0.0180 | 97.77% | 94.42% |

**Response Table for Means**

| Level | CNG (%) | CR | RPM |
|---|---|---|---|
| 1 | 0.4500 | 0.3325 | 0.4400 |
| 2 | 0.4475 | 0.5350 | 0.4425 |
| 3 | 0.4425 | 0.4475 | 0.4500 |
| 4 | 0.4375 | 0.4625 | 0.4450 |
| Delta | 0.0125 | 0.2025 | 0.0100 |
| Rank | 2 | 1 | 3 |

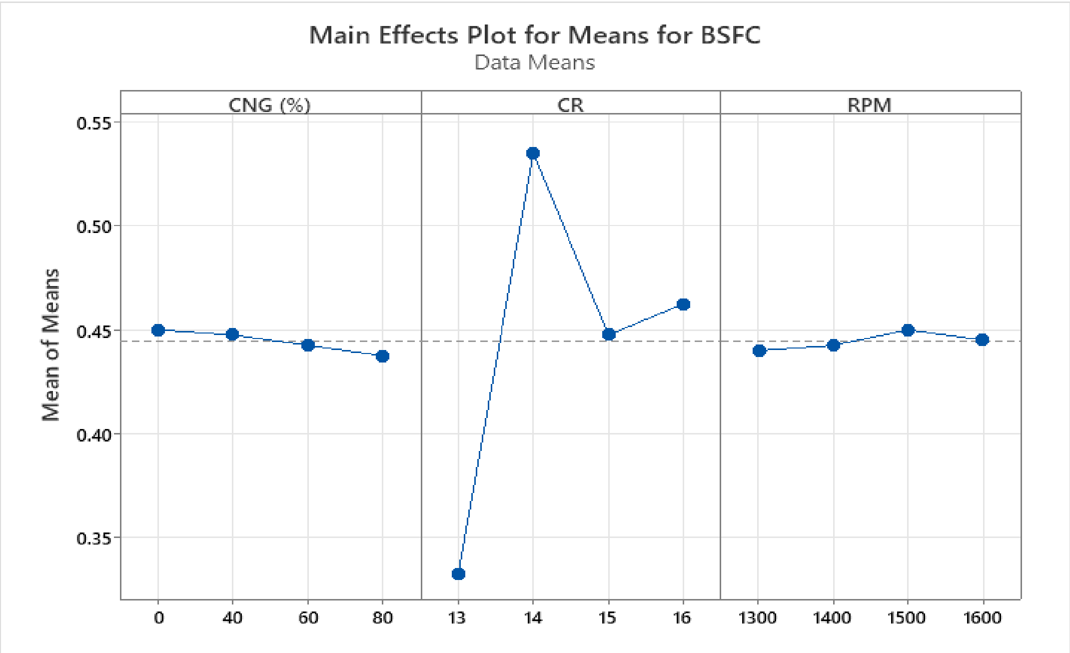


Fig. 4.3. (b) Mean of Means for BSFC

The coefficient of determination ($R^2$), was determined to be 98.09% for the SN ratio analysis and 97.77% for the means analysis. The findings were visually presented in Figure 4.3 (a and b). According to the statistical analysis of the mean SN ratio and mean of means, the optimum BSFC value was achieved at CR of 13, CNG substitution ratio of 80%, and at 1300 rpm.

## 4.4 Analysis of SNR and Means for CO

The relationship between the SNR and Means on the performance of diesel CNG dual fuel combustion on CO emission is shown in Figure 4.4 (a and b). The results of this analysis are summarized in Tables 4.5 and 4.6 for CO, highlighting the findings on their interrelation.

Table 4.5: Linear Model Analysis for CO: SN ratios versus CNG (%), CR, RPM

**Estimated Model Coefficients for SN ratios**

| Term | Coef | SE Coef | T | P |
|---|---|---|---|---|
| Constant | 21.5967 | 0.1310 | 164.842 | 0.000 |
| CNG (%) 0 | -2.6119 | 0.2269 | -11.510 | 0.000 |
| CNG (%) 40 | -0.1346 | 0.2269 | -0.593 | 0.575 |
| CNG (%) 60 | 0.6767 | 0.2269 | 2.982 | 0.025 |
| CR 13 | 1.3730 | 0.2269 | 6.050 | 0.001 |
| CR 14 | 0.4901 | 0.2269 | 2.160 | 0.074 |
| CR 15 | -0.2490 | 0.2269 | -1.097 | 0.315 |
| RPM 1300 | -0.1633 | 0.2269 | -0.720 | 0.499 |
| RPM 1400 | 0.0313 | 0.2269 | 0.138 | 0.895 |
| RPM 1500 | 0.0520 | 0.2269 | 0.229 | 0.826 |

**Analysis of Variance for SN ratios**

| Source | DF | Seq SS | Adj SS | Adj MS | F | P |
|---|---|---|---|---|---|---|
| CNG (%) | 3 | 46.3279 | 46.3279 | 15.4426 | 56.23 | 0.000 |
| CR | 3 | 19.1694 | 19.1694 | 6.3898 | 23.27 | 0.001 |
| RPM | 3 | 0.1471 | 0.1471 | 0.0490 | 0.18 | 0.907 |
| Residual Error | 6 | 1.6478 | 1.6478 | 0.2746 | | |
| Total | 15 | 67.2923 | | | | |

**Model Summary**

| S | R-Sq | R-Sq(adj) |
|---|---|---|
| 0.5241 | 97.55% | 93.88% |

**Response Table for Signal to Noise Ratios**

Smaller is better

| Level | CNG (%) | CR | RPM |
|---|---|---|---|
| 1 | 18.98 | 22.97 | 21.43 |
| 2 | 21.46 | 22.09 | 21.63 |
| 3 | 22.27 | 21.35 | 21.65 |
| 4 | 23.67 | 19.98 | 21.68 |
| Delta | 4.68 | 2.99 | 0.24 |
| Rank | 1 | 2 | 3 |

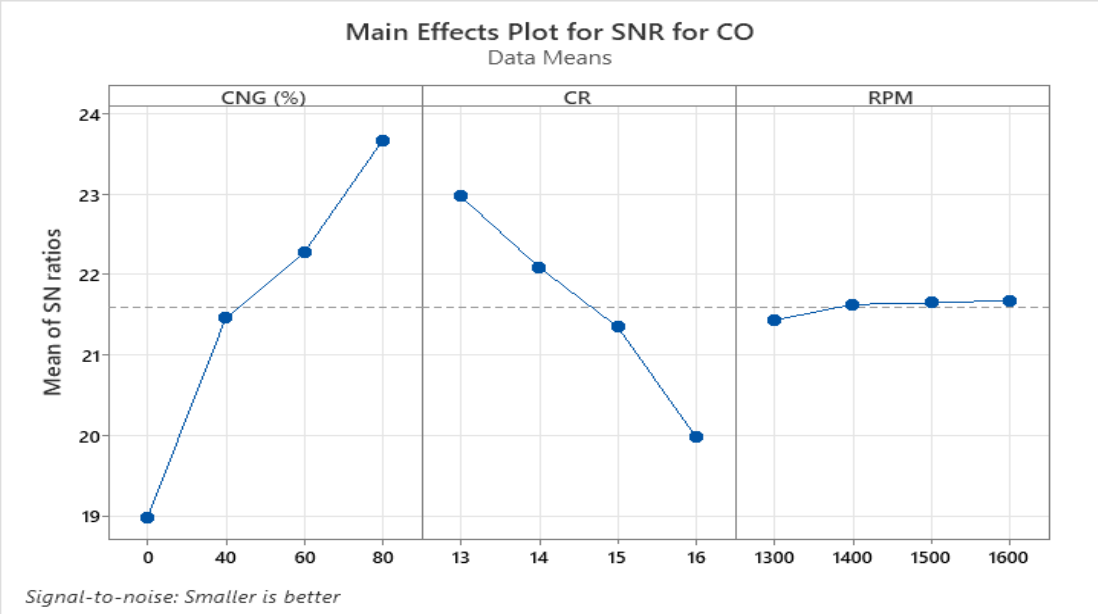


Fig.4.4. (a) Mean of SNR for CO

Table 4.6: Linear Model Analysis for CO: Means versus CNG (%), CR, RPM

**Estimated Model Coefficients for Means**

| Term | Coef | SE Coef | T | P |
|---|---|---|---|---|
| Constant | 0.085625 | 0.001804 | 47.458 | 0.000 |
| CNG (%) 0 | 0.028125 | 0.003125 | 9.000 | 0.000 |
| CNG (%) 40 | -0.000625 | 0.003125 | -0.200 | 0.848 |
| CNG (%) 60 | -0.008125 | 0.003125 | -2.600 | 0.041 |
| CR 13 | -0.013125 | 0.003125 | -4.200 | 0.006 |
| CR 14 | -0.005625 | 0.003125 | -1.800 | 0.122 |
| CR 15 | 0.001875 | 0.003125 | 0.600 | 0.570 |
| RPM 1300 | -0.000625 | 0.003125 | -0.200 | 0.848 |
| RPM 1400 | -0.001875 | 0.003125 | -0.600 | 0.570 |
| RPM 1500 | 0.000625 | 0.003125 | 0.200 | 0.848 |

**Analysis of Variance for Means**

| Source | DF | Seq SS | Adj SS | Adj MS | F | P |
|---|---|---|---|---|---|---|
| CNG (%) | 3 | 0.004931 | 0.004931 | 0.001644 | 31.56 | 0.000 |
| CR | 3 | 0.001969 | 0.001969 | 0.000656 | 12.60 | 0.005 |
| RPM | 3 | 0.000031 | 0.000031 | 0.000010 | 0.20 | 0.893 |
| Residual Error | 6 | 0.000312 | 0.000312 | 0.000052 | | |
| Total | 15 | 0.007244 | | | | |

**Model Summary**

| S | R-Sq | R-Sq(adj) |
|---|---|---|
| 0.0072 | 95.69% | 89.21% |

**Response Table for Means**

| Level | CNG (%) | CR | RPM |
|---|---|---|---|
| 1 | 0.11375 | 0.07250 | 0.08500 |
| 2 | 0.08500 | 0.08000 | 0.08375 |
| 3 | 0.07750 | 0.08750 | 0.08625 |
| 4 | 0.06625 | 0.10250 | 0.08750 |
| Delta | 0.04750 | 0.03000 | 0.00375 |
| Rank | 1 | 2 | 3 |

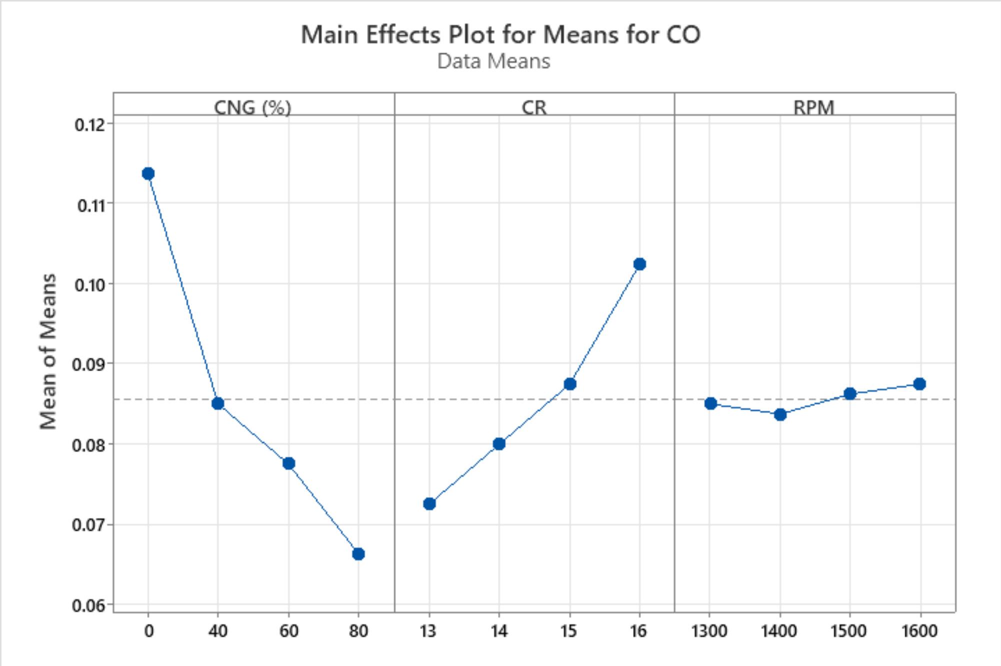


Fig. 4.4. (b) Mean of Means for CO

The coefficient of determination ($R^2$) was calculated to be 97.55% for the analysis of the SNR and 95.69% for the means analysis. Through statistical analysis of the mean SN ratio and the mean of means, it was determined that the optimal CO value was attained at CR of 13, a CNG substitution ratio of 80%, and an engine speed of 1600 rpm.

4.5 Analysis of SNR and Means for HC

Figure 4.5 (a and b) illustrates the correlation between the Signal to Noise ratio (SNR) and the Means in the context of diesel CNG dual fuel combustion performance concerning HC emissions. The outcomes of this examination are succinctly presented in Tables 4.7 and 4.8 for HC emissions, emphasizing the insights gained from their relationship.

Table 4.7: Linear Model Analysis for HC: SN ratios versus CNG (%), CR, RPM

**Estimated Model Coefficients for SN ratios**

| Term | Coef | SE Coef | T | P |
|---|---|---|---|---|
| Constant | -35.6707 | 0.3032 | -117.640 | 0.000 |
| CNG (%) 0 | -1.1274 | 0.5252 | -2.147 | 0.075 |
| CNG (%) 40 | -0.3069 | 0.5252 | -0.584 | 0.580 |
| CNG (%) 60 | 0.4016 | 0.5252 | 0.765 | 0.473 |
| CR 13 | 5.9237 | 0.5252 | 11.279 | 0.000 |
| CR 14 | 3.6027 | 0.5252 | 6.860 | 0.000 |
| CR 15 | -4.3006 | 0.5252 | -8.189 | 0.000 |
| RPM 1300 | 0.4141 | 0.5252 | 0.788 | 0.460 |
| RPM 1400 | -0.2126 | 0.5252 | -0.405 | 0.700 |
| RPM 1500 | 0.0555 | 0.5252 | 0.106 | 0.919 |

**Model Summary**

| S | R-Sq | R-Sq(adj) |
|---|---|---|
| 1.2129 | 97.77% | 94.43% |

**Analysis of Variance for SN ratios**

| Source | DF | Seq SS | Adj SS | Adj MS | F | P |
|---|---|---|---|---|---|---|
| CNG (%) | 3 | 10.372 | 10.372 | 3.457 | 2.35 | 0.172 |
| CR | 3 | 375.494 | 375.494 | 125.165 | 85.08 | 0.000 |
| RPM | 3 | 1.143 | 1.143 | 0.381 | 0.26 | 0.853 |
| Residual Error | 6 | 8.826 | 8.826 | 1.471 | | |
| Total | 15 | 395.835 | | | | |

**Response Table for Signal to Noise Ratios**

Smaller is better

| Level | CNG (%) | CR | RPM |
|---|---|---|---|
| 1 | -36.80 | -29.75 | -35.26 |
| 2 | -35.98 | -32.07 | -35.88 |
| 3 | -35.27 | -39.97 | -35.62 |
| 4 | -34.64 | -40.90 | -35.93 |

| | | | |
|---|---|---|---|
| Delta | 2.16 | 11.15 | 0.67 |
| Rank | 2 | 1 | 3 |

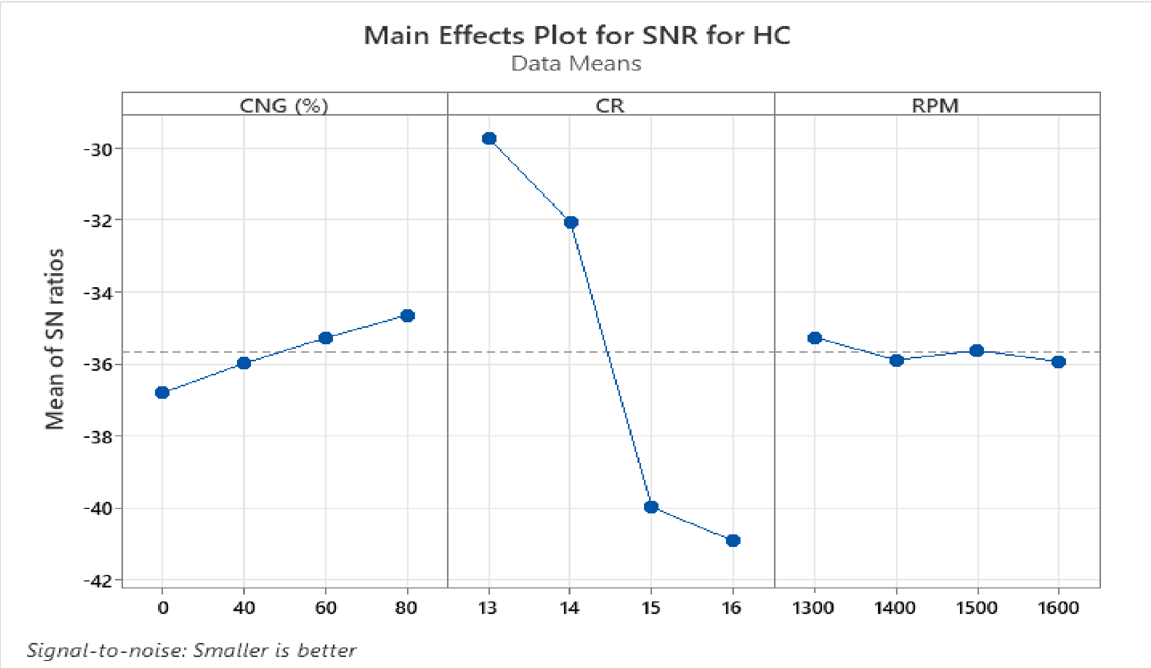


Fig.4.5. (a) Mean of SNR for HC

Table 4.8: Linear Model Analysis for HC: Means versus CNG (%), CR, RPM

**Estimated Model Coefficients for Means**

| **Term** | **Coef** | **SE Coef** | **T** | **P** |
|---|---|---|---|---|
| Constant | 71.0000 | 2.803 | 25.334 | 0.000 |
| CNG (%) 0 | 12.0000 | 4.854 | 2.472 | 0.048 |
| CNG (%) 40 | 1.5000 | 4.854 | 0.309 | 0.768 |
| CNG (%) 60 | -4.5000 | 4.854 | -0.927 | 0.390 |
| CR 13 | -40.2500 | 4.854 | -8.292 | 0.000 |
| CR 14 | -30.2500 | 4.854 | -6.232 | 0.001 |
| CR 15 | 28.7500 | 4.854 | 5.923 | 0.001 |
| RPM 1300 | -5.7500 | 4.854 | -1.185 | 0.281 |
| RPM 1400 | -1.7500 | 4.854 | -0.361 | 0.731 |
| RPM 1500 | 0.7500 | 4.854 | 0.155 | 0.882 |

**Model Summary**

| **S** | **R-Sq** | **R-Sq(adj)** |
|---|---|---|
| 11.2101 | 96.65% | 91.62% |

**Analysis of Variance for Means**

| Source | DF | Seq SS | Adj SS | Adj MS | F | P |
|---|---|---|---|---|---|---|
| CNG (%) | 3 | 990.0 | 990.0 | 330.0 | 2.63 | 0.145 |
| CR | 3 | 20419.0 | 20419.0 | 6806.3 | 54.16 | 0.000 |
| RPM | 3 | 329.0 | 329.0 | 109.7 | 0.87 | 0.506 |
| Residual Error | 6 | 754.0 | 754.0 | 125.7 | | |

**Response Table for Means**

| Level | CNG (%) | CR | RPM |
|---|---|---|---|
| 1 | 83.00 | 30.75 | 65.25 |
| 2 | 72.50 | 40.75 | 69.25 |
| 3 | 66.50 | 99.75 | 71.75 |
| 4 | 62.00 | 112.75 | 77.75 |
| Delta | 21.00 | 82.00 | 12.50 |
| Rank | 2 | 1 | 3 |

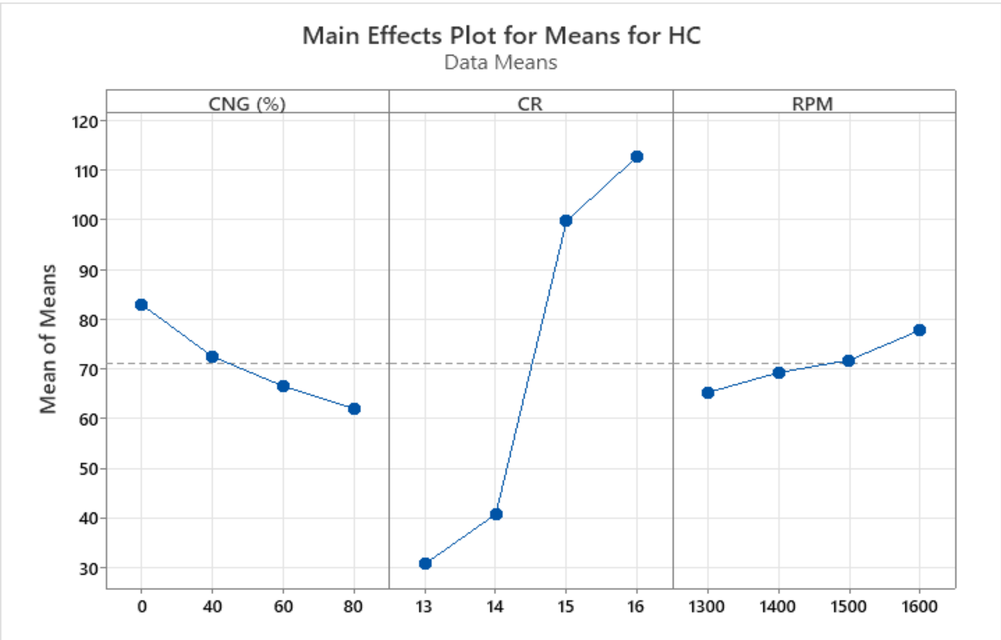


Fig. 4.5. (b) Mean of Means for HC

The coefficient of determination ($R^2$) was computed at 97.77% for the SNR analysis and 96.65% for the means analysis. Utilizing statistical methods on the mean SN ratio and the mean of means, it was established that the most favorable HC value was reached with a compression ratio (CR) of 16, a CNG substitution ratio of 0%, and an engine speed of 1600 rpm.

### 4.6 Analysis of SNR and Means for $CO_2$

Figure 4.6 (a and b) demonstrates how $CO_2$ emissions are influenced by CNG (%), CR, and RPM. It's evident from the figure that the lowest $CO_2$ emissions occur at a CNG (%) of 80%, a CR of 16, and at 1300 rpm when using the DF (diesel-CNG dual fuel) mode to optimize the "smaller is better" quality characteristics. Tables 4.9 and 4.10 provide the contribution ratios of CNG (%), CR, and RPM to $CO_2$ emissions, shedding light on their respective impacts in this context.

Table 4.9: Linear Model Analysis for $CO_2$: SN ratios versus CNG (%), CR, RPM

**Estimated Model Coefficients for SN ratios**

| Term | Coef | SE Coef | T | P |
|---|---|---|---|---|
| Constant | -10.1534 | 0.1272 | -79.827 | 0.000 |
| CNG (%) 0 | -0.1611 | 0.2203 | -0.731 | 0.492 |
| CNG (%) 40 | -0.1989 | 0.2203 | -0.903 | 0.401 |
| CNG (%) 60 | -0.0396 | 0.2203 | -0.180 | 0.863 |
| CR 13 | -3.0000 | 0.2203 | -13.618 | 0.000 |
| CR 14 | -0.3978 | 0.2203 | -1.806 | 0.121 |
| CR 15 | 0.1237 | 0.2203 | 0.562 | 0.595 |
| RPM 1300 | 0.1736 | 0.2203 | 0.788 | 0.461 |
| RPM 1400 | 0.0205 | 0.2203 | 0.093 | 0.929 |
| RPM 1500 | 0.1449 | 0.2203 | 0.658 | 0.535 |

**Model Summary**

| S | R-Sq | R-Sq(adj) |
|---|---|---|
| 0.5088 | 98.12% | 95.31% |

**Analysis of Variance for SN ratios**

| Source | DF | Seq SS | Adj SS | Adj MS | F | P |
|---|---|---|---|---|---|---|
| CNG (%) | 3 | 0.9071 | 0.9071 | 0.3024 | 1.17 | 0.397 |
| CR | 3 | 79.5750 | 79.5750 | 26.5250 | 102.47 | 0.000 |
| RPM | 3 | 0.6660 | 0.6660 | 0.2220 | 0.86 | 0.512 |
| Residual Error | 6 | 1.5531 | 1.5531 | 0.2588 | | |
| Total | 15 | 82.7012 | | | | |

**Response Table for Signal to Noise Ratios**

Smaller is better

| Level | CNG (%) | CR | RPM |
|---|---|---|---|
| 1 | -10.314 | -13.153 | -9.980 |
| 2 | -10.352 | -10.551 | -10.133 |
| 3 | -10.193 | -10.030 | -10.008 |
| 4 | -9.754 | -6.879 | -10.492 |
| Delta | 0.598 | 6.274 | 0.513 |
| Rank | 2 | 1 | 3 |

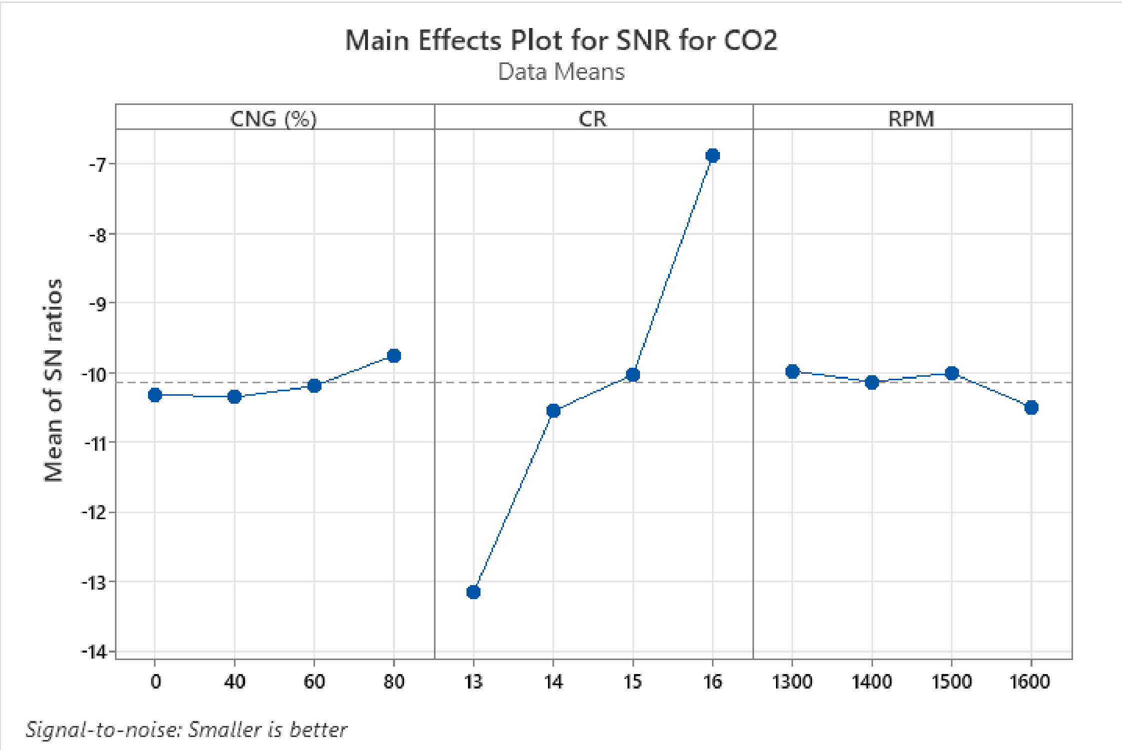


Fig.4.6. (a) Mean of SNR for $CO_2$

Table 4.10. Linear Model Analysis for $CO_2$: Means versus CNG (%), CR, RPM

**Estimated Model Coefficients for Means**

| Term | Coef | SE Coef | T | P |
|---|---|---|---|---|
| Constant | 3.32813 | 0.05189 | 64.144 | 0.000 |
| CNG (%) 0 | 0.02188 | 0.08987 | 0.243 | 0.816 |
| CNG (%) 40 | 0.07187 | 0.08987 | 0.800 | 0.454 |
| CNG (%) 60 | 0.00937 | 0.08987 | 0.104 | 0.920 |
| CR 13 | 1.22188 | 0.08987 | 13.596 | 0.000 |
| CR 14 | 0.04688 | 0.08987 | 0.522 | 0.621 |
| CR 15 | -0.15313 | 0.08987 | -1.704 | 0.139 |
| RPM 1300 | -0.05312 | 0.08987 | -0.591 | 0.576 |

| | | | | |
|---|---|---|---|---|
| RPM 1400 | -0.01563 | 0.08987 | -0.174 | 0.868 |
| RPM 1500 | -0.05312 | 0.08987 | -0.591 | 0.576 |

**Model Summary**

| S | R-Sq | R-Sq(adj) |
|---|---|---|
| 0.2075 | 97.74% | 94.36% |

**Analysis of Variance for Means**

| Source | DF | Seq SS | Adj SS | Adj MS | F | P |
|---|---|---|---|---|---|---|
| CNG (%) | 3 | 0.0655 | 0.0655 | 0.02182 | 0.51 | 0.692 |
| CR | 3 | 11.0530 | 11.0530 | 3.68432 | 85.54 | 0.000 |
| RPM | 3 | 0.0830 | 0.0830 | 0.02766 | 0.64 | 0.615 |
| Residual Error | 6 | 0.2584 | 0.2584 | 0.04307 | | |
| Total | 15 | 11.4598 | | | | |

**Response Table for Means**

| Level | CNG (%) | CR | RPM |
|---|---|---|---|
| 1 | 3.350 | 4.550 | 3.275 |
| 2 | 3.400 | 3.375 | 3.313 |
| 3 | 3.337 | 3.175 | 3.275 |
| 4 | 3.225 | 2.212 | 3.450 |
| Delta | 0.175 | 2.337 | 0.175 |
| Rank | 3 | 1 | 2 |

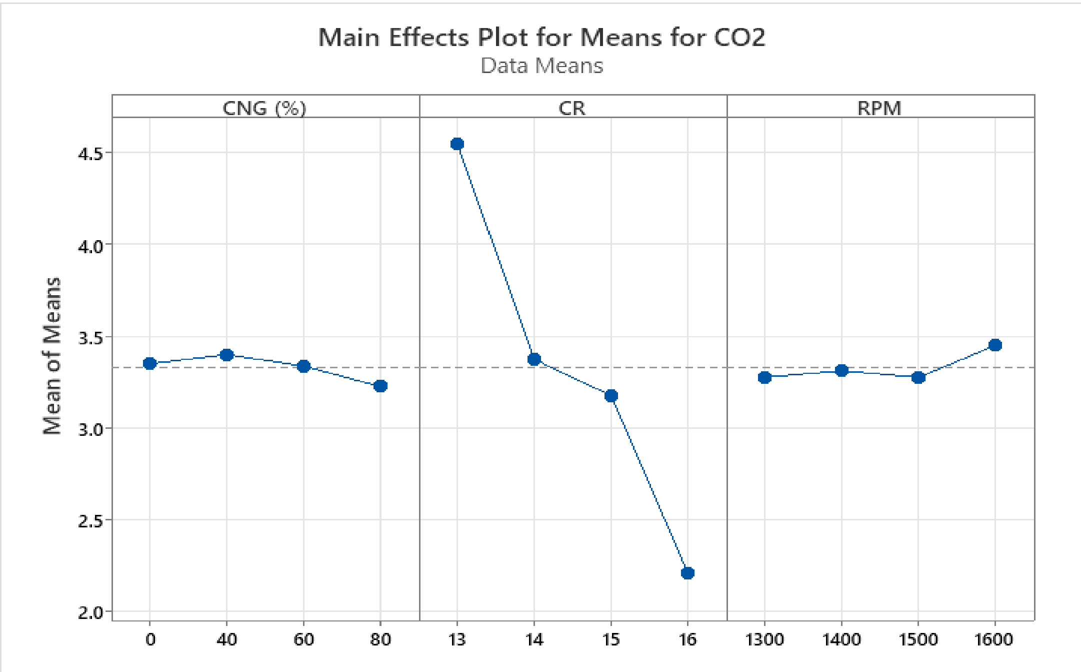


Fig. 4.6. (b) Mean of Means for $CO_2$

The coefficient of determination ($R^2$) was calculated to be 98.12% for the SNR analysis and 97.74% for the means analysis. This indicates a strong correlation between the variables in both analyses, with the vast majority of the variance in the data being explained by the respective models.

## 4.7 Analysis of SNR and Means for $NO_X$

In Figure 4.7 (a and b), the relationship between the SNR and the Means is depicted within the framework of diesel-CNG dual fuel combustion performance, specifically in relation to $NO_X$ emissions. The findings from this investigation are succinctly summarized in Table 4.11 and Table 4.12, with a focus on accentuating the insights derived from their interconnection.

Table 4.11. Linear Model Analysis for NOx: SN ratios versus CNG (%), CR, RPM

**Estimated Model Coefficients for SN ratios**

| Term | Coef | SE Coef | T | P |
|---|---|---|---|---|
| Constant | -58.9909 | 0.1648 | -357.974 | 0.000 |
| CNG (%) 0 | 0.5272 | 0.2854 | 1.847 | 0.114 |
| CNG (%) 40 | 0.0156 | 0.2854 | 0.055 | 0.958 |
| CNG (%) 60 | -0.2886 | 0.2854 | -1.011 | 0.351 |
| CR 13 | -4.3503 | 0.2854 | -15.241 | 0.000 |
| CR 14 | -3.1499 | 0.2854 | -11.036 | 0.000 |
| CR 15 | 1.9187 | 0.2854 | 6.722 | 0.001 |
| RPM 1300 | -0.5163 | 0.2854 | -1.809 | 0.120 |
| RPM 1400 | -0.0834 | 0.2854 | -0.292 | 0.780 |
| RPM 1500 | 0.1494 | 0.2854 | 0.523 | 0.619 |

**Model Summary**

| S | R-Sq | R-Sq(adj) |
|---|---|---|
| 0.6592 | 99.00% | 97.50% |

**Analysis of Variance for SN ratios**

| Source | DF | Seq SS | Adj SS | Adj MS | F | P |
|---|---|---|---|---|---|---|
| CNG (%) | 3 | 1.705 | 1.705 | 0.5682 | 1.31 | 0.356 |
| CR | 3 | 254.724 | 254.724 | 84.9079 | 195.42 | 0.000 |
| RPM | 3 | 1.994 | 1.994 | 0.6648 | 1.53 | 0.300 |
| Residual Error | 6 | 2.607 | 2.607 | 0.4345 | | |
| Total | 15 | 261.030 | | | | |

**Response Table for Signal to Noise Ratios**

Smaller is better

| Level | CNG (%) | CR | RPM |
|---|---|---|---|
| 1 | -58.46 | -63.34 | -59.51 |
| 2 | -58.98 | -62.14 | -59.07 |
| 3 | -59.28 | -57.07 | -58.84 |
| 4 | -59.25 | -53.41 | -58.54 |
| Delta | 0.82 | 9.93 | 0.97 |
| Rank | 3 | 1 | 2 |

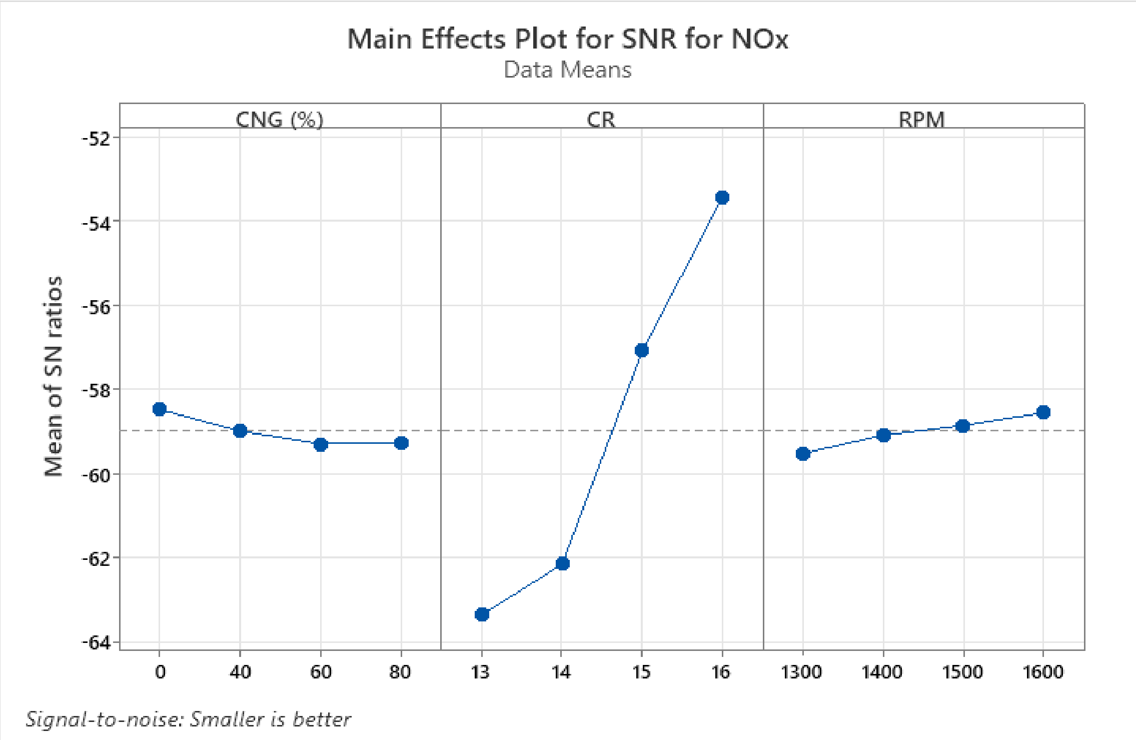


Fig.4.7. (a) Mean of SNR for $NO_X$

Table 4.12. Linear Model Analysis for NOx: Means versus CNG (%), CR, RPM

**Estimated Model Coefficients for Means**

| Term | Coef | SE Coef | T | P |
|---|---|---|---|---|
| Constant | 984.000 | 10.51 | 93.639 | 0.000 |
| CNG (%) 0 | -30.500 | 18.20 | -1.676 | 0.145 |
| CNG (%) 40 | 0.500 | 18.20 | 0.027 | 0.979 |
| CNG (%) 60 | 19.000 | 18.20 | 1.044 | 0.337 |
| CR 13 | 485.250 | 18.20 | 26.660 | 0.000 |
| CR 14 | 295.750 | 18.20 | 16.249 | 0.000 |
| CR 15 | -269.500 | 18.20 | -14.807 | 0.000 |
| RPM 1300 | 33.500 | 18.20 | 1.841 | 0.115 |
| RPM 1400 | 2.500 | 18.20 | 0.137 | 0.895 |

| | | | | |
|---|---|---|---|---|
| RPM 1500 | -14.750 | 18.20 | -0.810 | 0.449 |

**Model Summary**

| S | R-Sq | R-Sq(adj) |
|---|---|---|
| 42.0337 | 99.60% | 99.00% |

**Analysis of Variance for Means**

| Source | DF | Seq SS | Adj SS | Adj MS | F | P |
|---|---|---|---|---|---|---|
| CNG (%) | 3 | 5650 | 5650 | 1883 | 1.07 | 0.431 |
| CR | 3 | 2628793 | 2628793 | 876264 | 495.95 | 0.000 |
| RPM | 3 | 7190 | 7190 | 2397 | 1.36 | 0.342 |
| Residual Error | 6 | 10601 | 10601 | 1767 | | |
| Total | 15 | 2652234 | | | | |

**Response Table for Means**

| Level | CNG (%) | CR | RPM |
|---|---|---|---|
| 1 | 953.5 | 1469.3 | 1017.5 |
| 2 | 984.5 | 1279.8 | 986.5 |
| 3 | 1003.0 | 714.5 | 969.3 |
| 4 | 995.0 | 472.5 | 962.8 |
| Delta | 49.5 | 996.8 | 54.8 |
| Rank | 3 | 1 | 2 |

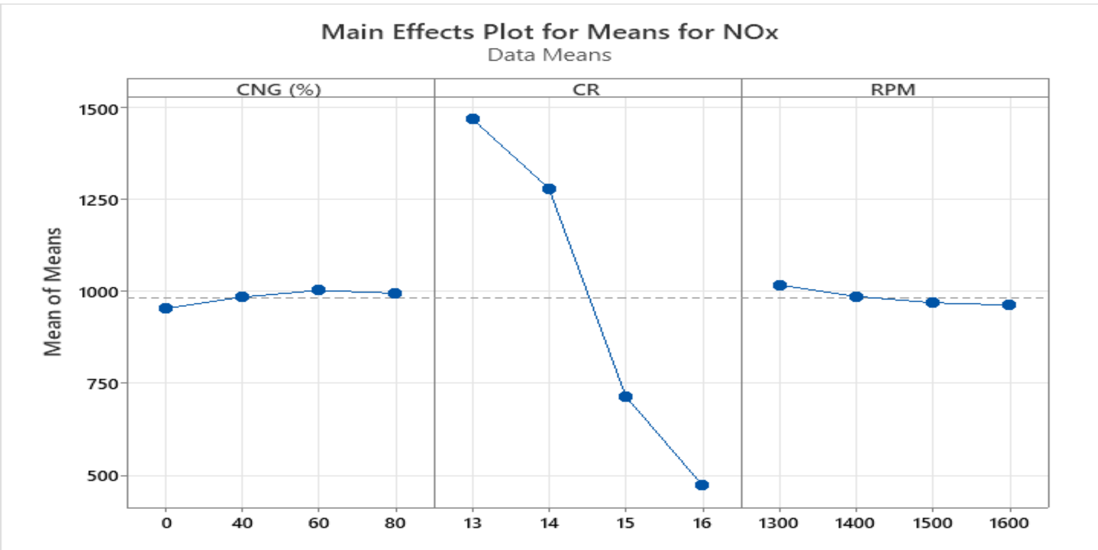


Fig.4.7. (b) Mean of Means for NOx

The coefficient of determination ($R^2$) was computed at 99.00% for the SNR analysis and 99.60% for the means analysis. Utilizing statistical methods on the mean SN ratio and the mean of means, it was established that the most favourable $NO_X$ value was reached with a compression ratio (CR) of 16, a CNG substitution ratio of 80%, and an engine speed of 1600 rpm.

## 4.8 Analysis of SNR and Means for Smoke

Figure 4.8 (a and b) illustrates the impact of CNG (%), CR, and RPM on smoke emissions. It is apparent from the figure that the lowest smoke opacity is achieved at a CNG percentage of 80%, a CR of 16, and an RPM of 1600 when utilizing the diesel-CNG dual fuel (DF) mode to optimize the "smaller is better" quality characteristics. Tables 4.13 and 4.14 present the contribution ratios of CNG percentage, CR, and RPM to smoke opacity, providing insight into their influences within this context.

Table 4.13. Linear Model Analysis: SN ratios versus CNG (%), CR, RPM

**Estimated Model Coefficients for SN ratios**

| Term | Coef | SE Coef | T | P |
|---|---|---|---|---|
| Constant | -2.937 | 1.150 | -2.555 | 0.043 |
| CNG (%) 0 | -9.645 | 1.991 | -4.844 | 0.003 |
| CNG (%) 40 | -4.344 | 1.991 | -2.182 | 0.072 |
| CNG (%) 60 | 5.082 | 1.991 | 2.553 | 0.043 |
| CR 13 | -5.043 | 1.991 | -2.533 | 0.045 |
| CR 14 | -3.000 | 1.991 | -1.507 | 0.183 |
| CR 15 | 3.420 | 1.991 | 1.718 | 0.137 |
| RPM 1300 | 1.847 | 1.991 | 0.928 | 0.389 |
| RPM 1400 | 4.513 | 1.991 | 2.267 | 0.064 |
| RPM 1500 | -5.168 | 1.991 | -2.596 | 0.041 |

**Model Summary**

| S | R-Sq | R-Sq(adj) |
|---|---|---|
| 4.5983 | 91.39% | 78.46% |

**Analysis of Variance for SN ratios**

| Source | DF | Seq SS | Adj SS | Adj MS | F | P |
|---|---|---|---|---|---|---|
| CNG (%) | 3 | 868.2 | 868.2 | 289.40 | 13.69 | 0.004 |
| CR | 3 | 270.0 | 270.0 | 90.01 | 4.26 | 0.062 |
| RPM | 3 | 207.7 | 207.7 | 69.22 | 3.27 | 0.101 |

| | | | | | | |
|---|---|---|---|---|---|---|
| Residual Error | 6 | 126.9 | 126.9 | 21.14 | | |
| Total | 15 | 1472.8 | | | | |

**Response Table for Signal to Noise Ratios**

Smaller is better

| Level | CNG (%) | CR | RPM |
|---|---|---|---|
| 1 | -12.5820 | -7.9807 | -1.0901 |
| 2 | -7.2818 | -5.9376 | 1.5758 |
| 3 | 2.1450 | 0.4824 | -8.1059 |
| 4 | 5.9691 | 1.6862 | -4.1296 |
| Delta | 18.5511 | 9.6670 | 9.6817 |
| Rank | 1 | 3 | 2 |

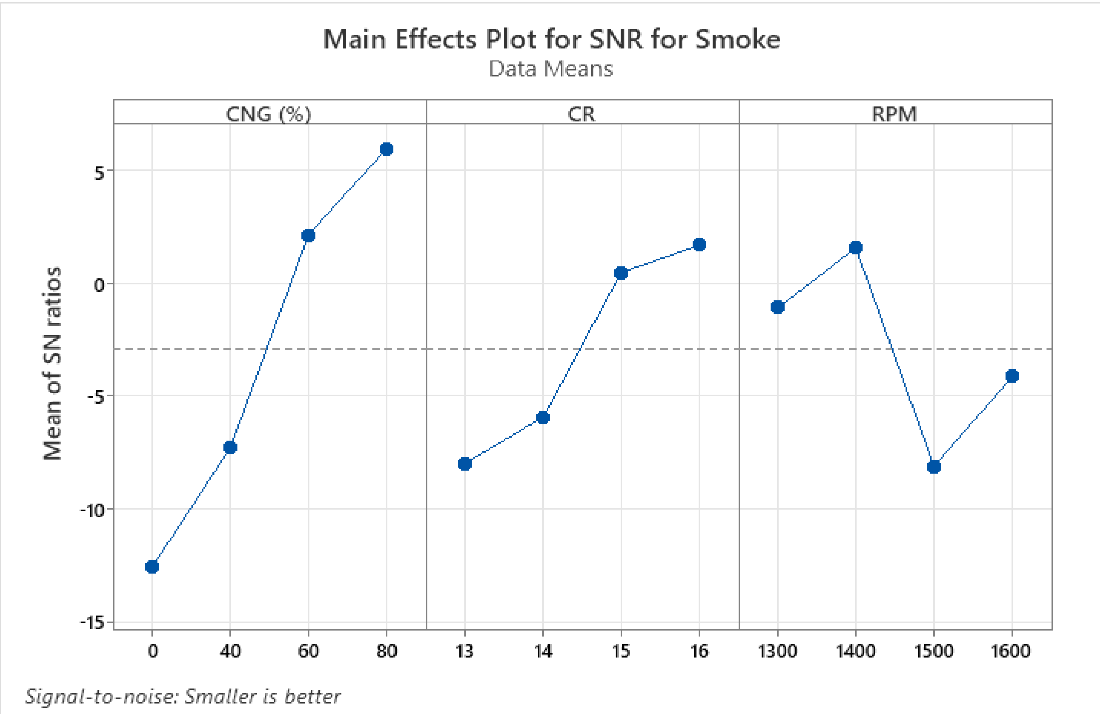


Fig. 4.8. (a) Mean of SNR for Smoke

Table 4.14: Linear Model Analysis: Means versus CNG (%), CR, RPM

**Estimated Model Coefficients for Means**

| Term | Coef | SE Coef | T | P |
|---|---|---|---|---|
| Constant | 2.23750 | 0.3343 | 6.693 | 0.001 |
| CNG (%) 0 | 2.28750 | 0.5791 | 3.950 | 0.008 |

| | | | | |
|---|---|---|---|---|
| CNG (%) 40 | 0.38750 | 0.5791 | 0.669 | 0.528 |
| CNG (%) 60 | -1.18750 | 0.5791 | -2.051 | 0.086 |
| CR 13 | 0.66250 | 0.5791 | 1.144 | 0.296 |
| CR 14 | 0.23750 | 0.5791 | 0.410 | 0.696 |
| CR 15 | -0.58750 | 0.5791 | -1.015 | 0.349 |
| RPM 1300 | -0.03750 | 0.5791 | -0.065 | 0.950 |
| RPM 1400 | -0.21250 | 0.5791 | -0.367 | 0.726 |
| RPM 1500 | 0.83750 | 0.5791 | 1.446 | 0.198 |

**Model Summary**

| S | R-Sq | R-Sq(adj) |
|---|---|---|
| 1.3373 | 80.45% | 51.12% |

**Analysis of Variance for Means**

| Source | DF | Seq SS | Adj SS | Adj MS | F | P |
|---|---|---|---|---|---|---|
| CNG (%) | 3 | 36.022 | 36.022 | 12.007 | 6.71 | 0.024 |
| CR | 3 | 3.753 | 3.753 | 1.251 | 0.70 | 0.586 |
| RPM | 3 | 4.372 | 4.372 | 1.457 | 0.82 | 0.531 |
| Residual Error | 6 | 10.730 | 10.730 | 1.788 | | |
| Total | 15 | 54.877 | | | | |

**Response Table for Means**

| Level | CNG (%) | CR | RPM |
|---|---|---|---|
| 1 | 4.5250 | 2.9000 | 2.2000 |
| 2 | 2.6250 | 2.4750 | 2.0250 |
| 3 | 1.0500 | 1.6500 | 3.0750 |
| 4 | 0.7500 | 1.9250 | 1.6500 |
| Delta | 3.7750 | 1.2500 | 1.4250 |
| Rank | 1 | 3 | 2 |

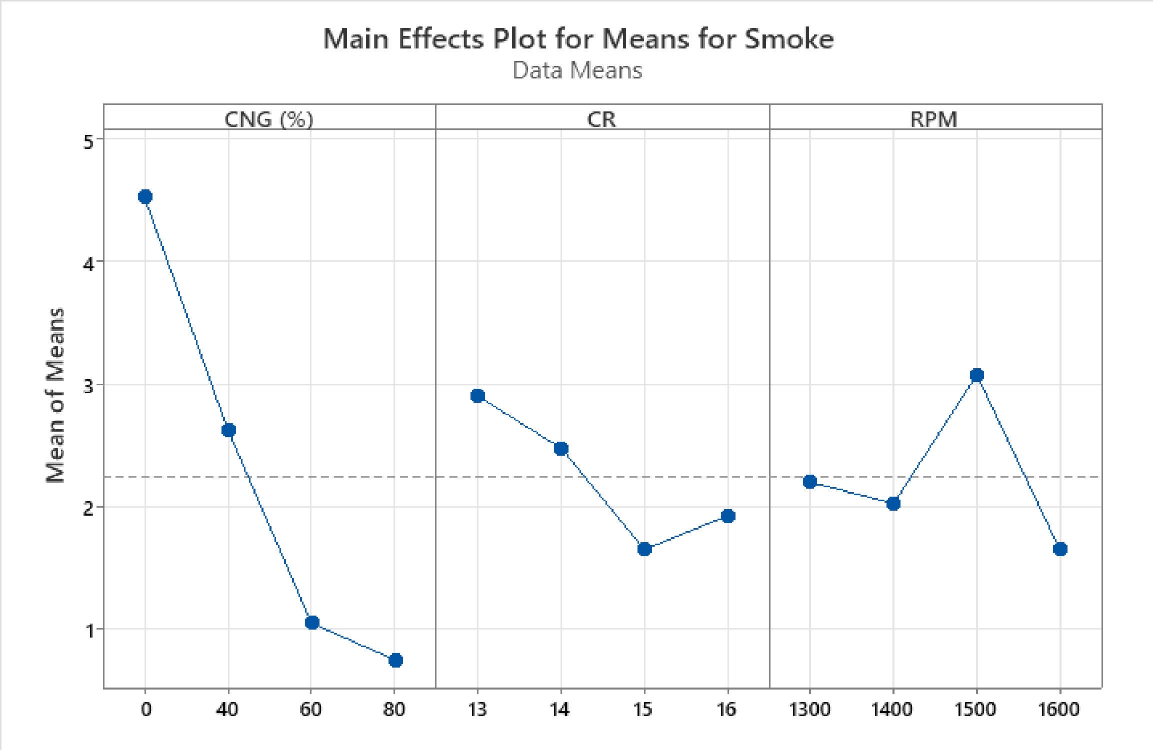


Fig. 4.8. (b) Mean of Means for Smoke

The coefficient of determination ($R^2$) was calculated to be 91.39% for the SNR analysis and 80.45% for the means analysis. Employing statistical methods on the mean signal-to-noise ratio (SNR) and the mean of means, it was determined that the optimal smoke value was attained with a compression ratio (CR) of 16, a CNG substitution ratio of 80%, and an engine speed of 1400 rpm.

# CHAPTER 5. EXPERIMENTAL RESULTS & DISCUSSIONS

The experimental setup encompassed two distinct operating modes: baseline diesel and dual fuel, which are extensively outlined in the experimental setup section. In the dual fuel mode, a diesel engine was employed to harness electricity from the utilization of gaseous fuel. To facilitate this mode of operation, comprehensive upgrades were executed in the diesel engine. This chapter presents the outcomes of the performance and emission characteristics of both a conventional diesel engine and a dual fuel engine across various Compression Ratios (CRs), engine speeds, and fuel Injection Pressures (IPs).

The investigation delves into the performance evaluation of a 4-stroke, single-cylinder Direct Injection (DI) engine functioning under a constant engine load in the dual fuel mode. Furthermore, an analysis of a CNG/diesel engine under different compression ratios, engine speeds, and injection pressures is provided. Performance metrics such as Brake Thermal Efficiency (BTE), Brake Specific Fuel Consumption (BSFC), and Volumetric Efficiency, Heat balance are utilized to assess engine performance. Moreover, an array of emission parameters including Hydrocarbons (HC), Carbon Monoxide (CO), Carbon Dioxide ($CO_2$), Nitrogen oxide (NOx), and smoke emissions are scrutinized.

The primary objective of this study is to investigate the impact of compression ratio, engine speeds, and injection pressure on the behavior of a CNG/diesel dual fuel mode in the diesel engine. Comparative analysis was conducted by exclusively testing the CI engine with diesel fuel under similar conditions for both operating modes.

## *5.1 Performance of diesel and dual fuel mode varying compression ratio*

In the experiment, a dual-fuel approach employing diesel/CNG fuel was adopted to assess performance characteristics. Comparative analysis was conducted against the performance achieved through 100% diesel fuel operation. The dual fuel engine underwent testing across a range of compression ratios (13, 13.5, 14, 14.5, and 15) in diesel mode, alongside operation in dual fuel mode utilizing diesel/CNG, all while maintaining a constant engine load and a rotational speed of 1500 rpm.

### *5.1.1 Air Flow and Fuel Flow*

Figure 5.1 shows the airflow and fuel flow variation. Airflow refers to the volume or mass of air that is drawn into the engine's combustion chamber during the intake stroke while fuel flow refers to the rate at which fuel is delivered to the engine's combustion chamber. The fuel is mixed with the incoming air before entering the combustion chamber. In diesel CNG dual fuel combustion, airflow is higher than fuel flow. CNG typically requires a higher air-to-fuel ratio for complete combustion compared to diesel. This means that more air is needed to burn a given amount of CNG effectively. Therefore, to ensure the complete combustion of CNG, a higher airflow rate is necessary. The stoichiometric ratio is the ideal ratio of air to fuel required for complete combustion. For CNG, the stoichiometric ratio is higher than for diesel due to the different chemical compositions and combustion characteristics of the fuels. Therefore, to achieve stoichiometric combustion, more air is required relative to the amount of CNG compared to diesel. Diesel is often used as a pilot fuel in dual-fuel combustion systems to ignite the CNG-air mixture. Therefore, only a small amount of diesel is required for ignition purposes. The higher airflow rate ensures sufficient oxygen availability for the combustion of both the diesel pilot fuel and the CNG.

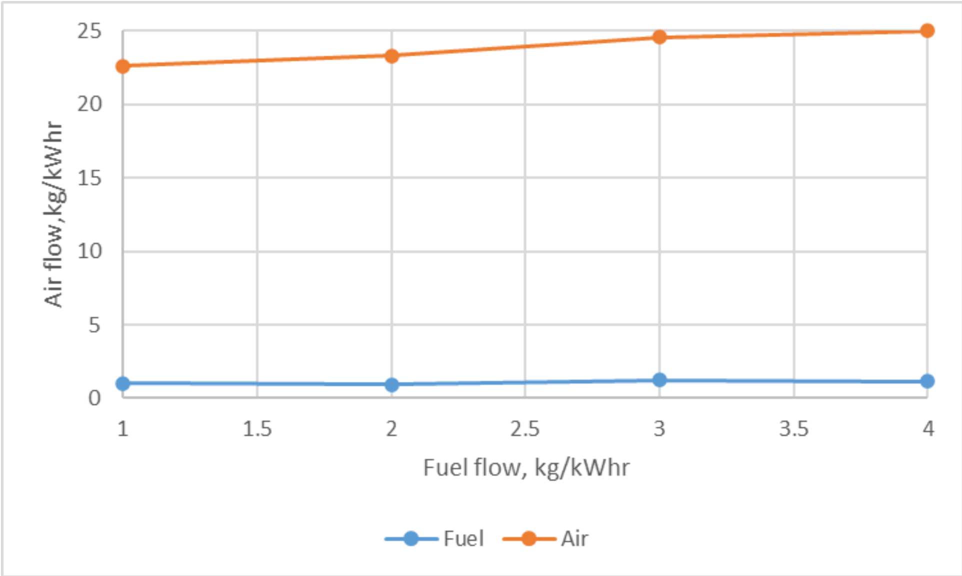


Fig. 5.1. Airflow vs fuel flow

### *5.1.2 Air Fuel Ratio*

The compression ratio influences the amount of air drawn into the engine, the conditions under which combustion occurs, and the stability of combustion. These factors collectively impact the optimal air-fuel ratio (AFR) required for efficient and effective engine operation. Figure 5.2 visually depicts the AFR variations observed in a dual-fuel engine operating in both diesel mode and diesel/CNG dual-fuel mode.

The compression ratio influences the temperature and pressure of the air-fuel mixture during the compression stroke. Higher compression ratios lead to higher temperatures and pressures in the combustion chamber before ignition. This elevated temperature and pressure can improve the efficiency of combustion by facilitating better atomization of the fuel and a more complete mixing of fuel and air. The compression ratio indirectly affects the ideal air-fuel ratio for combustion. Engines with higher compression ratios typically require slightly richer air-fuel mixtures to prevent knocking and ensure proper combustion. This adjustment is necessary to compensate for the increased pressure and temperature within the combustion chamber.

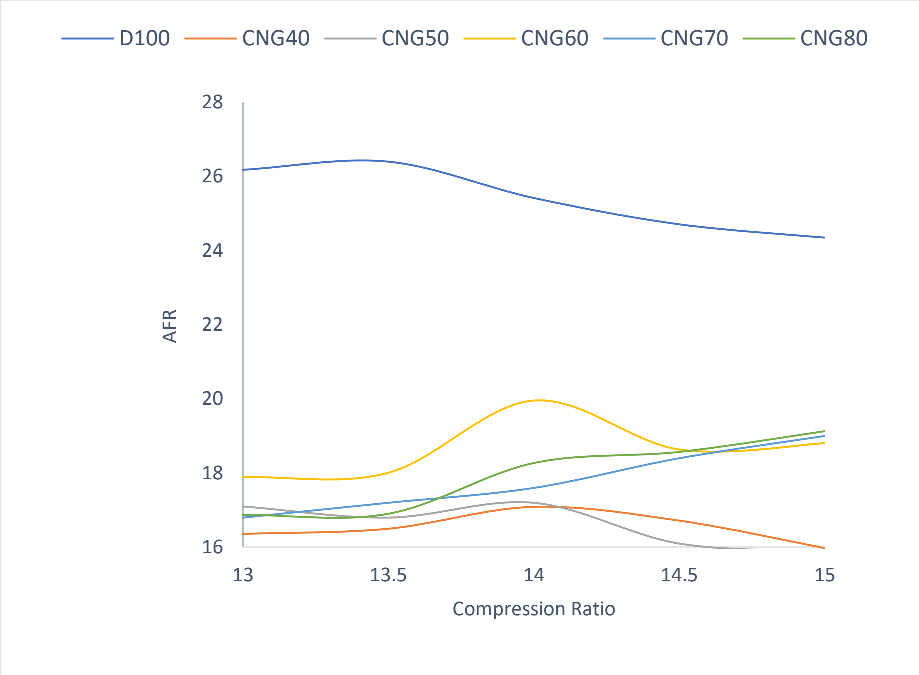


Fig. 5.2. Variation of AFR with variation of CR of diesel engine

### *5.1.3 Brake thermal efficiency*

Brake Thermal Efficiency (BTE) serves as a crucial metric, converting the chemical energy present in fuel into useful work output. Figure 5.3 visually depicts the BTE variations observed in a dual-fuel engine operating in both diesel mode and diesel/CNG dual-fuel mode. It's noteworthy that BTE exhibits a consistent increase with the rise in compression ratio [94].

The extent of gaseous energy introduced also influences BTE within the dual-fuel mode. With increasing CR, the injection of fuel into the charge occurs within an environment of heightened temperature and pressure, fostering improved air-fuel mixture conditions and accelerated fuel evaporation. Consequently, this leads to enhanced brake thermal efficiency, particularly evident at higher CR values. Notably, the diesel/CNG dual-fuel mode showcases superior BTE levels at both lower and higher CR ranges compared to the single diesel fuel mode.

Moreover, it's observed that a lower CNG energy share in dual-fuel combustion results in heightened BTE compared to combustion with 100% diesel (D100). The pinnacle of BTE, reaching 63.9% with a 40% CNG share (CNG40), is attained at CR 15 (as depicted in Figure 5.3). This phenomenon can be attributed to the greater availability of diesel fuel at lower CNG energy shares, consequently enhancing combustion efficiency due to the higher maximum flame temperature compared to situations with a higher CNG energy share. The BTE increases by 60.63%, 58.27%, 59.07%, 60.94%, and 63.71% for CNG40 dual fuel combustion compared to D100. For CNG50, BTE raised by 56.36%, 53.73%, 52.12%, 57.65%, and 58.84% compared to D100. For the CNG60 dual fuel combustion, BTE increased by 51.64%, 49.02%, 49.83%, 56.47%, and 55.81% to D100 fuel combustion. For CNG70 , the BTE is increased by 49.48%, 45.33%, 43.24%, 46.47%, and 52.13% compared to D100 .The same pattern is observed for the CNG80 combustion. As the CR increased, BTE increased by 46.11%, 42.13%, 42.63%, 47.91%, and 48.45% at all CR than D100 fuel combustion.

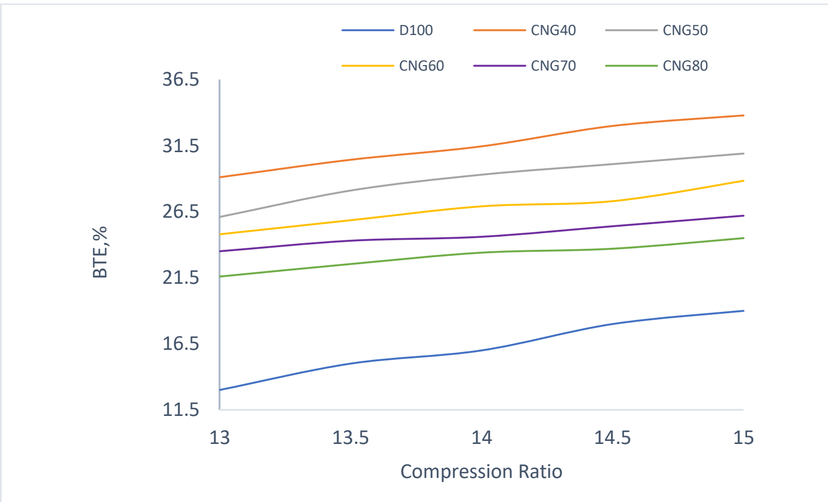


Fig. 5.3. Variation of BTE with variation of CR of diesel engine

Figure 5.4 shows the variation of BTE with respect to AFR of dual fuel. As increase the percentage of CNG in the fuel mixture, the overall air-fuel ratio tends to increase. This is because CNG has a higher octane rating compared to diesel, meaning it requires more air for complete combustion. Therefore, more air needs to be mixed with the increasing amount of CNG to maintain proper combustion stoichiometry. Higher air-fuel ratios can lead to lower combustion temperatures due to the excess air present in the mixture. While lower combustion temperatures can reduce thermal efficiency, as lower temperatures lead to less efficient energy conversion from heat to mechanical work.

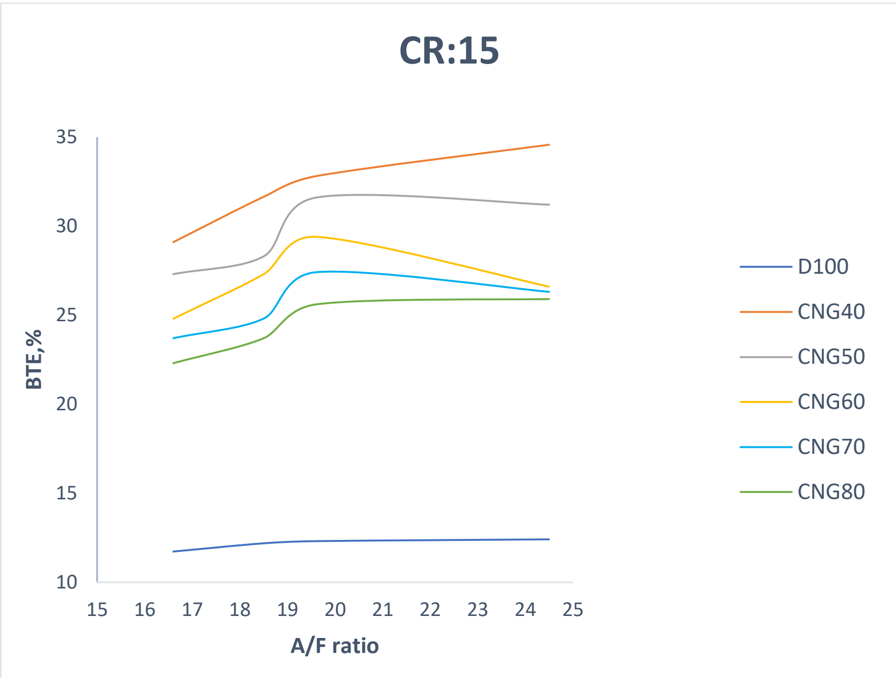


Fig. 5.4. Variation of BTE with different AFR of diesel engine

*5.1.4 Heat Balance*

The heat balance of a diesel-CNG dual-fuel combustion system refers to the distribution of the heat generated during the combustion process among various components of the engine. It provides insights into how effectively the energy from fuel is being converted into useful work and lost through various heat transfer mechanisms. Higher engine speeds may lead to shorter combustion durations and less time for complete combustion, affecting combustion efficiency and heat release characteristics. The heat generated during combustion is transferred to various engine components, including the cylinder walls, piston, cylinder head, and cooling system. The rate of heat transfer depends on engine speed, load, and cooling system efficiency. Higher engine speeds generally result in increased heat transfer rates due to higher combustion rates and frictional losses within the engine. The efficiency of the engine's cooling system plays a crucial role in dissipating excess heat generated during combustion. At higher engine speeds, the cooling system must work harder to dissipate heat effectively. Figure 5.5 shows the heat balance of dual fuel.

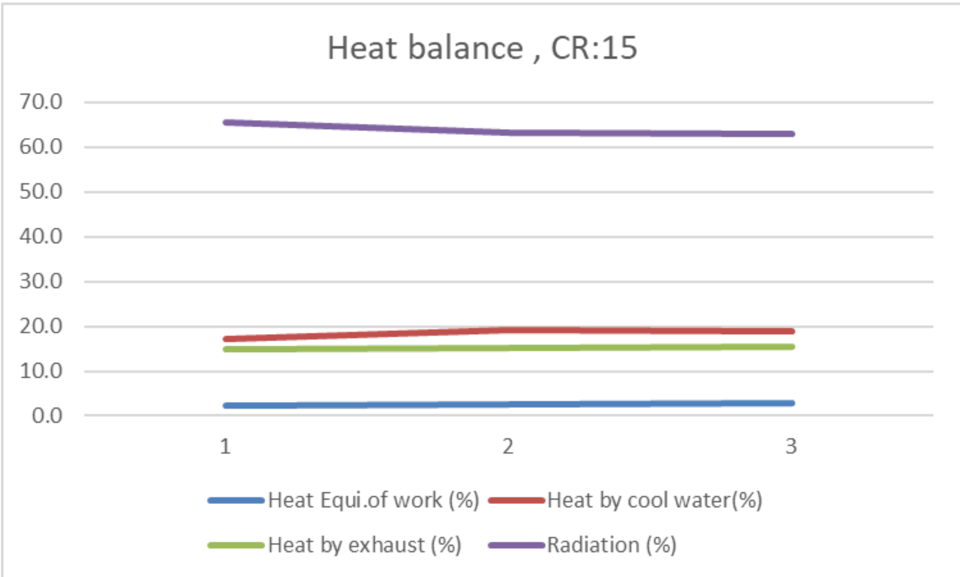


Fig. 5.5. Heat balance of diesel/CNG dual fuel diesel engine

Figure 5.6 (a) shows that as increased in BP, the exhaust heat increased in diesel/CNG dual fuel combustion. The increase in exhaust heat with increasing brake power (BP) suggests that as the engine output increases, more fuel is combusted per cycle, leading to higher heat generation and subsequently higher exhaust temperatures. With a higher proportion of CNG, the combustion characteristics can shift towards a more rapid and complete combustion process. This can lead to higher combustion temperatures and increased heat release, thus resulting in higher exhaust heat. Changes in the combustion process due to varying proportions of CNG can affect the overall efficiency of combustion. CNG has different combustion properties compared to diesel, such as higher octane rating and different flame speed. CNG combustion tends to release heat differently compared to diesel combustion. This can alter the combustion temperature and consequently, the amount of heat transferred to the exhaust gases.

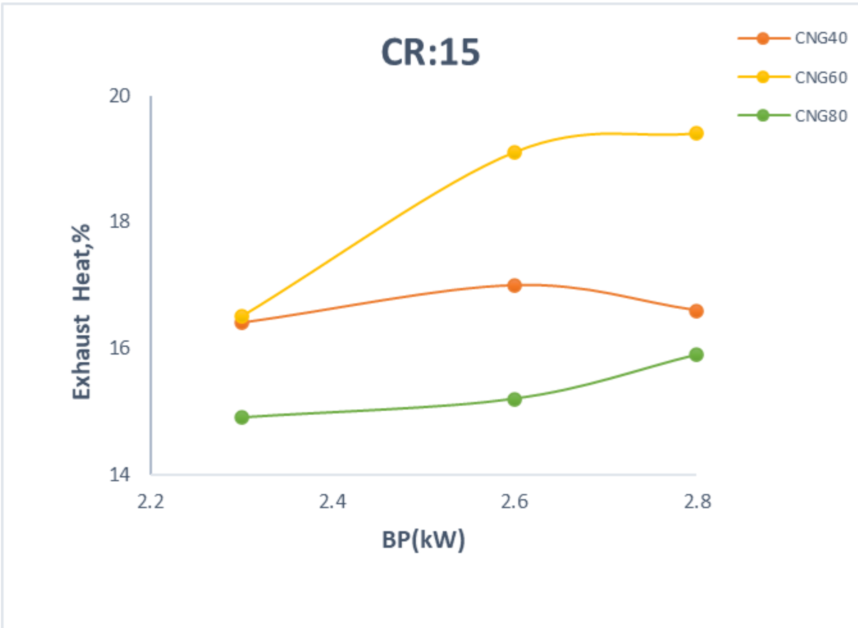


Fig.5.6 (a). Variation of Exhaust heat with variation of BP of dual fuel engine

### 5.1.5 *Brake Specific fuel consumption*

Brake Specific Fuel Consumption (BSFC) represents the amount of fuel consumed per unit of engine power output, a crucial metric influenced by both diesel and CNG fuel consumption rates, as well as their respective calorific values, particularly in diesel and dual-fuel modes. Notably, findings revealed that the dual-fuel mode exhibited a higher BSFC compared to the diesel mode [64]. An interesting observation emerged regarding the impact of natural gas quantity on BSFC: as the amount of natural gas increased, BSFC values decreased, albeit remaining higher across all-natural gas rates compared to single diesel fuel operation [95]. Furthermore, BSFC displayed an increase in dual-fuel combustion across all compression ratios compared to single diesel fuel combustion, as depicted in Figure 5.6 (b). This trend was particularly pronounced with the highest BSFC observed across all CR values when employing a 40% CNG energy share. This phenomenon can be attributed to the substantially higher excess air ratio in the air-fuel mixture when utilizing a lower CNG energy share. In lean air-fuel mixtures, the combustion chamber receives additional CNG, effectively replacing diesel fuel and influencing BSFC levels accordingly.

The BSFC increases by 30.43%, 35.27%, 37.07%, 40.83%, and 39.10% for CNG40 dual fuel combustion compared to D100. For the case of CNG50, the BSFC is enhanced by 28.2%, 34.51%, 32.64%, 32.27% and 35.34% . For the CNG60 dual fuel combustion, BSFC increased by 27.64%, 34.02%, 29.83%, 26.47%, and 31.81% to D100 fuel combustion. For the case of CNG50, the BSFC is enhanced by 27.52%, 34.46%, 31.54%, 28.16% and 29.63% than D100. The same pattern is observed for the CNG80 combustion. As the CR increased, BSFC increased by 27.11%, 35.13%, 32.63%, 29.91%, and 32.15% at all CR than D100 fuel combustion.

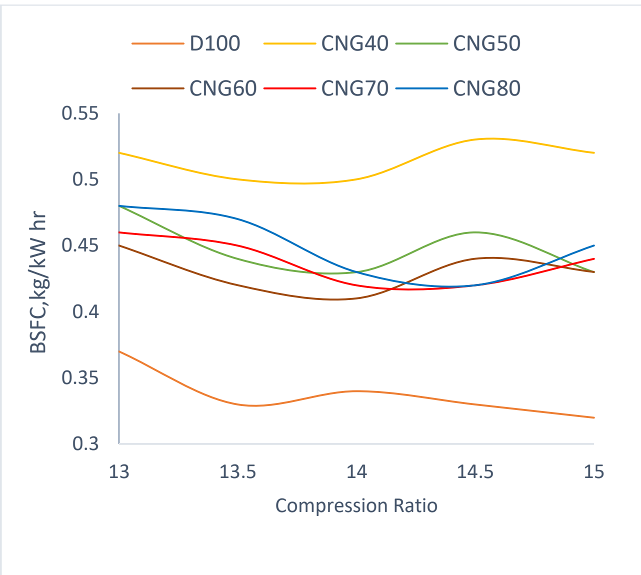


Fig. 5.6 (b). Variation of BSFC with variation of CR of diesel engine

Figure 5.7 illustrates the variation of BSFC versus AFR of DF combustion. As increasing the CNG percentage the BSFC decreased in diesel CNG dual fuel Combustion but BSFC is higher at all CNG energy share compared to pure diesel. This is because diesel fuel typically has a higher energy density compared to CNG. Therefore, even though diesel combustion may not be as efficient as CNG combustion, it provides more energy per unit of fuel consumed, resulting in lower BSFC when compared to a mixture with higher proportions of CNG. Higher air-fuel ratios can lead to lower combustion temperatures, reducing heat losses to the engine components and the surrounding environment. This reduction in heat losses contributes to lower BSFC.

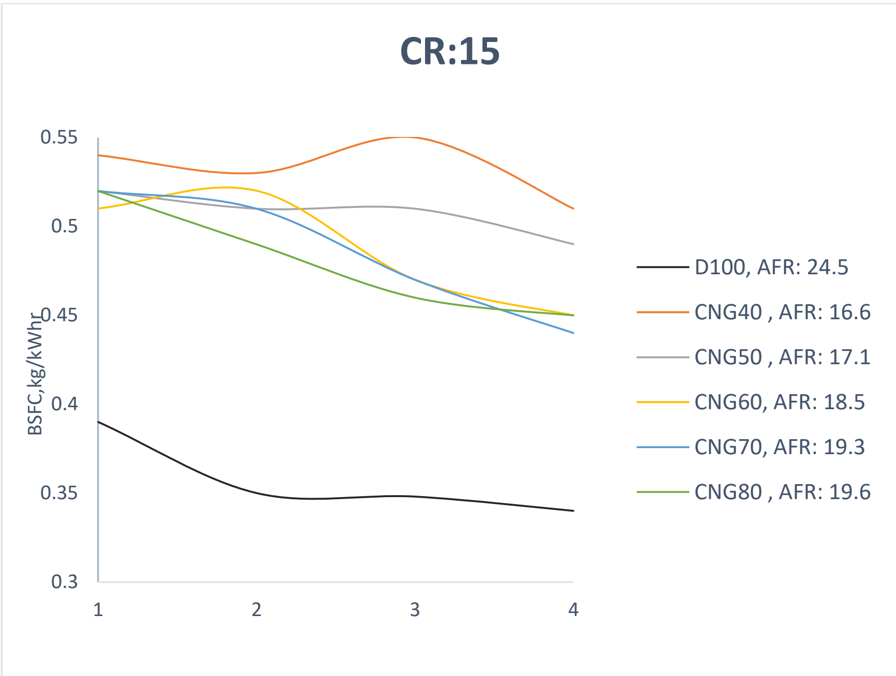


Fig. 5.7. Variation of BSFC with different AFR of diesel engine

### *5.2 Emission of diesel and dual fuel mode varying compression ratio*

Emission analysis was conducted on the engine operating in both dual fuel and diesel modes across different compression ratios. This section presents the experimental examination of pollutants such as CO, HC, $CO_2$, NOx, and smoke emissions.

### *5.2.1 CO emission*

The primary influence of CO emission is low flame temperature and poor air/fuel mixture from the engine. CO emissions are the result of incomplete combustion [96]. Generally, CO emission increases as increasing in the CNG substitution ratio [65]. With increasing CNG supply, the ignition fuel quantity and spray combustion region decrease at a lower CNG substitution ratio. The lower equivalence ratio in the CNG/air mixture indicates that the quenching region expands, and the CO emissions increase more than pure diesel. For a higher CNG substitution ratio, the equivalence ratio rises by increasing the CNG quantity and reducing pilot fuel quantity, decreasing the ignition temperature and leading to CO emissions. Figure 5.8 displays the relationship between CO emissions and CR for both operating modes. In comparison to D100, CO emissions increased by 11.1%, 20%, 7.6%, 7.1%, and 7% at all CR for CNG40 dual fuel combustion. For CNG50, it raised by 136.6%, 87.7%, 35.2%, 16.7% and 11.4% than D100. Similarly, The CO emissions incresed by 277.7%, 180%,69.2%, 28.5%, and 13.3% at CNG60 substitution ratio than D100 fuel combustion. For CNG70, it raised by 296.7%, 214.4%, 89.6%, 87.7%, 56.1%, and 14.6% compared to D100. The same pattern was observed for the CNG80 substitution ratio, and CO emission increased by 322.2%, 240%, 115.5%, 57.1%, and 20% than D100% fuel at all CR of 13:1 to 15:1. The maximum increment of CO emission of 322.2% was achieved at CR13 by CNG80 substitution ratio.

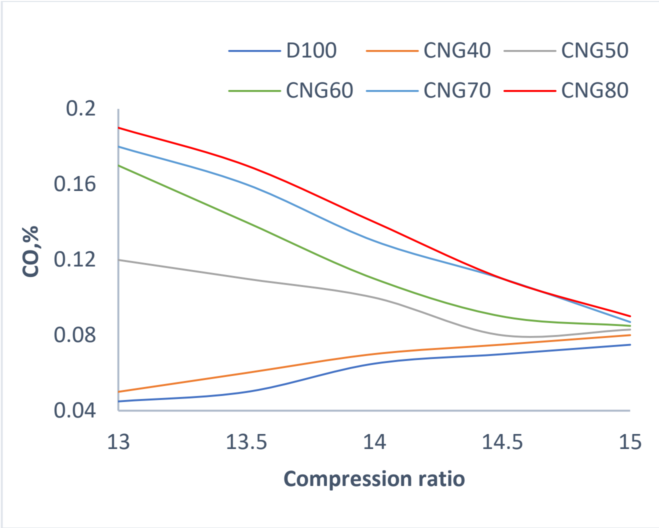


Fig. 5.8. Variation CO emission with variation of CR of diesel engine

### *5.2.2 HC emission*

The emission of hydrocarbons (HC) primarily stems from incomplete combustion, a phenomenon exacerbated by oxygen scarcity and reduced combustion rates in dual-fuel combustion. Notably, research indicates that HC emissions are notably higher in dual-fuel combustion compared to single-diesel fuel combustion, as illustrated in Figure 5.9. Moreover, HC emissions display an increasing trend with higher gas flow rates, likely due to incomplete combustion of liquid fuel [97]. Insufficient oxygen availability for complete combustion is a plausible explanation for this phenomenon. Compared to conventional diesel fuel, burning CNG necessitates a larger volume of air for complete combustion. Additionally, during dual-fuel (DF) operation with CNG, the volumetric efficiency tends to be lower compared to normal CI engine operation. This reduction in volumetric efficiency, particularly at higher gas flow rates, contributes to increased HC emission levels. This can be attributed to lower oxygen availability for combustion and reduced charge temperature associated with CNG usage.

Furthermore, the lower charge temperature with CNG utilization leads to slower combustion during the later stages of the diffusion combustion phase. Consequently, unburnt HC molecules escape through the exhaust port during valve overlaps, exacerbating combustion deterioration and resulting in higher HC emission levels. The HC emissions are higher at CNG40 dual fuel combustion compared to D100 fuel by 46%, 40.1%, 30.3%, 16.6%, and 6.06% at all CR. For CNG50, it increased by 71.3%, 55%, 46.4%, 81.3% and 85.7% . At CNG60 combustion, HC emissions increased by 98.6%, 66.6%, 70%, 105.5%, and 142.4% compared to D100 combustion. For CNG70, it increased by 136.6%, 108.7%, 98.6%, 129.3% and 157.7% than D100. The substitution ratio of CNG80 combustion, HC emissions increased by 180%, 144.4%, 130%, 161.1%, and 187.8%, respectively, compared to D100 fuel at CR of 13:1 to 15:1. It is observed that the maximum increased HC emission was achieved at CR13 by CNG80 substitution ratio.

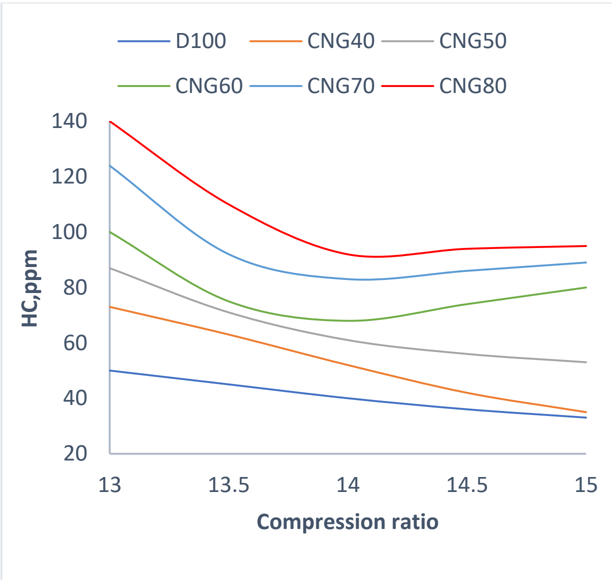


Fig. 5.9. Variation of HC emission with variation of CR of diesel engine

### 5.2.3 $CO_2$ emission

Carbon dioxide ($CO_2$) is a significant contributor to greenhouse gases, playing a role in global warming. The substitution of CNG in place of diesel fuel influences $CO_2$ emissions due to the differing carbon atom availability and oxygen content. Typically, in dual-fuel (DF) mode, $CO_2$ emissions are lower compared to combustion using only diesel fuel. Research findings support this notion, indicating that $CO_2$ emissions decrease as the ratio of CNG substitution increases compared to combustion using 100% diesel fuel (D100) [98][99]. This reduction in $CO_2$ emissions can be attributed to the inherent properties of CNG, such as its lower carbon content and the availability of oxygen during combustion, which leads to more efficient fuel utilization and consequently lower $CO_2$ emissions compared to diesel fuel combustion.

Figure 5.10 shows that $CO_2$ emission was lower in DF combustion at all CRs. At the CNG40 substitution ratio, the $CO_2$ emissions are reduced by 7.5%, 2.6%, 22.4%, 18.9%, and 18.4% at all CR from 13:1 to 15:1 compared to D100 fuel. For CNG50 gas substitution ratio, $CO_2$ decreased by 16.6%, 13.4%, 38.6%, 29.3% and 25.8% than D100. The $CO_2$ emissions decreased by 26.4%, 21.8%, 48.2%, 41.9%, and 36.3% for the CNG60 substitution ratio. For CNG70 gas substitution ratio, $CO_2$ decreased by 43.6%, 28.1%, 58.6%, 69.3% and 77.8% than D100. The same pattern was observed for the CNG80 substitution ratio, and $CO_2$ emissions were reduced by 59.2%, 34.4%, 79.1%, 91.3 %, and 114.3% than D100 fuel combustion. The maximum reduction of $CO_2$ emission was attained at the CNG80 substitution ratio at CR 15.

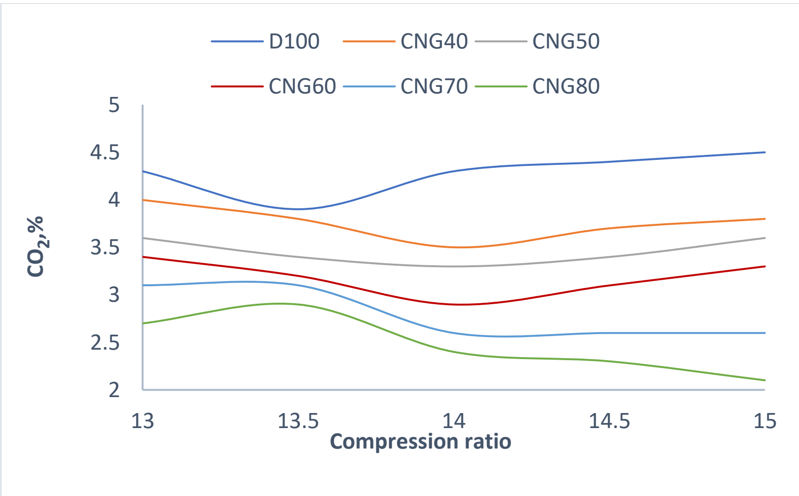


Fig. 5.10. Variation of $CO_2$ emission with variation of CR of diesel engine

### *5.2.4 $NO_X$ emission*

The formation of nitrogen oxides (NOx) is influenced by various factors including oxygen levels, cylinder temperatures, and the duration of combustion reactions. Typically, NOx emissions decrease in dual-fuel (DF) mode, as supported by research findings [100][101]. In diesel/CNG DF combustion, the combustion process shifts towards a lean, premixed regime due to the increased stoichiometric air/fuel ratio. This transition lowers cylinder temperatures, resulting in decreased NOx emissions. In contrast, in single diesel combustion, the majority of the fuel burns as a diffusion flame near the stoichiometric equivalence ratio, leading to stoichiometric combustion and higher NOx emissions due to elevated combustion temperatures.

As depicted in Figure 5.11, NOx emissions decrease with increasing CNG substitution ratios compared to combustion using 100% diesel fuel (D100%). This reduction in NOx emissions can be attributed to the leaner combustion conditions facilitated by CNG substitution, which effectively mitigates the formation of nitrogen oxides. At the CNG40 dual fuel combustion substitution ratio, $NO_X$ emissions are reduced by 3.02%, 10.5%, 25.9%, 19.1%, and 16.9% at all CR. For CNG50 gas substitution ratio, $NO_X$ decreased by 118.6%, 113.4%, 116.3%, 63.3% and 35.8% than D100. The $NO_X$ emissions were reduced by 222.3%, 207%, 204%, 103.4%, and 52.7% for CNG60 substitution ratio DF combustion. For CNG70 gas substitution ratio, $NO_X$ reduced by 297.6%, 473.4%, 593.7%, 503.3% and 445.8% compared to D100.

The same pattern was observed for the CNG80 substitution ratio, and $NO_X$ emissions decreased by 396.8%, 746.7%, 990%, 904%, and 840.5%, respectively, compared to D100 fuel combustion at CR of 13:1 to 15:1. At the CNG80 substitution ratio, the lowest $NO_X$ were achieved at CR 14.

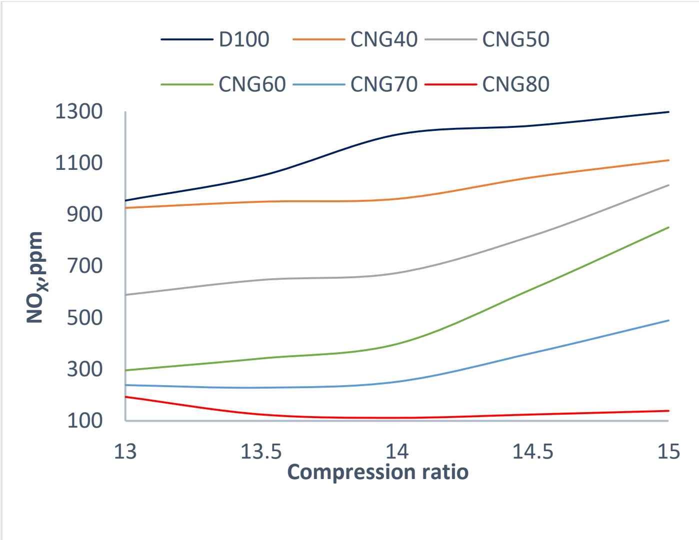


Fig. 5.11. Variation of $NO_X$ emission with Variation of CR of diesel engine

### *5.2.5 Smoke emission*

Figure 5.12 illustrates the variation in smoke opacity across different CR and CNG substitution ratios. The primary factor influencing smoke opacity is the volume of liquid fuel injected into the combustion chamber. In a dual-fuel engine, the necessity for diesel fuel decreases as it is partially replaced by cleaner-burning CNG fuel, resulting in lower smoke emissions. Increasing the CNG substitution ratio enhances the combustion of the fuel mixture and reduces the Carbon-to-Hydrogen (C/H) ratio, resulting in decreased smoke emissions and a greater heat contribution from the CNG fuel. The clean-burning nature of CNG aids in reducing soot emissions and facilitates soot oxidation, particularly at higher CNG substitution ratios [102][103]. This is attributed to the composition of CNG, which primarily consists of methane and belongs to the lower paraffin family, thereby mitigating significant soot production.

At lower CNG substitution ratios, the heat input contribution from CNG fuel diminishes, while the pilot liquid fuel increases the combustion carbon content and smoke levels compared to higher CNG substitution ratios. Figure 5.12 further illustrates that as the CNG substitution ratio increases, the smoke level decreases compared to combustion using 100% diesel fuel (D100). This trend highlights the beneficial impact of higher CNG substitution ratios in reducing smoke emissions in dual-fuel combustion systems. When the CNG40 substitution ratio is used in DF combustion, the smoke emissions are reduced by 35.2%, 64.7%, 14.2%, 38.6%, and 50% at CR from 13:1 to 15:1 compared to D100 fuel combustion. For CNG50 gas substitution ratio, smoke opacity decreased by 23.6%, 37.4%, 17.6%, 28.2% and 82.8% than D100. The smoke emissions decreased by 17.1%, 16.6%, 23%, 16% and 125% for the CNG60 substitution ratio. For CNG70 gas substitution ratio, smoke opacity reduced by 39.8%, 104.4%, 27.6%, 37.4% and 237.8% compared to D100.

Similarly, The same pattern was at the CNG80 substitution ratio, and the smoke emission was reduced by 68.4%, 194.6%, 33.5%,55.3%, and 350% than D100 fuel combustion for all CR. At the CNG80 substitution ratio, the lowest smoke emissions were obtained at CR 15.

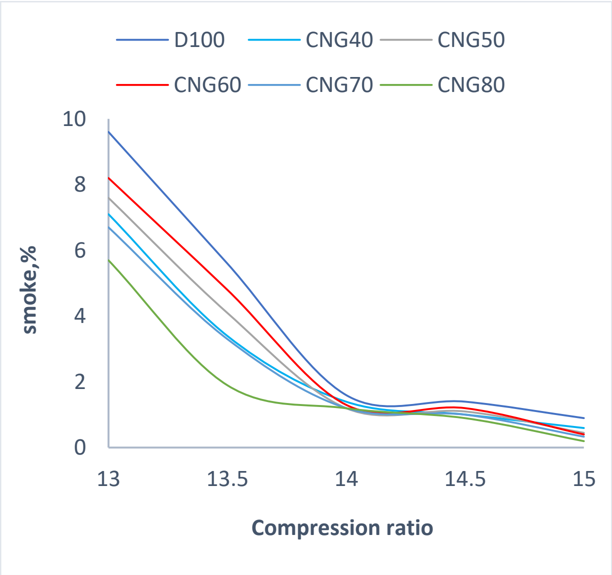


Fig. 5.12. Variation of smoke emission with variation of CR of diesel engine

## 5.3 Performance of diesel and dual fuel engine mode varying Engine speed

In the experimental setup, a Compression Ignition (CI) engine was utilized to assess the performance of dual-fuel operation using diesel/CNG fuel, contrasting it with the performance achieved through 100% diesel fuel operation. To facilitate a comparative analysis of the dual-fuel engine's performance across various engine speeds, the compression ratio was standardized at 15:1. Consequently, the performance evaluation of the dual-fuel engine was conducted under diesel/CNG dual-fuel mode at different engine speeds ranging from 1200 to 1500 rpm, with increments of 50 rpm. This standardized setup ensured consistent conditions for assessing the engine's performance across the specified range of engine speeds while operating under dual-fuel mode with a compression ratio of 15:1.

### *5.3.1 Air Fuel Ratio*

In the realm of IC engines, the AFR undergoes dynamic adjustments as the engine RPM climbs. This fluctuation is meticulously managed by the engine control unit, which fine-tunes the balance between fuel and air intake based on a multitude of factors including engine load, temperature, and rotational speed. During lower engine speeds, the management system opts for a richer mixture, favouring a higher proportion of fuel to air. This deliberate choice is aimed at promoting smooth combustion and bolstering low-end torque output. As the engine's revolutions per minute escalate, a transition occurs towards a leaner mixture, characterized by a higher ratio of air to fuel. This adjustment is crafted to optimize efficiency while concurrently curbing emissions. Crucially, modern engines are outfitted with an array of sensors engineered to gauge the prevailing AFR with precision. These sensors serve as vigilant custodians, ensuring that the engine operates within the bounds of its optimal performance spectrum across diverse operating conditions.

Figure 5.13 visually depicts the AFR variations observed in a dual-fuel engine operating in both diesel mode and diesel/CNG dual-fuel mode. In a CNG-diesel dual fuel engine, the introduction of CNG into the air intake reduces the volume of air available for combustion in the cylinder. Since combustion requires a sufficient supply of oxygen from the air, this reduction in combustion air can hinder the combustion process. With less oxygen available, there are fewer ignition sources generated, leading to diminished combustion performance. Moreover, when the airflow rate decreases due to the reduced intake of air, the air-fuel mixture becomes richer. This means there is a higher concentration of fuel compared to air, which can result in incomplete combustion. Incomplete combustion occurs when not all the fuel is burned, leading to wasted fuel and potentially higher emissions. Thus, the engine may not operate at its optimal efficiency, and there could be adverse effects on both performance and emissions.

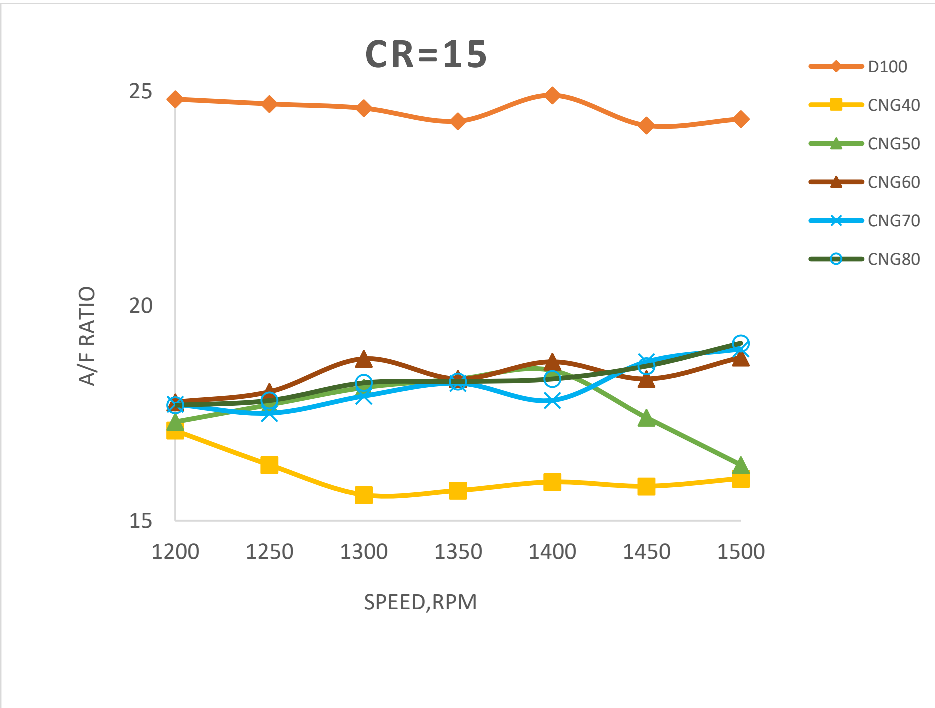


Fig.5.13. Variation of AFR with different engine speed of diesel engine

### 5.3.2 *Volumetric efficiency*

Volumetric efficiency is a measure of how effectively an engine's cylinders are filled with air (or air-fuel mixture) during the intake stroke compared to their maximum possible capacity. It is expressed as a percentage and represents the ratio of the actual volume of air (or air-fuel mixture) drawn into the cylinders during the intake stroke to the theoretical maximum volume that the cylinders could hold at ambient conditions. As shown in the figure as the speed increased, the volumetric efficiency decreased in diesel CNG dual fuel engines. At higher engine speeds, the intake valve timing may be optimized for maximum power output rather than volumetric efficiency. This optimization can result in shorter intake valve opening durations or less overlap between intake and exhaust valve opening periods. Reduced intake valve timing optimization limits the amount of air that can enter the combustion chamber during each intake stroke, thereby reducing volumetric efficiency. At higher engine speeds, the air intake system may experience increased airflow restrictions due to factors such as air turbulence, and pressure losses. These restrictions impede the flow of air into the combustion chamber, reducing volumetric efficiency by limiting the amount of air available for combustion. Figure 5.14, observe shows the volumetric Efficiency affected by both D100 (pure diesel) combustion and dual-fuel combustion as engine speeds vary.

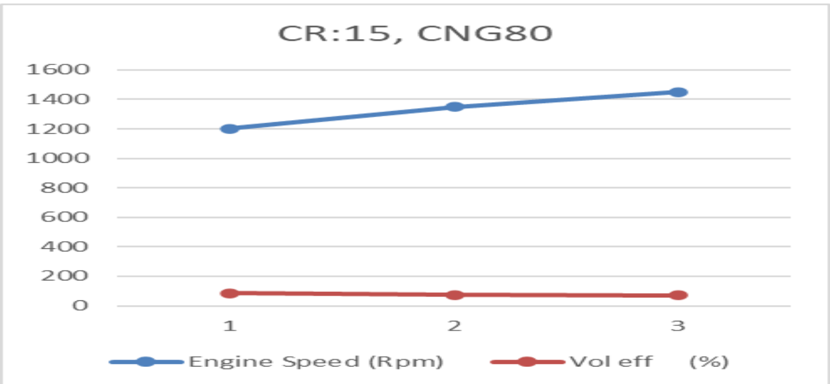


Fig. 5.14. Volumetric Efficiency with different speed of dual fuel engine

### *5.3.3 Brake Thermal Efficiency*

Figure 5.15 illustrates the influence of both D100 and dual-fuel combustion on Brake Thermal Efficiency (BTE) across various engine speeds. Notably, BTE demonstrates an increase with both increasing CNG energy share and engine speed, as depicted in the figure. One noteworthy observation is that dual-fuel combustion with a lower CNG energy share yields higher BTE compared to D100 combustion. This phenomenon can be attributed to the slower flame propagation of the air-gas mixture, particularly with a higher CNG substitution ratio. Additionally, an increase in the CNG energy share results in a longer igniting delay time.

The availability of diesel fuel is more pronounced at lower CNG energy shares, contributing to better combustion efficiency due to the higher maximum flame temperature achieved compared to higher CNG energy shares. This observation underscores the intricate interplay between fuel composition, combustion efficiency, and resultant BTE levels in dual-fuel combustion scenarios. Figure 5.15 shows that when the engine speed increases, the BTE increases by 59.72%, 57.27%, 57.07%, 60.94%, 61.77%, 64.02%, and 65.59% for CNG40 dual fuel combustion compared to D100. For CNG50, BTE raised by 55.36%, 53.37%, 53.24% 57.41%, 58.32%, 60.33%, and 59.89% compared to D100. For the CNG60 dual fuel combustion, BTE increased by 52.74%, 49.72%, 49.83%, 55.38%, 55.37%, 57.82%, and 59.93% to D100 fuel combustion. For CNG70, BTE raised by 48.62%, 43.86%, 42.24% 57.41%, 58.32%, 60.33%, and 59.89% compared to D100. The same pattern is observed for the CNG80 combustion. As the engine speeds increased, BTE increased by 45.71%, 42.32%, 48.61%, 49.3%, 52.46%, 54.26%, and 58.37% at all engine speeds than D100 fuel combustion.

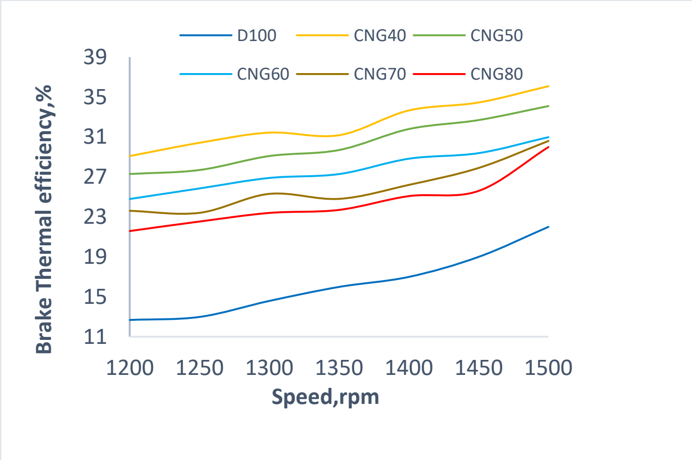


Fig. 5.15. Variation of BTE versus engine speed of diesel engine

### *5.3.4 Brake Specific Fuel Consumption*

BSFC increased in dual fuel combustion at all engine speeds than single diesel fuel combustion. The highest BSFC was achieved for all engine speeds with CNG40 energy share. Because the excess air ratio of the air-fuel mixture is substantially higher for a lower CNG energy share. When the air-fuel mixture is lean, the combustion chamber receives additional CNG, which replaces the diesel fuel. Because of the decrease in diesel fuel quantity, the spark energy of the air-fuel mixture is reduced at a higher CNG energy share, which is also responsible for incomplete combustion. Complete combustion happens when the air-fuel mixture is too rich, lowering BSFC at a higher CNG energy share.

Figure 5.16 shows that BSFC increased in dual fuel combustion for all CNG energy shares and engine speed compared to D100 fuel. When comparing D100 fuel combustion to CNG40 dual fuel combustion, the BSFC increased by 31.48%, 34%, 40.74%, 37.5%, 40%, 33.33%, and 37.03% at all engine speeds in dual fuel mode. For CNG50, BSFC raised by 29.33%, 32.96%, 36.14%, 31.44%, 34.52%, 30.13%, and 29.77% compared to D100. Compared to D100, the value of BSFC increased by 28.84%, 36.53%, 30.43%, 25.53%, 28.26%, 24.44%, and 20.93% for CNG60 dual fuel combustion. For CNG70, BSFC raised by 28.33%, 35.56%, 31.18%, 26.41%, 28.52%, 26.37%, and 21.85% compared to D100. Same pattern is repeated for CNG80, BSFC was increased by 28.84%, 34%, 33.33%, 28.57%, 28.26%, 27.65%, and 22.72% compared to D100 fuel.

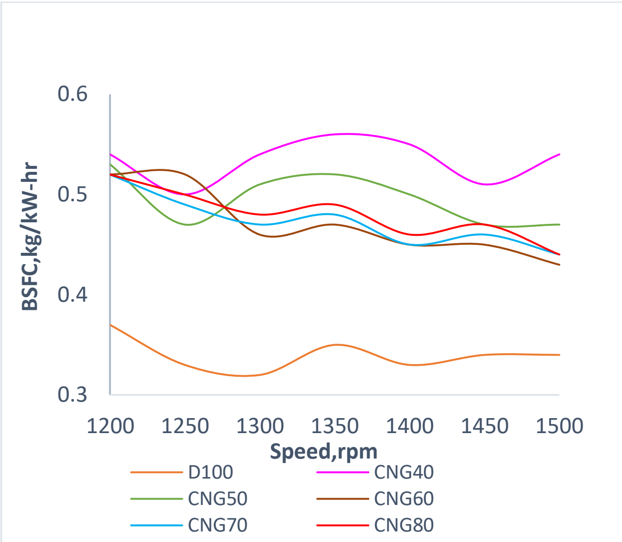


Fig. 5.16. Variation of BSFC versus engine speed of diesel engine

## 5.4 Emission of diesel and dual fuel mode varying engine speed

The investigation of emissions was performed for the engine in both dual fuel and diesel fuel modes at various engine speeds. This section discusses the experimental investigation of pollutants including CO, HC, $CO_2$, NOx, and smoke.

### *5.4.1 CO emission*

Figure 5.17 shows the CO emission deviations for D100 fuel and dual fuel combustion at different engine speeds. The engine's low flame temperature and a lack of air-fuel mixture are the primary causes of CO emissions. When a lower CNG energy share is used, CO emissions are lower than a higher CNG energy share. Because at lower CNG energy share, the ignition fuel quantity and spray combustion region decrease with increasing CNG supply due to the lower equivalence ratio in the CNG/air mixture. It indicates that the quenching region expands, and the CO emissions increase compared to single diesel fuel. For a higher CNG energy share, the equivalence ratios increase with increasing the CNG supply and decreased pilot fuel quantity, resulting in decreased ignition temperature and increased CO emission.

In comparison to D100, CO emissions increased by 18.9%, 10%, 9.4%, 9.2%, 12.5%, 14.28%, and 16.66% at all engine speeds for CNG40 dual fuel combustion, as shown in Figure 5.17. For CNG50, CO raised by 15.21%, 12.26%, 9.11%, 7.44%, 12.52%, 19.35%, and 22.72% compared to D100. The CO emissions increased by 13.33%, 15.38%, 9.09%, 5.8%, 12.5%, 25%, and 28.57% for CNG60 energy share than D100 fuel combustion. For CNG70, CO raised by 18.41%, 21.16%, 19.11%, 20.24%, 21.12%, 30.26%, and 32.52% than D100. The same pattern was observed for CNG80 energy share, CO emission increased by 23.52%, 26.66%, 28.57%,33.33%, 30%, 33.33%, and 37.5% than D100 fuel at engine speeds 1200 rpm to 1500 rpm.

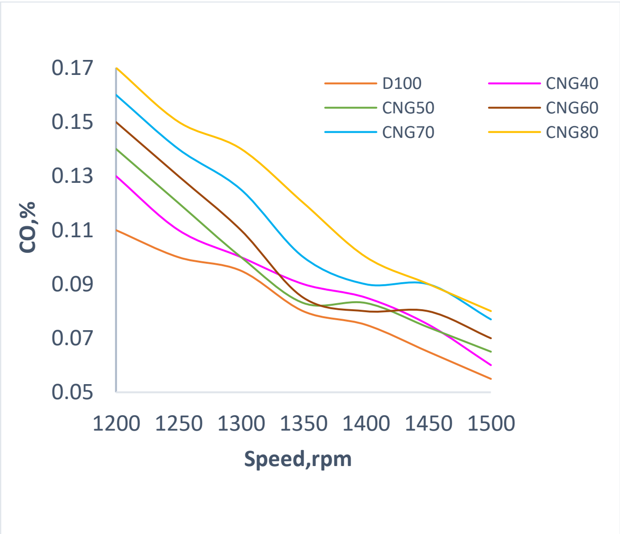


Fig.5.17 . Variation of CO emission versus engine speed of diesel engine

### 5.4.2 HC emission

Figure 5.18 shows that the HC emissions are significantly higher in dual-fuel combustion than in single-diesel fuel combustion. In dual-fuel combustion, the gaseous fuels are incompletely burned due to the lower combustion temperature caused by the high specific heat content of the gases, poor burning rate, and poor injection characteristics of the pilot fuel. Increases in HC emission are also caused by the release of unburned gas in both the crevice and squish zones during the power stroke. Compared to D100 combustion, HC emissions increased as the CNG energy share, and engine speeds increased.

The HC emission at CNG40 dual fuel combustion is higher than D100 fuel by 40.9%, 42.37%, 39.21%, 36.95%, 22.5%, 5.71%, and 8.68%. For CNG50, HC raised by 53.25%, 57.46%, 54.11%, 53.64%, 46.62%, 37.45%, and 42.58% compared to D100. At engine speeds of 1200-1500 rpm, HC emissions increased by 64.54%, 68.51%, 70.75%, 72.38%, 69%, 66%, and 63.15% for CNG60 energy share. For CNG70, HC raised by 73.15%, 75.66%, 74.21%, 73.64%, 71.32%, 67.51%, and 62.18% compared to D100. The same pattern was observed for CNG80 dual-fuel combustion in Figure 5.18. The HC emissions increased by 80.2%, 79.14%, 78.76%, 76.42%, 73.04%, 67%, and 61.11%, respectively, compared to D100 fuel.

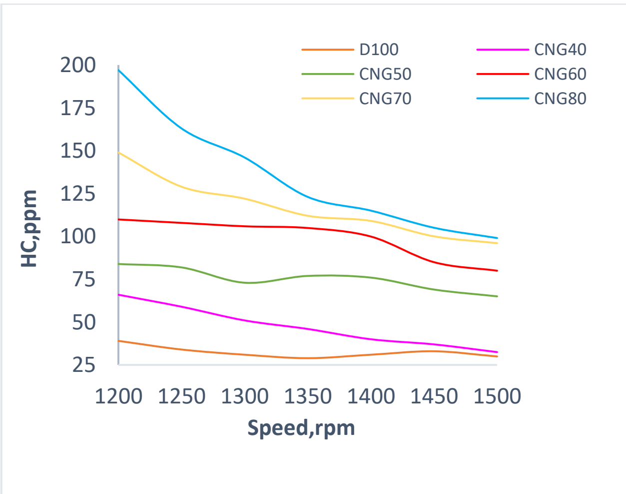


Fig.5.18. Variation of HC emission versus engine speed of diesel engine

### *5.4.3 $CO_2$ emission*

Figure 5.19 depicts the fluctuation of Carbon Dioxide ($CO_2$) emissions at various engine speeds in both diesel and dual-fuel modes. $CO_2$ emissions serve as primary contributors to greenhouse gas (GHG) emissions, thereby contributing to environmental degradation. The quantity of $CO_2$ emissions in the exhaust gas serves as a reliable indicator of complete combustion. Our observations reveal a correlation between $CO_2$ emissions and both the level of CNG substitution and engine speed in dual-fuel mode. As the CNG substitution ratio and engine speed increase, the concentration of $CO_2$ emissions in the exhaust gas also rises.

In the case of diesel fuel combustion, the temperature of combustion plays a significant role in influencing $CO_2$ emissions. Higher combustion temperatures tend to elevate $CO_2$ emissions, highlighting the complex interplay between combustion conditions, fuel composition, and resultant $CO_2$ emissions.

In the current study, there was a reduction in $CO_2$ by 2.4%, 9.3%, 11.4%, 18.6%, 20.6%, 26.6%, and 33.7% in the case of CNG40 energy share compared to D100. For CNG50, $CO_2$ decreased by 11.15%, 17.46%, 18.13%, 23.64%, 21.62%, 77.75%, and 32.28% compared to D100. The $CO_2$ emissions decreased by 17.1%, 23.8%, 26.7%, 29.6%, 25.2%, 29.6%, and 37.3% for the CNG60 substitution ratio at all rpm than D100. For CNG70, $CO_2$ decreased by 27.25%, 31.56%, 36.13%, 35.44%, 39.62%, 39.15%, and 45.88% compared to D100.The same pattern was observed for the CNG80 substitution ratio, and $CO_2$ emissions were reduced by 34.1%, 38.4%, 44.1%, 47.7%, 49.3%, 50.5%, and 56.3% than D100 fuel combustion. The maximum reduction of $CO_2$ emission was attained at the CNG80 substitution ratio at engine speeds.

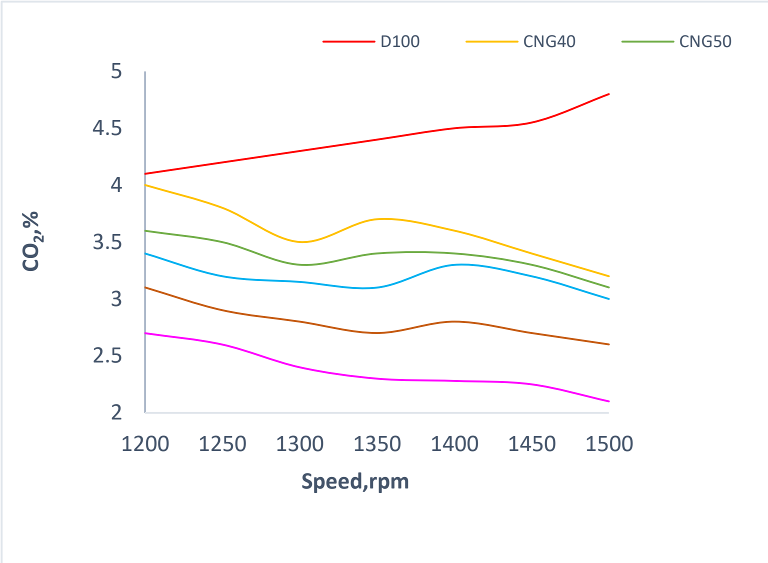


Fig. 5.19. Variation of $CO_2$ emission versus engine speed of diesel engine

### *5.4.4 $NO_X$ emission*

Figure 5.20 shows that $NO_X$ emissions are lower in dual-fuel combustion than in single-fuel combustion. In dual-fuel combustion, the combustion process occurs in the lean, premixed regime due to an increase in Stoichiometric air/fuel ratio, which may decrease the cylinder temperature, resulting decrease the $NO_X$ emission. For single diesel combustion, maximum fuel is burned as a diffusion flame near stoichiometric equivalence ratio, producing higher combustion temperatures and increased NOx emission.

Figure 5.20 shows that when CNG40 is used as the primary fuel, $NO_X$ emissions are reduced by 20.94%, 16.41%, 11.24%, 6.8%, 11.29%, 16.82%, and 20.08% at all engine speeds compared to D100 fuel. For CNG50, $NO_X$ decreased by 93.45%, 87.46%, 72.11%, 45.64%, 55.62%, 57.45%, and 62.58% compared to D100. $NO_X$ emissions were reduced by 160%, 133.3%, 108.6%, 80%, 105%, 93%, and 114% for CNG60 dual fuel compared to D100 fuel. For CNG50, $NO_X$ decreased by 432.5%, 274.46%, 192.11%, 165.14%, 155.82%, 142.55%, and 164.58% compared to D100. The same pattern was observed for CNG80 energy share, with $NO_X$ emissions reduced by 705.4%, 416.9%, 282%, 248.2%, 213.5%, 192.8%, and 164.6%, respectively, compared to D100 fuel.

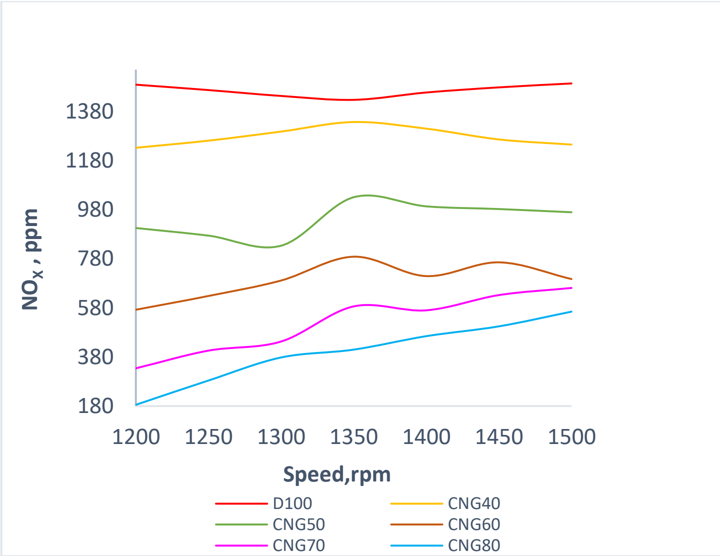


Fig.5.20. Variation of $NO_X$ emission versus engine speed of diesel engine

### 5.4.5 *Smoke emission*

The fluctuation in smoke opacity for various CNG energy shares is depicted in Figure 5.21. The amount of liquid fuel injected has the greatest impact on the opacity of the smoke. In a dual-fuel engine, diesel fuel consumption is reduced since it is replaced by a CNG-air mixture that produces less smoke. Increased CNG energy share increases its quantity of heat contribution and decreases the C/H ratio in the fuel mixture, resulting in better combustion and reduced smoke opacity.

A higher ratio of CNG energy share enhances soot oxidation, and the clean burning gas quality helps reduce soot emissions. CNG is primarily composed of methane, and as a lower paraffin family member, it has a low tendency to generate soot. The heat input contribution of CNG fuel is reduced at lower CNG energy share, and pilot liquid fuel increases the carbon proportion in the combustion and the smoke levels in the exhaust. Figure 5.21 shows a great reduction in smoke opacity in dual fuel compared to single D100 fuel.

When CNG40 is used as the primary fuel, smoke opacity is reduced by 20%, 26.1%, 11.2%, 22.8%, 10.29%, 34.82%, and 45.08% at all engine speeds 1200 to 1500 rpm compared to D100 fuel. For CNG50, smoke opacity decreased by 43.45%, 41.48%, 38.34%, 45.84%, 39.2%, 141.75%, and 386.58% compared to D100. The smoke opacity decreased by 69.54%, 58.32%, 27.75%, 60.3%, 69%, 216.1%, and 700.15% for D40CNG60 energy share. For CNG70, smoke opacity decreased by 153.5%, 129.41%, 101.44%, 145.43%, 229.72%, 536.41%, and 836.38% compared to D100. The same pattern was observed for CNG80 energy share, and smoke opacity decreased by 230.52%, 192.66%, 168.57%,220%, 388%, 850.43%, and 973.22% than D100 fuel combustion.

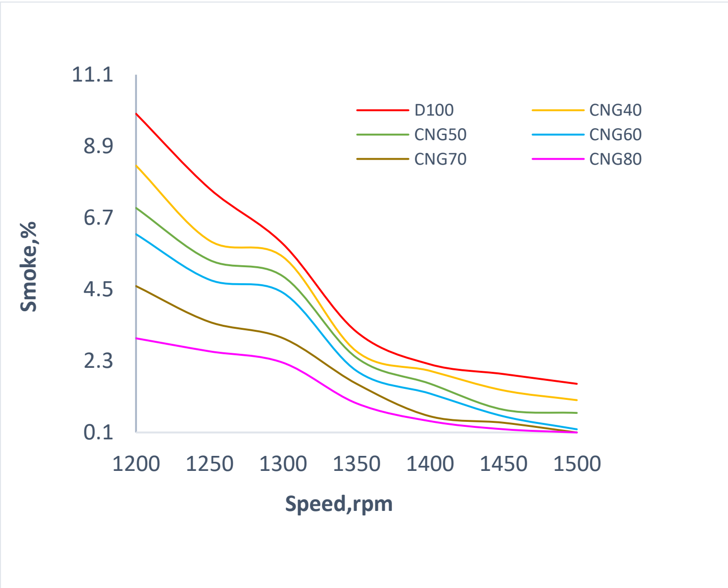


Fig. 5.21. Variation of Smoke opacity versus engine speed of diesel engine

## 5.5 Effect of injection pressure (IP) on the performance of diesel and dual fuel mode

Based on the experimental findings, it was observed that the emission characteristics and performance of a dual-fuel engine showed enhancements at higher Compression Ratios (CRs). Consequently, to conduct a comparative analysis of the dual-fuel engine's performance under various Injection Pressures (IPs) and engine speeds, the compression ratio was maintained at 15:1. Therefore, the performance evaluation of the dual-fuel engine was conducted under diesel/CNG dual-fuel mode at different injection pressures of 500 and 600 bar, while varying engine speeds. This standardized approach allowed for a systematic comparison of the engine's performance across different injection pressures and engine speeds while operating under dual-fuel mode with a compression ratio of 15:1.

### *5.5.1 Brake thermal efficiency*

The Brake Thermal Efficiency (BTE) of the engine serves as a key indicator of its performance. In Figure 5.22, BTE is plotted against engine speeds for different fuel compositions, including D100, CNG40, CNG50,CNG60, CNG70 and CNG80 substitution ratios, at injection pressures (IP) of 500 and 600 bar. Observations indicate that increasing the injection pressure from 500 to 600 bar results in a 2.1% increase in BTE when using diesel fuel across all engine speeds. However, in diesel/CNG dual-fuel mode, this increase in BTE is even more substantial, reaching 2.6% at all speeds. Figure 5.22 illustrates a notable increase in BTE for both diesel mode and dual-fuel mode at an injection pressure of 600 bar. This increase in BTE can be attributed to the production of smaller droplets due to the precise atomization of the pilot fuel and enhanced spray penetration [82]. These factors contribute to improved uniformity in the mixing process of gas and air, leading to more complete combustion. Interestingly, the study identifies an optimum injection pressure of 600 bar at an engine speed of 1500 rpm, highlighting the importance of injection pressure optimization for achieving optimal engine performance.

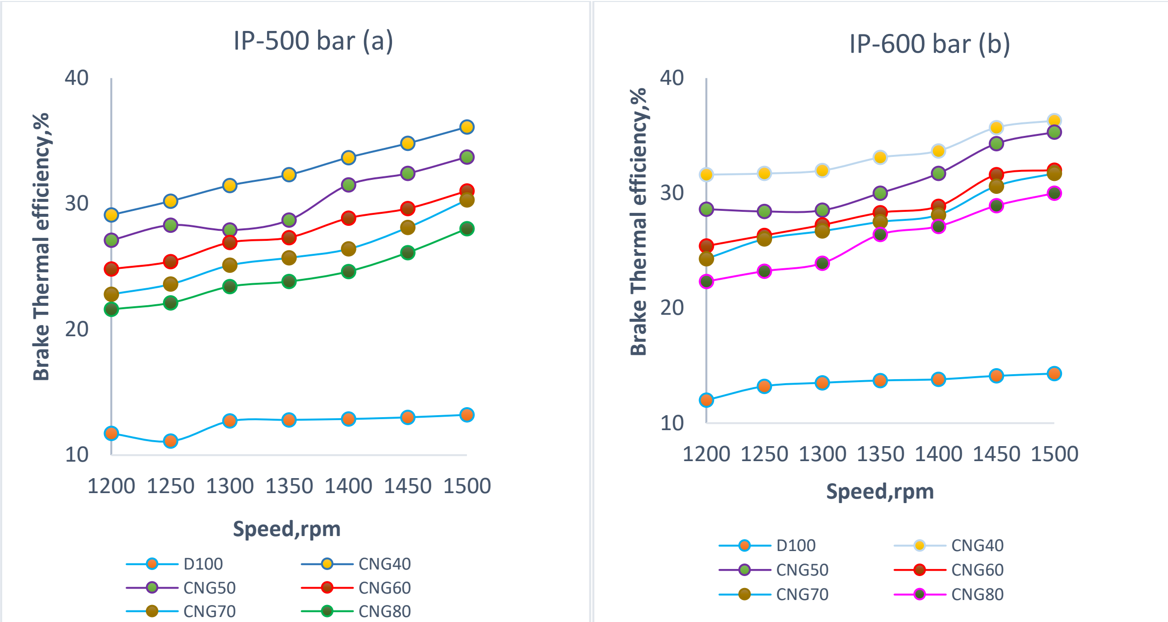


Fig. 5.22. Variation of BTE at IPs of (a) 500 bar ; (b) 600 bar of diesel engine

### *5.5.2 Brake Specific Fuel Consumption*

Figure 5.23 illustrates the variation in Brake Specific Fuel Consumption (BSFC) for both single D100 and dual-fuel combustion across different Injection Pressures (IP) of 500 and 600 bar. Upon observation, it was noted that increasing the IP from 500 to 600 bar led to an increase in BSFC for both single diesel and dual-fuel combustion scenarios.

Specifically, the BSFC rose by 5.1% when utilizing single diesel fuel and increased by 7.9% in dual-fuel mode as the IP increased from 500 to 600 bar. Experimental results consistently showed that an IP of 600 bar exhibited the maximum increment in BSFC compared to an IP of 500 bar across all engine speeds. This phenomenon can be attributed to the higher injection pressure facilitating the production of smaller droplet diameters during fuel injection. Consequently, this reduction in droplet size decreases the ignition delay during combustion, leading to a higher BSFC at the elevated injection pressure of 600 bar.

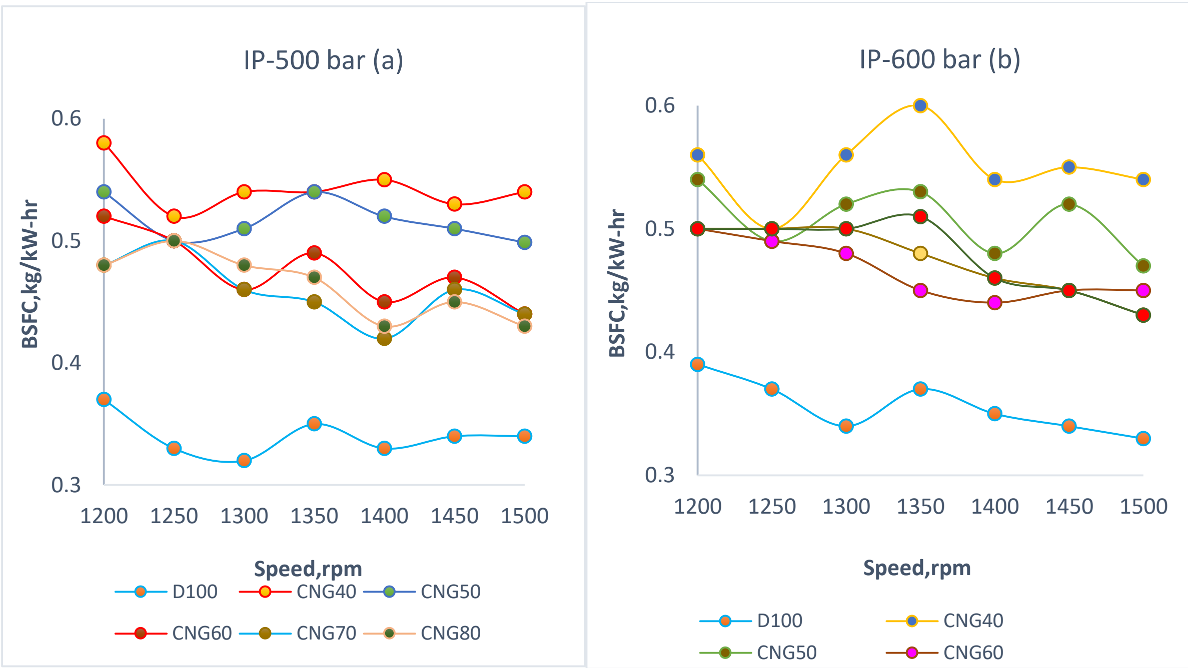


Fig. 5.23. Variation of BSFC at IPs of (a) 500 bar ; (b) 600 bar of diesel engine

## 5.6 Effect of injection pressure on emission under diesel and dual fuel mode

The emissions analysis was conducted for the engine under both dual-fuel and diesel fuel modes across various Injection Pressures (IP). This section presents the experimental examination of pollutants such as Carbon Monoxide (CO), Hydrocarbons (HC), Carbon Dioxide ($CO_2$), and Nitrogen oxide (NOx).

### *5.6.1 CO emission*

Figure 5.24 illustrates the deviation of Carbon Monoxide (CO) emissions for both D100 fuel and dual-fuel combustion scenarios with CNG substitution ratios of CNG40, CNG60, and CNG80, at Injection Pressures (IP) of 500 and 600 bar across various engine speeds. The primary factor influencing CO emissions is the low flame temperature and the deficiency of the air-fuel mixture in the engine.

Upon observation, it was noted that as the IP increased from 500 to 600 bar in both combustion modes, CO emissions decreased. Specifically, when single diesel fuel was used, CO emissions decreased by 2.1%, while in dual-fuel mode, the reduction was more pronounced at 4.9% across all engine speeds. This reduction in CO emissions can be attributed to the higher injection pressure facilitating improved fuel atomization and combustion efficiency, resulting in more complete combustion and consequently lower CO emissions.

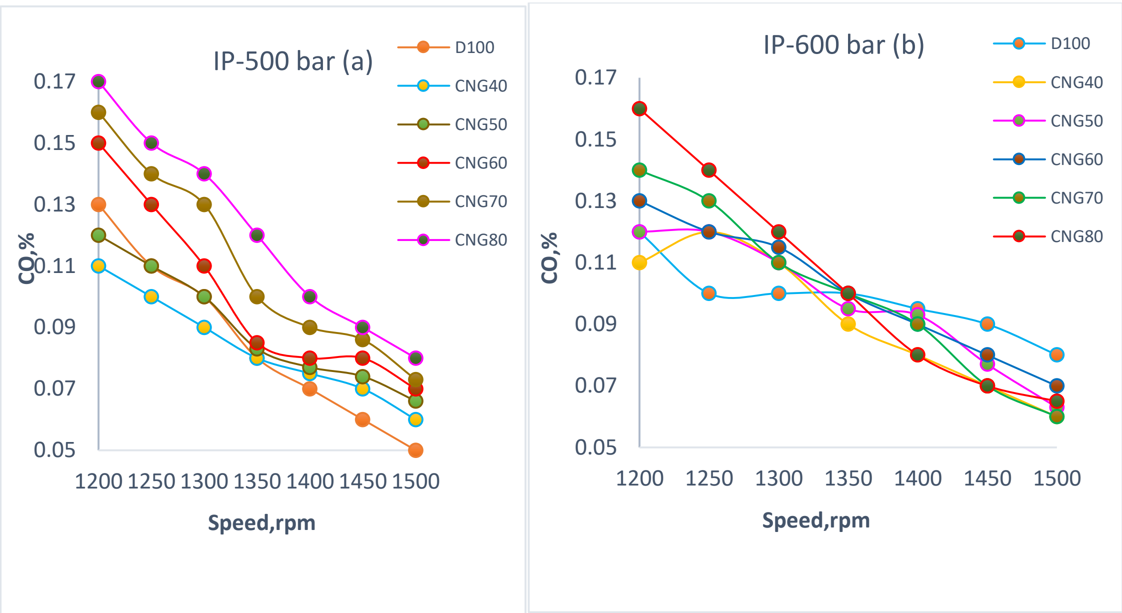


Fig. 5.24. Variation of CO emission at IPs of (a) 500 bar ; (b) 600 bar of diesel engine

### *5.6.2 HC emission*

Figure 5.25 illustrates that increasing Injection Pressure (IP) led to a reduction in Hydrocarbon (HC) emissions both in diesel and dual-fuel modes. This reduction can be attributed to improved atomization and air-fuel mixing facilitated by higher IP, enhancing combustion efficiency. However, a notable observation is that increasing IP from 500 to 600 bar resulted in higher HC emissions. This unexpected outcome is attributed to the reduction in fuel droplet size, which diminishes the momentum required for the fuel to transit into the air-gas mixture effectively. Consequently, despite the improved atomization and mixing, the overall combustion efficiency decreases as IP increases.

Specifically, when single diesel fuel was used, HC emissions decreased by 3.6%, while in dual-fuel mode, the reduction was more significant at 11.9% as IP increased from 500 to 600 bar across all engine speeds. This highlights the complex relationship between injection pressure, fuel atomization, combustion efficiency, and resultant HC emissions in both diesel and dual-fuel combustion scenarios.

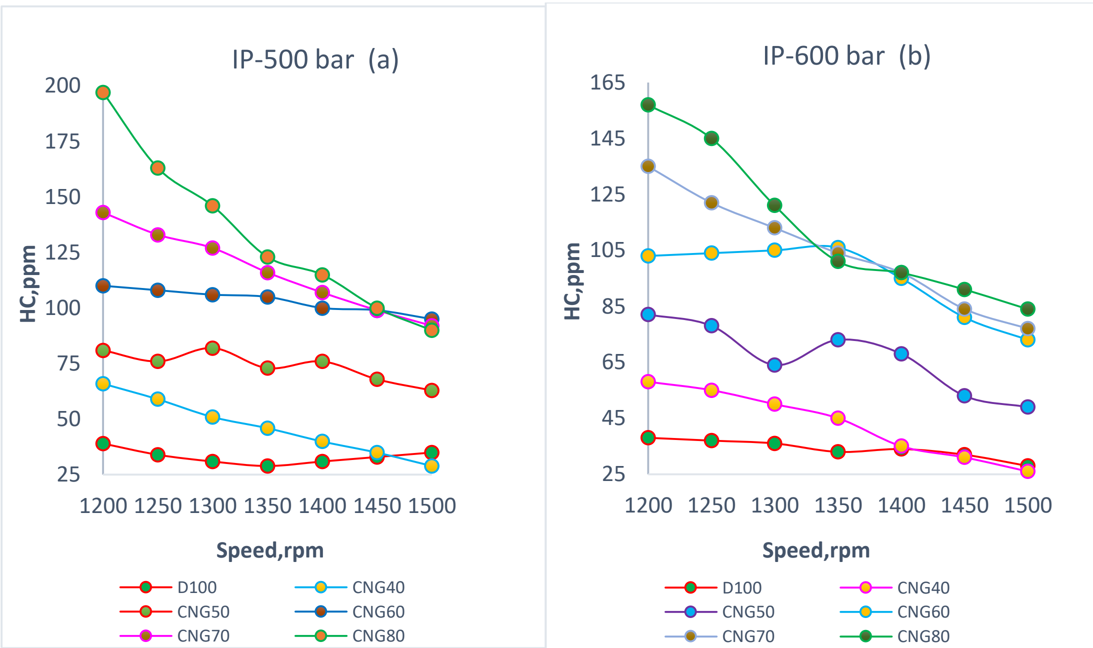


Fig. 5.25. Variation of HC emission at IPs of (a) 500 bar ; (b) 600 bar of diesel engine

### *5.6.3 $CO_2$ emission*

Figure 5.26 illustrates the behavior of Carbon Dioxide ($CO_2$) emissions with both D100 fuel and various CNG substitution ratios (CNG40, CNG60, and CNG80) at injection pressures (IP) of 500 and 600 bar across different engine speeds. $CO_2$ emissions are significant contributors to greenhouse gases, which are associated with global warming. Observations from Figure 5.26 indicate that $CO_2$ emissions decrease with increasing IP in both modes of combustion. Specifically, when single diesel fuel was used, $CO_2$ emissions decreased by 6.7%, while in dual-fuel mode, the reduction was more substantial at 14.3% at higher IP across all speeds.

This reduction in $CO_2$ emissions with increasing IP can be attributed to improved combustion efficiency and more complete combustion achieved through better fuel atomization and air-fuel mixing at higher injection pressures. Consequently, the decrease in $CO_2$ emissions observed at higher injection pressures aligns with efforts to mitigate the environmental impact of engine emissions.

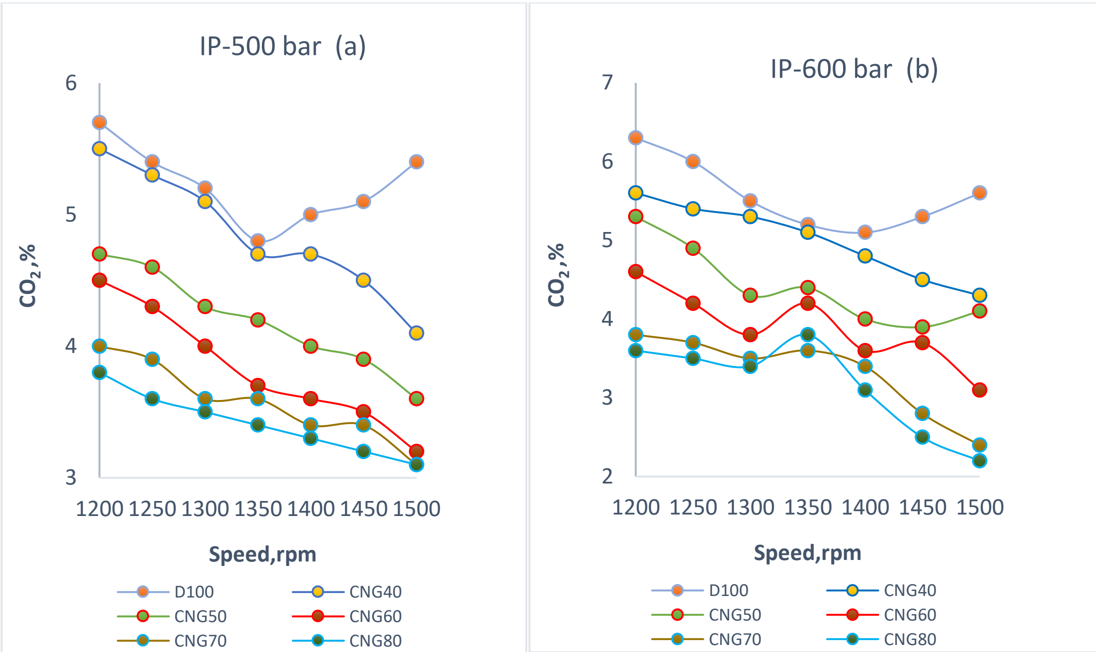


Fig. 5.26. Variation of $CO_2$ emission at IPs of (a) 500 bar ; (b) 600 bar of diesel engine

### *5.6.4 $NO_X$ emission*

Figure 5.27 presents the variation in Nitrogen Oxide (NOx) emissions across different engine speeds at injection pressures (IP) of 500 and 600 bar. Experimental observations reveal a consistent decrease in NOx emissions for both modes of engine operation as the IP increases. Specifically, when single diesel fuel was used, NOx emissions decreased by 16.7% with an increase in IP from 500 to 600 bar. Similarly, in dual-fuel mode, NOx emissions exhibited a more substantial reduction of 34.3% with the same increase in IP across all engine speeds.

This reduction in NOx emissions aligns with efforts to mitigate the environmental impact of engine emissions. The decrease in NOx emissions observed at higher injection pressures can be attributed to improved combustion efficiency and reduced combustion temperatures facilitated by better fuel atomization and air-fuel mixing at elevated injection pressures. Overall, the findings highlight the potential of higher injection pressures to effectively reduce NOx emissions in both diesel and dual-fuel combustion modes.

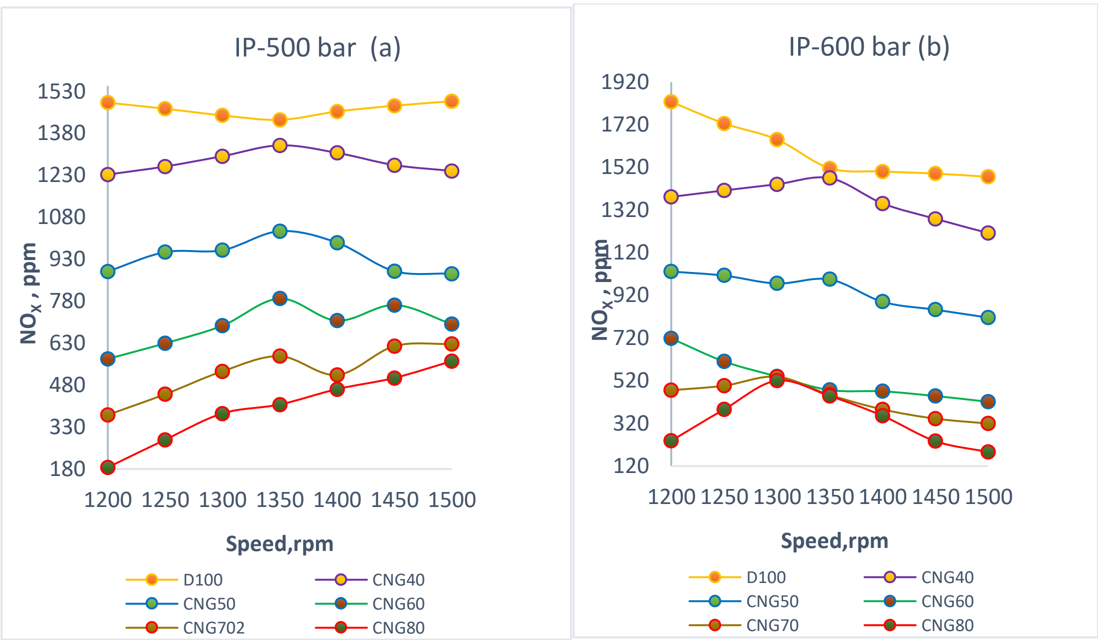


Fig. 5.27. Variation of NOx emission at IPs of (a) 500 bar ; (b) 600 bar of diesel engine

# CHAPTER 6. CONCLUSIONS & FUTURE RECOMMENDATIONS

The analysis and experimental investigation aims to determine the effect of compression ratio of a diesel engine by varying various parameter such as engine speed, injection pressure (IP) in order to measure the performance and emission characteristics of a dual fuel diesel engine. In this study, gaseous fuels (CNG) were employed to conduct experiments in the dual fuel mode of a diesel engine. The studies were carried out on four-stroke, DI, single-cylinder, and VCR diesel engines. The dual fuel engine was tested with 100% diesel fuel to provide reference results for comparison. The engine was tested with varying compression ratios (13 to 15) and engine speed (1200 to 1500 rpm). Also, the effects of IP on dual fuel engines are studied in the present study. The experiment's observation of performance and emission characteristics was analyzed under similar operating conditions. The performance and emission characteristics of a dual fuel engine operating on diesel/CNG were compared to those of a 100% diesel fuel mode. Finally, the impact of the current work has been highlighted.

**(1) Effects of compression ratio on performance and emission**

The specific interaction between compression ratio and CNG substitution ratio can influence combustion characteristics, temperature profiles, and the completeness of combustion, affecting performance and emissions.

- At a Compression Ratio of 15, the fuel injection into the charge, which has higher temperature and pressure, contributes to a better air-fuel mixture and faster fuel evaporation. This optimal condition at CR 15 results in the observed maximum Brake Thermal Efficiency with a CNG40 substitution ratio than D100 fuel.
- Increasing the compression ratio from 13 to 15 led to an increase in brake specific fuel consumption. The maximum brake specific fuel consumption was observed at a substitution ratio of CNG40 when the compression ratio was 15.

- CO emissions typically rise in DF combustion due to incomplete combustion of the gaseous fuel. The combustion characteristics of gaseous fuels, such as CNG (Compressed Natural Gas), differ from liquid diesel fuel. Incomplete combustion can occur because gaseous fuels may have different ignition characteristics or combustion rates compared to liquid fuels. The maximum increment in CO emissions occurred at a Compression Ratio of 13 by the substitution of CNG80.
- The higher HC emissions in DF combustion, especially with the substitution of CNG at 80%, can be attributed to factors like incomplete combustion and the specific chemical composition of the gaseous fuel. Gaseous fuels may introduce additional hydrocarbons into the combustion process, contributing to elevated HC emissions.
- The use of CNG in dual fuel combustion, especially at higher substitution ratios like CNG80%, has the potential to significantly reduce $CO_2$ emissions compared to pure diesel combustion. This outcome is attributed to the favorable characteristics of CNG, including its higher calorific value and lower carbon content. The findings emphasize the environmental benefits of using CNG as an alternative fuel in internal combustion engines.
- The benefits of CNG in reducing NOx and smoke emissions during Dual Fuel (DF) combustion are attributed to the gaseous fuel's combustion characteristics. Higher substitution ratios of CNG, particularly at CNG80, result in longer ignition delay times. This ignition delay contributes to a more controlled combustion process. Slower flame propagation speeds associated with CNG combustion can lead to better mixing with air, promoting more complete combustion and reducing the formation of NOx. The slower combustion process and lower temperatures associated with CNG combustion, especially at higher substitution ratios, contribute to a reduction in smoke emissions. Complete combustion and optimized air-fuel mixing minimize the production of particulate matter, resulting in cleaner exhaust gas.

**(2) Effects of engine speed on performance and emission**

- Brake Thermal Efficiency and Brake Specific Fuel Consumption increased in dual fuel combustion at all engine speeds compared to D100% combustion. The maximum raised in BTE and BSFC detected at CNG40% energy share due to higher flame temperature excess air ratio mixture and pressure, resulting in a better air/fuel mixture and faster fuel evaporation at a lower CNG energy share.

- Carbon Monoxide (CO) and hydrocarbon (HC) emissions were increased in dual fuel combustion compared to single diesel fuel combustion. CNG's energy share of CNG80 produced higher CO and HC emissions. Because at a higher CNG energy share, the equivalence ratios increase with increasing the CNG supply rate, which decreases the liquid fuel quantity resulting in lower ignition temperature and sparks energy of mixture. These facts increase CO and HC emissions in dual-fuel combustion.
- A high substitution ratio of CNG80 led to the maximum reduction in $CO_2$ emissions at all specified engine speeds. This finding aligns with the environmental benefits often associated with the use of natural gas as a cleaner-burning fuel compared to conventional fossil fuels.
- Adding the CNG to the diesel fuel reduces the NOx and smoke opacity in the Exhaust Gas. The Minimal $NO_X$ emission and smoke opacity were attained at CNG80 energy share. At a higher CNG energy share, the ignition delay period prolongs, slows the flame propagation speed, and decreases the cylinder temperature and C/H ratio, reducing the $NO_X$ emission and smoke opacity in dual fuel combustion.

**(3) Effects of injection pressure on performance and emission**

- It is observed that increasing the injection pressure to 600 bar was beneficial for both diesel and dual-fuel combustion modes in terms of Brake Thermal Efficiency. The observed increase in BTE with higher injection pressure indicates that the combustion process became more efficient. Higher injection pressure can result in better atomization of the fuel, improved mixing with air, and more complete combustion, contributing to higher BTE.
- It is found that an increase in BSFC occurred in both single diesel mode and dual-fuel mode at higher IP. Maximum brake specific fuel consumption achieved at CNG40% dual fuel combustion than D100% fuel combustion at 600 bar for all engine rpm. The reasons for the increase in BSFC could be related to changes in combustion characteristics, air-fuel mixing, or other factors influenced by the higher injection pressure.
- CO emission is decreased in both cases as IP is raised at all engine speeds. In both cases, higher injection pressure seems to have a beneficial effect on reducing carbon monoxide emissions. This could be due to improved combustion efficiency with the higher injection pressure.
- The reduction in hydrocarbon emissions can be attributed to the potential improvement in combustion efficiency, better atomization of the fuel, and enhanced mixing of fuel and air at higher injection pressures. These factors contribute to a more complete combustion process, resulting in lower unburned hydrocarbons in the exhaust.
- Higher injection pressure (IP) has led to a reduction in carbon dioxide ($CO_2$) emissions in both combustion modes. Improved combustion efficiency at higher injection pressures can result in a more complete burning of the fuel, leading to less wasted energy and lower $CO_2$ emissions per unit of work produced by the engine.
- Similarly, Higher injection pressure (IP) has led to a reduction in nitrogen oxide ($NO_X$) emissions in both combustion modes. The reduction in NOx emissions could be attributed to

several factors associated with higher injection pressures. These factors may include improved combustion efficiency, enhanced mixing of fuel and air, and better control over combustion temperatures. Generally, higher injection pressures can promote more complete combustion, reducing the formation of nitrogen oxides.

## (4) Recommendations For Future Work

The recommendation to conduct additional work on simulation at various load conditions and different CNG energy share ratios is a prudent approach for a comprehensive understanding of dual-fuel engine combustion and emissions. Here are some aspects that could be considered in the proposed research:

1. Simulation Studies:

    - Perform simulations at different load conditions and gaseous energy share to understand the behavior of the dual-fuel engine across its operating range.

    - Investigate the effects of varying different injection pressures on combustion efficiency, heat release rates, and emissions.

    - Study the impact of diesel displacement variations on overall engine performance and emissions.

2. Combustion and Emission Analysis:

    - Analyze combustion characteristics such as ignition delay, combustion duration, and peak pressure at different load points.

- Investigate emissions of nitrogen oxides (NOx), particulate matter (PM), carbon monoxide (CO), and hydrocarbons (HC) under different operating conditions.
- Assess the trade-offs between NOx and PM emissions and explore ways to optimize for both.

3. Oxidation Catalyst Integration:

- Explore the use of oxidation catalysts to reduce CO and HC emissions in dual-fuel engines. Oxidation catalysts can be effective in converting unburned hydrocarbons and carbon monoxide into less harmful substances.
- Investigate the optimal location for integrating the oxidation catalyst within the exhaust system.
- Study the impact of oxidation catalysts on overall engine performance, emissions, and fuel efficiency.

4. Economic and Practical Consideration:

- Assess the economic feasibility and practicality of implementing the recommended changes in injection pressure and timing, diesel displacement, and oxidation catalyst integration.
- Consider factors such as component durability, maintenance requirements, and the cost-effectiveness of emission reduction strategies.

# REFERENCES


1. Gupta, H. N. (2013). *Fundamentals of Internal Combustion Engines.* PHI Learning Private Limited.

2. Heywood, John B. (1988). *Internal Combustion Engine Fundamentals.* Tata McGraw-Hill.

3. Worldometer. (n.d.). $CO_2$ emissions by country. Retrieved from https://www.worldometers.info/co2-emissions/co2-emissions-by-country/

4. Dimaratos, A., Toumasatos, Z., Doulgeris, S., Triantafyllopoulos, G., Kontses, A., & Samaras, Z. (2019). Assessment of $CO_2$ and NOx Emissions of One Diesel and One Bi-Fuel Gasoline/CNG Euro 6 Vehicles During Real-World Driving and Laboratory Testing. *Frontiers in Mechanical Engineering, 62.*

5. Manisalidis, I., Stavropoulou, E., Stavropoulos, A., & Bezirtzoglou, E. (2020). Environmental and health impacts of air pollution: a review. *Frontiers in Public Health, 14.*

6. OPIndia. (2023, January 14). Delhi's air quality remains good for 1,096 hours in 45 days amid smog and pollution. https://www.opindia.com/2023/01/delhi-air-quality-good-1096-hours-45-days-smog-pollution/

7. https://indianexpress.com/article/cities/delhi/delhi-ranks-4-on-list-of-worlds-most-polluted-cities-8497423/

8. Selim, M. Y. E. (2004). Sensitivity of dual fuel engine combustion and knocking limits to gaseous fuel composition. *Energy Conversion and Management, 45*(3), 411-425.

9. Sahoo, B. B., Sahoo, N., & Saha, U. K. (2009). Effect of engine parameters and type of gaseous fuel on the performance of dual-fuel gas diesel engines—A critical review. *Renewable and Sustainable Energy Reviews, 13*(5), 1151–1184.

10. Bora, B. J., Saha, U. K., Chatterjee, S., & Veerb, V. (2014). Effect of compression ratio on performance, combustion and emission characteristics of a dual fuel diesel engine run on raw biogas. *Energy Conversion and Management, 80*, 1000–1009.

11. Kafle, G. K., & Kim, S. H. (2013). Effects of chemical compositions and ensiling on the biogas productivity and degradation rates of agricultural and food processing by-products. *Bioresource Technology, 150*, 553-561.

12. Bedoya, I. D., Arrieta, A. A., & Cadavid, F. J. (2009). Effects of mixing system and pilot fuel quality on diesel-biogas dual fuel engine performance. *Bioresource Technology, 100*(23), 6624-6629.

13. Bari, S. (1996). Effect of carbon dioxide on the performance of biogas/diesel dual-fuel engine. *Renewable Energy, 9*(7-8), 1007-1010.

14. Roy, M. M., Tomita, E., Kawaraha, N., Hadara, Y., & Sakane, A. (2009). Performance and emission comparison of a supercharged dual-fuel engine fueled by producer gases with varying hydrogen content. *International Journal of Hydrogen Energy, 34*(19), 7811–7822.

15. Banapurmath, N. R., & Tewari, P. G. (2009). Comparative performance studies of a 4-stroke CI engine operated on dual fuel mode with producer gas and Honge oil and its methyl ester (HOME) with and without carburetor. *Renewable Energy, 34*(5), 1009-0015.

16. Sombatwong, P., Thaiyasuit, P., & Pianthong, K. (2013). Effect of Pilot Fuel Quantity on the Performance and Emission of a Dual Producer Gas–Diesel Engine. *Energy Procedia, 34*, 218-227.

17. Renald, C. J. T., & Somasundaram, P. (2012). Experimental Investigation on Attenuation of Emission with Optimized LPG Jet Induction in a Dual Fuel Diesel Engine and Prediction by ANN Model. *Energy Procedia, 14*, 1427-1438.

18. Jothi, N. K., Miller, G., Nagarajan, G., & Renganarayanan, S. (2007). Experimental studies on homogeneous charge CI engine fueled with LPG using DEE as an ignition enhancer. *Renewable Energy, 32*(9), 1581–1593.

19. Goto, S., Lee, D., Shakal, J., Harayama, N., Honyo, F., & Ueno, H. (1999). Performance and Emissions of an LPG Lean-Burn Engine for Heavy Duty Vehicles. *SAE Technical Paper, 1999–01-1513*.

20. Saleh, H. E. (2008). Effect of variation in LPG composition on emissions and performance in a dual fuel diesel engine. *Fuel, 87*(13-14), 3031-3039.

21. Surawski, N. C., Miljevica, B., Bodisco, T. A., Situ, R., Ristovski, Z. D., & Brown, R. J. (2014). Performance and gaseous and particle emissions from a liquefied petroleum gas (LPG) fumigated compression ignition engine. *Fuel, 122*, 17-25.

22. Lata, D. B., Misra, A., & Medhekar, S. (2012). Effect of hydrogen and LPG addition on the efficiency and emissions of a dual fuel diesel engine. *International Journal of Hydrogen Energy, 37*(7), 6084–6096.

23. Lata, D. B., Misra, A., & Medhekar, S. (2011). Investigations on the combustion parameters of a dual fuel diesel engine with hydrogen and LPG as secondary fuels. *International Journal of Hydrogen Energy, 36*(21), 13808–13819.

24. Lounici, M. S., Loubar, K., Tarabet, L., Balistrou, M., Niculescu, D. C., & Tazerout, M. (2014). Towards improvement of natural gas-diesel dual fuel mode: An experimental investigation on performance and exhaust emissions. *Energy, 69*, 200-211.

25. Papagiannakis, R. G., & Hountalas, D. T. (2004). Combustion and exhaust emission characteristics of a dual fuel compression ignition engine operated with pilot Diesel fuel and natural gas. *Energy Conversion and Management, 45*(18-19), 2971–2987.

26. Papagiannakis, R. G., & Hountalas, D. T. (2003). Experimental investigation concerning the effect of natural gas percentage on performance and emissions of a DI dual fuel diesel engine. *Applied Thermal Engineering, 23*(3), 353–365.

27. Papagiannakis, R. G., et al. (2010). Emission characteristics of high-speed, dual fuel, compression ignition engine operating in a wide range of natural gas/diesel fuel proportion. *Fuel, 89*(6), 1397–1406.

28. Yang, B., Wei, X., Xi, C., Liu, Y., Zheng, K., & Lai, M. C. (2014). Experimental study of the effects of natural gas injection timing on the combustion performance and emissions of a turbocharged common rail dual-fuel engine. *Energy Conversion and Management, 85*, 297–304.

29. Alonso, A. S. (2012). The Expansion of Unconventional Production of Natural Gas (Tight Gas, Gas Shale and Coal Bed Methane). In *Advances in Natural Gas Technology* (pp. 123-146). Intech.

30. Perry, K. F. (2010). Hydraulic Fracturing – A Historical and Impact Perspective. Gas Technology Institute. Slide 33.

31. Perry, K. F. (2010). Hydraulic Fracturing – A Historical and Impact Perspective. Gas Technology Institute. Slide 33.

32. Liu, Z. (2002). Knock characteristics of dual-fuel engines fueled with hydrogen fuel. *International Journal of Hydrogen Energy, 20*, 919–924. doi:10.1016/0360-3199(95)00023-7.

33. Mansor, W., Vaughn, J. S., & Olsen, D. B. (2014). Emissions and efficiency evaluations of a 6.8-liter diesel derivative dual fuel engine. *Proceedings of The Canadian Society for Mechanical Engineering International Congress*. Retrieved from http://www.dwppon.com/bifuel.pdf

34. ComAp System. (2009). DWPPON Elektric. Retrieved from http://www.dwppon.com/bifuel.pdf.

35. Naber, J., Siebers, D.L., Caton, J.A., Westbrook, C.K., Di Julio, S.S. (2010). Natural Gas Autoignition Under Diesel Conditions: Experiments and Chemical Kinetic Modeling. *SAE Technical Paper Series, 1*. doi:10.4271/942034.

36. Hodgins, K.B., Hill, P.G., Ouellette, P. (n.d.). Fueling of Diesel Engines.

37. Liu, Z. (1995). An examination of the combustion characteristics of compression ignition engines fueled with gaseous fuels. *University of Calgary*.

38. Wang, Z., Fu, X., Wang, D., Xu, Y., Du, G., You, J. (2021). A multilevel study on the influence of natural gas substitution rate on combustion mode and cyclic variation in a diesel/natural gas dual fuel engine. *Fuel*.

39. Mansour, C., Bounif, A., Aris, A., Gaillard, F. (2001). Gas – Diesel (dual-fuel) modeling in diesel engine. *International Journal of Thermal Sciences, 0729*, 409–424.

40. Kim, W., Park, C., Bae, C. (2021). Characterization of combustion process and emissions in a natural gas/diesel dual-fuel compression-ignition engine. *Fuel, 291*, 120043.

41. Lee, S., Kim, C., Lee, S., Oh, S., Kim, J., & Lee, J. (2021). Characteristics of non-methane hydrocarbons and methane emissions in exhaust gases under natural-gas/diesel dual-fuel combustion. *Fuel, 290*, 120009.

42. Millo, F., Accurso, F., Piano, A., Caputo, G., Cafari, A., & Hyvönen, J. (2021). Experimental and numerical investigation of the ignition process in a large bore dual fuel engine. *Fuel, 290*, 120073.

43. Kim, S. C., & Jin, H. (2016). Pressure model based coordinated control of VGT and dual-loop EGR in a diesel engine air-path system. *International Journal of Automotive Technology, 17*, 11-34.

44. Li, W., Liu, Z., & Wang, Z. (2016). Experimental and theoretical analysis of the combustion process at low loads of a diesel natural gas dual-fuel engine.

45. Ryu, K. (2013). Effects of pilot injection timing on the combustion and emissions characteristics in a diesel engine using biodiesel-CNG dual fuel. *Applied Energy, 111*, 721–730.

46. Yousefi, A., Guo, H., & Birouk, M. (2019). Effect of diesel injection timing on the combustion of natural gas/diesel dual-fuel engine at low-high load and low-high speed conditions. *Fuel, 235*, 838-846.

47. Wang, Z., Zhao, Z., Wang, D., Tan, M., Han, Y., Liu, Z., et al. (2016). Impact of pilot diesel ignition mode on combustion and emissions characteristics of a diesel/natural gas dual fuel heavy-duty engine. *Fuel, 167*, 248–256.

48. Nithyanandan, K., Gao, Y., Wu, H., Lee, C., Liu, F., & Yan, J. (2017). An optical investigation on multiple diesel injections in CNG/diesel dual-fuel combustion in a light-duty optical diesel engine. *SAE Technical Paper 2017–01-0755*.

49. Papagiannakis, R. G., Krishnan, S. R., Rakopoulos, D. C., Srinivasan, K. K., & Rakopoulos, C. D. (2017). A combined experimental and theoretical study of diesel fuel injection timing and gaseous fuel/diesel mass ratio effects on the performance and

emissions of natural gas-diesel HDDI engine operating at various loads. *Fuel, 202*, 675–687.

50. Liu, J., Yang, F., Wang, H., Ouyang, M., & Hao, S. (2013). Effects of pilot fuel quantity on the emissions characteristics of a CNG/diesel dual fuel engine with optimized pilot injection timing. *Applied Energy, 110*, 201–206.
51. Yang, B., Wang, L., Ning, L., & Zeng, K. (2016). Effects of pilot injection timing on the combustion noise and particle emissions of a diesel/natural gas dual-fuel engine at low load. *Applied Thermal Engineering, 102*(x), 822–828.
52. Guerry, E. S., Raihan, M. S., Srinivasan, K. K., Krishnan, S. R., & Sohail, A. (2016). Injection timing effects on partially premixed diesel-methane dual fuel low temperature combustion. *Applied Energy, 162*(x), 99–113.
53. Shu, J., Fu, J., Liu, J., Zhang, L., & Zhao, Z. (2018). Experimental and computational study on the effects of injection timing on thermodynamics, combustion and emission characteristics of a natural gas (NG)-diesel dual fuel engine at low speed and low load. *Energy Conversion and Management, 160*(January), 426–438.
54. Yuvenda, D., Sudarmanta, B., Wahjudi, A., & da Silva, J. (2019, August). Characterization of engine performance, combustion process and emission of diesel/CNG dual fuel engines with pilot injection timing variation at low load. *IOP Conference Series: Materials Science and Engineering, 588*(1), 012005.
55. Ouchikh, S., Lounici, M. S., Loubar, K., Tarabet, L., & Tazerout, M. (2022). Effect of diesel injection strategy on performance and emissions of CH4/diesel dual-fuel engine. *Fuel, 308*, 121911.

56. Ramachander, J., Gugulothu, S. K., Sastry, G. R., & Surya, M. S. (2021). Statistical and experimental investigation of the influence of fuel injection strategies on CRDI engine assisted CNG dual fuel diesel engine. *International Journal of Hydrogen Energy, 46*(42), 22149–22164.

57. Dou, Z., Yao, C., Wei, H., Wang, B., Liu, M., Chen, C., ... & Shi, J. (2017). Experimental study of the effect of engine parameters on ultrafine particle in diesel/methanol dual fuel engine. *Fuel, 192*, 45-52.

58. Papagiannakis, R. G., & Hountalas, D. T. (2004). Combustion and Exhaust Emissions Characteristics of a Dual Fuel Compression Ignition Engine Operated with Pilot Diesel Fuel and Natural Gas. *Energy Conversion and Management, 45*, 2971-2987.

59. Karim, G. (1991). An examination of some measures for improving the performance of gas fuelled diesel engines at light load. *SAE Technical Paper*.

60. Karim, G., Liu, Z., & Jones, W. (1993). Exhaust emissions from dual fuel engines at light load. *SAE Technical Paper*.

61. Gatts, T., et al. (2012). An experimental investigation of incomplete combustion of gaseous fuels of a heavy-duty diesel engine supplemented with hydrogen and natural gas. *International Journal of Hydrogen Energy, 37*(9), 7848-7859.

62. Lyu, M., Zhang, C., Bao, X., Song, J., & Liu, Z. (2017). Effects of the substitution rate of natural gas on the combustion and emission characteristics in a dual-fuel engine under full load. *Advances in Mechanical Engineering, 9*, 168781401774715.

63. Gharehghani, A., Hosseini, R., Mirsalim, M., Jazayeri, S., & Yusaf, T. (2015). An experimental study on reactivity-controlled compression ignition engine fueled with biodiesel/natural gas. *Energy, 89*, 558–567.

64. Bari, S., & Hossain, S. N. (2019). Performance of a diesel engine run on diesel and natural gas in dual-fuel mode of operation. *Energy Procedia, 160*, 215-222.

65. Lounici, M. S., Loubar, K., Tarabet, L., Balistrou, M., Niculescu, D. C., & Tazerout, M. (2014). Towards improvement of natural gas-diesel dual fuel mode: An experimental investigation on performance and exhaust emissions. *Energy, 64*, 200-211.

66. Tripathi, G., Sharma, P., & Dhar, A. (2020). Effect of methane augmentations on engine performance and emissions. *Alexandria Engineering Journal, 59*(1), 429-439.

67. Jamrozik, A., Tutak, W., & Grab-Rogaliński, K. (2019). An experimental study on the performance and emission of the diesel/CNG dual-fuel combustion mode in a stationary CI engine. *Energies, 12*(20), 3857.

68. Lee, C. F., Pang, Y., Wu, H., Nithyanandan, K., & Liu, F. (2020). An optical investigation of substitution rates on natural gas/diesel dual-fuel combustion in a diesel engine. *Applied Energy, 261*, 114455.

69. Rai, A. A., Narasimha, K. B., & Bailkeri, S. R. (2021). Effect of injection timings on performance and emission characteristics of CNG diesel dual fuel engine. *Materials Today: Proceedings*.

70. Di Blasio, G., Belgiorno, G., & Beatrice, C. (2017). Effects on performances, emissions and particle size distributions of a dual fuel (methane-diesel) light-duty engine varying the compression ratio. *Applied Energy, 204*, 726-740.

71. Ismail, M. M., Fawzi, M., Theerayut, L., Zulkifli, F. H., Osman, S. A., & Taweekun, J. (2020). Energy Consumption and Emissions of Diesel-CNG Dual Fuel Engine at High Load Operation. *International Journal of Integrated Engineering, 12*(2), 253-260.

72. Yuvenda, D., Sudarmanta, B., Wahjudi, A., & Muraza, O. (2020). Improved combustion performances and lowered emissions of CNG-diesel dual fuel engine under low load by optimizing CNG injection parameters. *Fuel, 269*, 117202.

73. Huang, H., Zhu, Z., Chen, Y., Chen, Y., Lv, D., Zhu, J., & Ouyang, T. (2019). Experimental and numerical study of multiple injection effects on combustion and emission characteristics of natural gas–diesel dual-fuel engine. *Energy Conversion and Management, 183*, 84-96.

74. Karabektas, M., Ergen, G., & Hosoz, M. (2016). The effects of using diethylether as additive on the performance and emissions of a diesel engine fuelled with CNG. Fuel, 115, 855–860.

75. Lebedevas, S., Pukalskas, S., Daukšys, V., Rimkus, A., Melaika, M., & Jonika, L. (2019). Research on fuel efficiency and emissions of converted diesel engine with conventional fuel injection system for operation on natural gas. Energies, 12(12), 2413.

76. Bayat, Y., & Ghazikhani, M. (2020). Experimental investigation of compressed natural gas using in an indirect injection diesel engine at different conditions. Journal of Cleaner Production, 271, 122450.

77. Gülcan, H. E., & Ciniviz, M. (2023). The effect of pure methane energy fraction on combustion performance, energy analysis and environmental-economic cost indicators in a single-cylinder common rail methane-diesel dual fuel engine. Applied Thermal Engineering, 230, 120712.

78. Tripathi, G., Sharma, P., & Dhar, A. (2020). Effect of methane augmentation on combustion stability and unregulated emissions in compression ignition engine. Fuel, 263, 116672.

79. Di Iorio, S., Magno, A., Mancaruso, E., & Vaglieco, B. M. (2016). Characterization of particle number and mass size distributions from a small compression ignition engine operating in diesel/methane dual fuel mode. Fuel, 180, 613-623.

80. Gulcan, H. E., & Ciniviz, M. (2023). Experimental study on the effect of piston bowl geometry on the combustion performance and pollutant emissions of methane-diesel common rail dual-fuel engine. Fuel, 345, 128175.

81. Mattson, J. M. S., Langness, C., & Depcik, C. (2018). An analysis of dual-fuel combustion of diesel with compressed natural gas in a single-cylinder engine. SAE International, Technical Paper 2018-01-0248.

82. YAŞAR, M. F., ERGEN, G., & CESUR, İ. (2023). Investigating the Use of Methane as an Alternative Fuel in Diesel Engines: A Numerical Approach. International Journal of Automotive Science And Technology, 7(4), 349-359.

83. Meng, X., Tian, H., Long, W., Zhou, Y., Bi, M., Tian, J., & Lee, C. F. F. (2019). Experimental study of using additive in the pilot fuel on the performance and emission trade-offs in the diesel/CNG (methane emulated) dual-fuel combustion mode. Applied Thermal Engineering, 157, 113718.

84. Jung, J., Song, S., & Hur, K. B. (2017). Numerical study on the effects of intake valve timing on performance of a natural gas-diesel dual-fuel engine and multi-objective Pareto optimization. Applied Thermal Engineering, 121, 604-616.

85. Zhou, H., Li, X., & Lee, C. F. F. (2019). Investigation on soot emissions from diesel-CNG dual-fuel. international journal of hydrogen energy, 44(18), 9438-9449.

86. Addy, J. M., Bining, A., Norton, P., Peterson, E., Campbell, K., & Bevillaqua, O. (2000). Demonstration of Caterpillar C10 DualFuel Natural Gas Engines in Commuter Buses. SAE Technical Paper 2000-01-1386.

87. Napolitano, P., Guido, C., Beatrice, C., & Del Giacomo, N. (2017). Application of a Dual Fuel Diesel-CNG Configuration in a Euro 5 Automotive Diesel Engine (No. 2017-01-0769). SAE Technical Paper.

88. Choi, G. H., & Lim, O. T. (2011). The Engine Performance and emission characteristics of CNG/Diesel dual-fuel engine by CNG mixing ratio. Transactions of the Korean Society of Automotive Engineers, 19(3), 38-43.

89. Maji, S., Pal, A., & Arora, B. B. (2008). Use of CNG and diesel in CI engines in dual fuel mode (No. 2008-28-0072). SAE Technical Paper.

90. Kline, S. J., & McClintock, F. A. (1953). Describing uncertainties in single sample experiments. *Mechanical Engineering, 75*(1), 3–8.

91. Shailaja, M., Raju, S. (2016). Optimization of diesel engine parameters for performance, combustion and emission parameters using Taguchi and grey relational analysis. *Global Journal of Researches in Engineering, A Mech. Mech. Eng.*, 16, 49–61. ISSN: 0975-5861.

92. Modi, M. A., Patel, T. M., Rathod, G. P. (2014). Parametric optimization of single cylinder diesel engine for palm seed oil and diesel blend for brake thermal efficiency using Taguchi method. *IOSR Journal of Engineering*, 4, 49–54. ISSN: 2278-8719.

93. Win, Z., Gakkhar, R. P., Jain, S. C., Bhattacharya, M. (2005). Investigation of diesel engine operating and injection system parameters for low noise, emissions, and fuel consumption using Taguchi methods. *Proceedings of the Institution of Mechanical Engineers, Part D: Journal of Automobile Engineering, 219*, 1237–1251.

94. Hosmath, R. S., Banapurmath, N. R., Khandal, S. V., Gaitonde, V. N., Basavarajappa, Y. H., & Yaliwal, V. S. (2016). Effect of compression ratio, CNG flow rate and injection timing on the performance of dual fuel engine operated on honge oil methyl ester (HOME) and compressed natural gas (CNG). *Renewable Energy, 93*, 579-590.

95. Cheenkachorn, K., Poompipatpong, C., & Ho, C. G. (2013). Performance and emissions of a heavy-duty diesel engine fuelled with diesel and LNG (liquid natural gas). *Energy, 53*, 52–57.

96. Wei, L., & Geng, P. (2016). A review on natural gas/diesel dual fuel combustion, emissions and performance. *Fuel Processing Technology, 142*, 264–278.

97. Karagöz, Y., Sandalcı, T., Koylu, U. O., Dalkılıç, A. S., & Wongwises, S. (2016). Effect of the use of natural gas–diesel fuel mixture on performance, emissions, and combustion characteristics of a compression ignition engine. *Advances in Mechanical Engineering, 8*(4), 1687814016643228.

98. Karczewski, M., & Szamrej, G. (2023). Experimental Evaluation of the Effect of Replacing Diesel Fuel by CNG on the Emission of Harmful Exhaust Gas Components and Emission Changes in a Dual-Fuel Engine. *Energies, 16*(1), 475.

99. Stettler, M. E., Midgley, W. J., Swanson, J. J., Cebon, D., & Boies, A. M. (2016). Greenhouse gas and noxious emissions from dual fuel diesel and natural gas heavy goods vehicles. *Environmental Science & Technology, 50*(4), 2018–2026.

100. Santoso, A., Sampurno, B., & Cahyono, B. (2021). Modifying Single-Cylinder Diesel Engine Become Dual-fuel System to Reduce NOx Emission and Maintain Fuel Efficiency. *IOP Conference Series: Materials Science and Engineering, 1052*(1), 012003. DOI 10.1088/1757-899X/1052/1/012003

101. Nithyanandan, K., Zhang, J., Li, Y., Meng, X., Donahue, R., Lee, C. F., & Dou, H. (2016). Diesel-like efficiency using compressed natural gas/diesel dual-fuel combustion. *Journal of Energy Resources Technology, 138*(5), 052201.

102. Felayati, F. M., Cahyono, B., Bakar, R. A., & Birouk, M. (2021). Performance and emissions of natural gas/diesel dual-fuel engine at low load conditions: Effect of natural gas split injection strategy. *Fuel*, *300*, 121012.

103. Yin, Z., Liu, S., Tan, D., Zhang, Z., Wang, Z., & Wang, B. (2023). A review of the development and application of soot modelling for modern diesel engines and the soot modelling for different fuels. *Process Safety and Environmental Protection*.

# List of Publications

This thesis is based on the following papers, which are underlined with bullet points. Papers are attached in the order stated below.

- **Kumar, Neeraj**, Bharat Bhushan Arora, and Sagar Maji. "Environmental impact evaluation of diesel engine fuelled with CNG." *Archives of Environmental Protection* (2023): 79-84. **(SCIE)**
- **KUMAR, Neeraj**, Bharat Bhushan ARORA, and MAJI Sagar. "Experimental Evaluation of CNG Substitution Ratio on Exhaust Gas Emissions of Diesel/CNG Dual Fuel Combustion." *Mechanics* 29, no. 5 (2023): 432-437. **(SCIE)**

- **Kumar, Neeraj**, Bharat Bhushan Arora, and Sagar Maji. 2021. Influence of Alternative Fuels on Exhaust Emissions of IC Engine: A Review. *International Conference of Renewable Technologies in Engineering* (ICRTE-2021), organized at Manav Rachna International Institute of Research and Studies, Faridabad, Haryana on 15th-16th April,2021. https://doi.org/10.1007/978-981-16-4663-8_2 **(Springer)**

- " Evaluation of Mixture Formation to Improve Combustion Efficiency and Reduce Emissions in Internal Combustion Engines: A Study'' , **Neeraj Kumar** , B.B. Arora , S. Maji , IJESPR , Vol. 48, Special Issue **(UGC Approved)**

# Annexure -A

**Engine performance calculations:**

**(i) Brake Power (kW) :**

$$BP = \frac{2x\pi xNxT}{60x1000}$$

$$BP = \frac{2x\pi xNxWxR}{60000}, \text{kW}$$

**(ii) Brake Specific fuel consumption (kg/kWh) :**

$$BSFC = \frac{Fuel\ flow\ in\ kg/hr}{BP}$$

**(iii) Brake thermal efficiency (%) :**

$$BTE = \frac{BPx3600x100}{Fuel\ flow\ in\frac{kg}{hr}\ x\ calorific\ value\ of\ fuel}$$

**(iv) Air fuel ratio :**

$$A/F\ ratio = \frac{Air\ flow}{Fuel\ flow}$$

# Annexure B

## Uncertainty Analysis

This section discusses the errors in experimental data for different variables. Kline and McClintok presented a method for assessing uncertainty in experimental data in 1953. The method is based on specifying the uncertainty in the basic experimental measurements. These are systematic errors that depend on the measurement instruments' accuracy. Consider the experiment outcome P, which is a function of independent variables x1, x2, x3, x4, …, xn. Thus P=P(x1,x2,x3,x4…….xn).

Let ΔR represent the uncertainty in the experiment's outcomes and ΔP1, ΔP2, ΔP3, ΔP4,... ΔPn represents the uncertainties in the independent variables. If the uncertainties in the independent variables are all given with the same odds, then the uncertainties in the results having these odds are as follows

$$\Delta P = \sqrt{\left(\frac{\partial P}{\partial x_1}\Delta P_1\right)^2 + \left(\frac{\partial P}{\partial x_2}\Delta P_2\right)^2 + \left(\frac{\partial P}{\partial x_3}\Delta P_3\right)^2 + \left(\frac{\partial P}{\partial x_4}\Delta P_4\right)^2 + \cdots .. \left(\frac{\partial P}{\partial x_n}\Delta P_n\right)^2}$$

The table shows the estimated relative errors for each measured independent variable in both modes of combustion. The table shows the overall measurement error for the performance metrics.

For example, the uncertainties resulting from measuring BTE in diesel mode are below:

$$\text{BP} = \frac{2x\pi xNxWxR}{60000}\text{, kW}$$

The independent variables used to calculate BP are N, W, and R, which are system constants when diesel fuel is used.

$$BTE = \frac{BPx3600x100}{\dot{m}_{Diesel} \times CV_{Diesel}}$$

Hence independent variable are N, W, $\dot{m}_{Diesel}$ and $CV_{Diesel}$.

The errors in measurement of N, W, $\dot{m}_{Diesel}$ and $CV_{Diesel}$ are 0.3%, 0.3%, 1%, 1%, respectively.

The uncertainty in the measurement of BTE of diesel mode

$$\Delta BTE = \sqrt{(0.003)^2 + (0.003)^2 + (0.01)^2 + (0.01)^2}$$

$$= .010$$

$$= 1.0\%$$

Table B1 shows the relative errors of independent variables

| Independent Variables | Relative error % |
|---|---|
| Engie speed (N) | 0.5 |
| Engine Load (W) | 0.5 |
| Cylinder pressure (CP) | 1 |
| diesel fuel flow rate ($\dot{m}_{Diesel}$) | 1 |
| CNG fuel flow rate ( $\dot{m}_{CNG}$) | 1.5 |
| calorific value of CNG | 1.5 |
| calorific value of diesel fuel. | 1 |

# CURRICULUM VITAE

NEERAJ KUMAR

- He is a highly motivated individual with a solid objective to pursue a career in leading engineering colleges and universities within a hi-tech environment. His educational background reflects his dedication and pursuit of excellence. He is pursuing a Ph.D. from Delhi Technological University (DTU) and has achieved a notable SGPA of 8.00. Before this, he completed his M.Tech in Thermal Engineering from M.D.U. Rohtak (Haryana), and his B.Tech. in Mechanical Engineering from M.D.U. Rohtak (Haryana).
- He possesses valuable work experience as an Assistant Professor in various esteemed institutions. He has served as a lecturer at the SGT Institute of Engineering and Technology, Gurgaon, DPG Institute of Technology & Management, Gurgaon. These roles have allowed him to develop expertise and skills in engineering education, contributing to his well-rounded teaching abilities.
- Notably, He has made significant research contributions, with several of his papers published in reputable journals. Some of his noteworthy articles include "An Effective Tool for Manufacturing Firms in Product Design & Development in Industry", published in the International Journal of Advanced Engineering Science and Technological Research. And "Concurrent Engineering –An Emerging Tool for Production Industries Design & Development " in the International Journal of  International Journal of Mechanical Engineering and Robotics Research.
- Neeraj Kumar's career aspirations, educational background, work experience, research contributions, and accolades showcase his unwavering commitment to excel in engineering, particularly within a hi-tech environment. His diverse experiences in teaching, research, and active participation in academic events demonstrate his dedication to continuous learning and determination to thrive in challenging settings.